

Appendix A

DETAILED RESULTS FOR ALL DECAY MODES

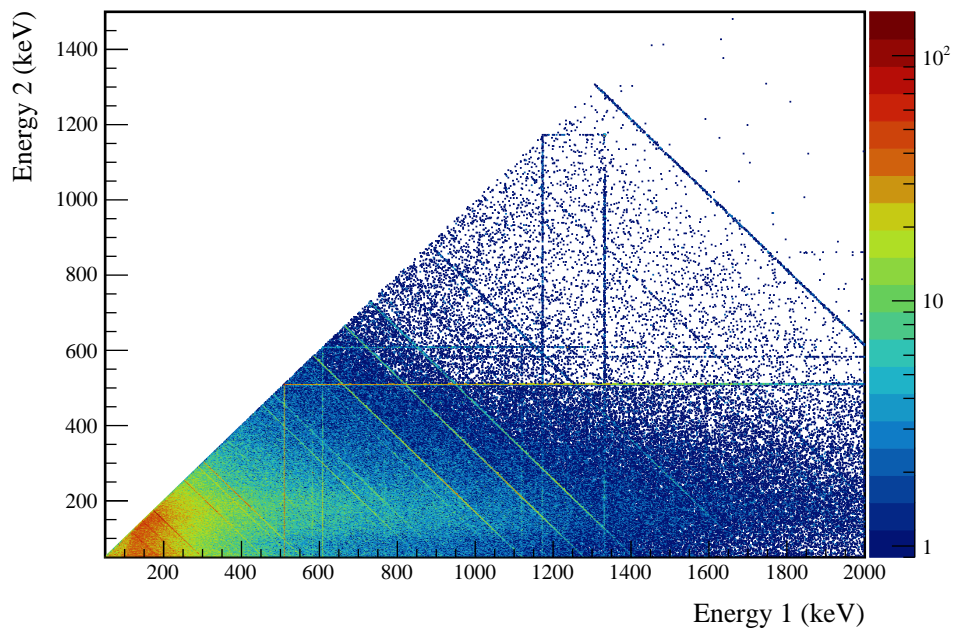


Figure A.1: Simulation using early version of background model.

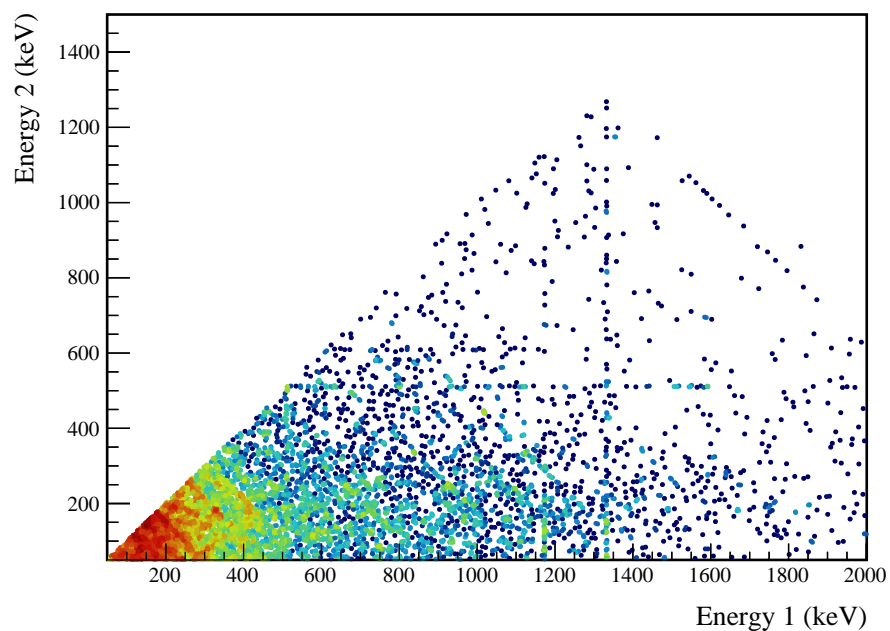


Figure A.2: All 2-detector events, colored using a Gaussian density kernel.

Decay Mode	Peak	Module	n_{ROI}	m_{BG}	Expected ROI BGs	$T^* (\times 10^{23} \text{y})$	$T_{1/2} (\times 10^{23} \text{y})$ 90% Limit	$T_{1/2} (\times 10^{23} \text{y})$ 90% Sensitivity
$0_{g.s.}^+ \xrightarrow{2\nu\beta\beta} 0_1^+$	559 keV	M1	2	51	1.77	16.63 ± 1.18	> 4.7	> 5.1
		M2	1	6	0.25	4.46 ± 0.82	> 1.3	> 3.2
	563 keV	M1	2	51	1.95	16.72 ± 1.19	> 4.9	> 5.2
		M2	0	6	0.22	4.41 ± 0.81	> 3.2	> 3.2
	Combined						> 7.6	> 10.5
	$0_{g.s.}^+ \xrightarrow{2\nu\beta\beta} 2_1^+$	559 keV	M1	0	35	19.23 ± 1.96	> 14.1	> 7.8
			M2	1	2	5.16 ± 1.73	> 1.2	> 3.3
		Combined					> 7.7	> 10.2
$0_{g.s.}^+ \xrightarrow{2\nu\beta\beta} 2_2^+$	559 keV	M1	3	76	2.64	13.89 ± 1.72	> 3.2	> 4.3
		M2	1	8	0.32	3.86 ± 1.78	> 0.8	> 2.4
		M1	0	30	0.98	10.66 ± 1.39	> 7.8	> 4.0
		M2	0	3	0.10	3.05 ± 1.53	> 1.8	> 1.8
	657 keV	M1	0	41	1.07	5.79 ± 1.60	> 4.0	> 2.1
		M2	0	7	0.24	1.52 ± 1.84	> 2.2	> 2.2
	Combined						> 12.6	> 8.8
	563 keV	M1	0	6	0.24	21.45 ± 1.81	> 15.8	> 15.8
		M2	0	1	0.06	5.69 ± 1.14	> 4.1	> 4.1
		M1	0	6	0.25	21.19 ± 1.79	> 15.6	> 15.6
		M2	0	1	0.06	5.58 ± 1.12	> 4.0	> 4.0
	Combined						> 39.8	> 39.8
$0_{g.s.}^+ \xrightarrow{0\nu\beta\beta} 0_1^+$	559 keV	M1	0	0	0.00	22.89 ± 2.48	> 16.8	> 16.8
		M2	0	0	0.00	5.98 ± 2.06	> 4.0	> 4.0
	Combined						> 21.2	> 21.2
	$0_{g.s.}^+ \xrightarrow{0\nu\beta\beta} 2_1^+$	559 keV	M1	0	8	0.29	13.38 ± 1.81	> 9.8
			M2	0	1	0.07	3.54 ± 1.70	> 2.1
		657 keV	M1	0	10	0.41	13.27 ± 1.86	> 9.7
			M2	0	1	0.01	3.48 ± 1.82	> 1.9
		1216 keV	M1	0	0	0.00	6.16 ± 1.67	> 4.3
			M2	0	0	0.00	1.62 ± 1.90	> 0.4
	Combined						> 30.4	> 18.7

Table A.1: Table of results. n_{ROI} and m_{BG} are the number of observed events, after all cuts, in the Signal ROI and BG counting regions, respectively. $T^* = \ln 2 \frac{N_A}{m_{76}} \epsilon_k M_{iso} T_{live}$ is used to calculate the number of expected signal counts from a half-life: $\langle s_k \rangle = \frac{T^*}{T_{1/2}}$. Physically, it represents the half-life that is expected to produce one count, based on exposure and detection efficiency. Limits and sensitivities were computed using the Rolke Confidence Intervals, which are similar to Feldman-Cousins, but account for nuisance parameter uncertainties in detection efficiency and exposure.

A.1 Exposure

DS	M1 Detector Mask	M2 Detector Mask	Run Time (days)	M1 L.T. (days)	M1 Eff.	M2 L.T. (days)	M2 Eff.	Exposure (kg·y)
DS1	061a08001e0e1c00	00000000000000000000	2.64	2.60	1.72%	0.00	0.00%	0.109
DS1	161a08341e0e1c00	00000000000000000000	0.02	0.02	2.00%	0.00	0.00%	0.001
DS1	161a0c341e0e1c00	00000000000000000000	4.51	4.48	1.94%	0.00	0.00%	0.188
DS1	161a0c361e0e1c00	00000000000000000000	3.49	3.48	1.47%	0.00	0.00%	0.146
DS1	1e1a00001e0e1c00	00000000000000000000	7.82	7.73	2.04%	0.00	0.00%	0.324
DS1	1e1a08001e0e1c00	00000000000000000000	37.30	36.87	2.23%	0.00	0.00%	1.547
DS1	1e1a08041e0e1c00	00000000000000000000	6.26	6.19	2.30%	0.00	0.00%	0.260
DS1	1e1a08141e0e1c00	00000000000000000000	0.26	0.25	2.32%	0.00	0.00%	0.011
DS1	1e1a08301e0e1c00	00000000000000000000	1.40	1.37	2.33%	0.00	0.00%	0.057
DS1	1e1a08341e0e1c00	00000000000000000000	7.58	7.50	2.12%	0.00	0.00%	0.315
DS1	1e1a0c001e0e1c00	00000000000000000000	2.83	2.78	2.25%	0.00	0.00%	0.117
DS1	1e1a0c041e0e1c00	00000000000000000000	0.04	0.04	2.24%	0.00	0.00%	0.002
DS1	1e1a0c341e0e1c00	00000000000000000000	0.67	0.67	2.32%	0.00	0.00%	0.028
DS2	1e1a08001e0e1c00	00000000000000000000	38.92	38.52	2.28%	0.00	0.00%	1.617
DS2	1e1a0c001e0e1c00	00000000000000000000	1.22	1.19	2.27%	0.00	0.00%	0.050
DS3	1e1a0c3e1e0e1c00	00000000000000000000	29.88	29.67	2.64%	0.00	0.00%	1.245
DS4	00000000000000000000	1c061a16060e1e00	19.15	0.00	0.00%	18.85	1.89%	0.622
DS5a	08000020040e1c00	18060a02040e1e00	1.49	1.48	0.72%	1.46	1.16%	0.110
DS5a	08080020040e1c00	18060a16060e1e00	2.51	2.49	0.86%	2.47	1.56%	0.186
DS5a	08080030040e1c00	18060a02040e1e00	0.01	0.01	0.91%	0.01	1.14%	0.001
DS5a	0e1a04321e0e1c00	08020a16060e1e00	2.69	2.71	2.33%	2.66	1.23%	0.201
DS5a	0e1a0c321e0e1c00	00000000000000000000	0.65	0.63	2.59%	0.00	0.00%	0.026
DS5a	0e1a0c321e0e1c00	08060a16060e1e00	1.24	1.24	2.58%	1.21	1.52%	0.092
DS5a	0e1a0c321e0e1c00	18060a02040e1e00	2.94	2.92	2.35%	2.89	1.15%	0.218
DS5a	0e1a0c321e0e1c00	18060a1406061600	0.04	0.04	2.56%	0.04	0.95%	0.003
DS5a	0e1a0c321e0e1c00	18060a1606060600	3.19	3.15	2.52%	3.16	0.82%	0.237
DS5a	0e1a0c321e0e1c00	18060a16060e0600	3.30	3.28	2.53%	3.29	0.84%	0.246
DS5a	0e1a0c3e1e0e1c00	1806020606081800	1.75	1.73	2.80%	1.73	0.76%	0.129
DS5a	0e1a0c3e1e0e1c00	18060216060c1c00	6.84	6.77	2.80%	6.74	1.12%	0.507
DS5a	0e1a0c3e1e0e1c00	18060216060e1e00	13.48	13.30	2.77%	13.27	1.26%	0.996
DS5a	0e1a0c3e1e0e1c00	18060816060e1c00	0.05	0.05	2.59%	0.05	1.30%	0.004
DS5a	0e1a0c3e1e0e1c00	18060a0606060c00	2.16	2.12	2.77%	2.12	1.02%	0.159
DS5a	0e1a0c3e1e0e1c00	18060a16040e1e00	0.76	0.76	2.76%	0.74	1.29%	0.056
DS5a	0e1a0c3e1e0e1c00	18060a1606060c00	0.25	0.25	2.78%	0.25	1.11%	0.019
DS5a	0e1a0c3e1e0e1c00	18060a1606061800	1.88	1.86	2.78%	1.86	1.04%	0.140
DS5a	0e1a0c3e1e0e1c00	18060a1606061c00	9.20	9.13	2.75%	9.06	1.41%	0.682

Continued on the next page

Table A.2: List of subdatasets

DS	M1 Detector Mask	M2 Detector Mask	Run Time (days)	M1 L.T. (days)	M1 Eff.	M2 L.T. (days)	M2 Eff.	Exposure (kg·y)
DS5a	0e1a0c3e1e0e1c00	18060a16060c1c00	7.89	7.79	2.78%	7.79	1.41%	0.584
DS5a	0e1a0c3e1e0e1c00	18060a16060e1c00	11.68	11.53	2.43%	11.51	1.42%	0.864
DS5a	0e1a0c3e1e0e1c00	18060a16060e1e00	5.21	5.15	2.76%	5.13	1.56%	0.386
DS5a	0e1a0c3e1e0e1c00	18061216060e1e00	2.39	2.37	2.77%	2.37	1.34%	0.178
DS5b	1e1a0c3e1e0c1c00	18061216060e1e00	24.46	24.09	2.75%	24.06	1.34%	1.805
DS5b	1e1a0c3e1e0c1c00	18061a16060e1e00	0.75	0.75	2.75%	0.75	1.73%	0.056
DS5b	1e1a0c3e1e0e1c00	18061216060e1e00	14.28	14.12	2.86%	14.07	1.24%	1.057
DS5c	1e1a0c3e1e0c1c00	00000000000000000000	0.67	0.67	2.65%	0.00	0.00%	0.028
DS5c	1e1a0c3e1e0c1c00	00060216060e0e00	0.78	0.76	2.65%	0.78	0.84%	0.058
DS5c	1e1a0c3e1e0c1c00	00060a16060e0e00	5.91	5.82	2.75%	5.83	1.07%	0.437
DS5c	1e1a0c3e1e0c1c00	00061216060e0e00	38.85	38.45	2.73%	38.29	0.91%	2.877
DS6a	120000000000c0800	1002020006040e00	4.94	4.89	0.16%	4.89	0.42%	0.366
DS6a	12000c20000c1c00	18061216060c1e00	17.22	17.03	0.78%	17.03	1.13%	1.277
DS6a	12020000040c0800	1802020006040e00	5.69	5.63	0.29%	5.62	0.50%	0.422
DS6a	12020c00040c1800	1802020006040e00	7.90	7.79	0.68%	7.78	0.50%	0.584
DS6a	12080c20000c1c00	18061216060c1e00	12.23	12.11	0.96%	12.09	1.13%	0.907
DS6a	12120c3e1c0c1c00	18061216060c1e00	0.56	0.54	1.90%	0.56	1.10%	0.041
DS6a	16020c10040c1800	1806020006060e00	14.89	14.73	0.90%	14.68	0.69%	1.103
DS6a	160a0c321c0c1c00	1806021006061e00	5.87	5.80	2.05%	5.80	0.89%	0.435
DS6a	1e0a0c321c0c1c00	0000000000000000	0.23	0.23	2.31%	0.00	0.00%	0.010
DS6a	1e0a0c321c0c1c00	1806020006040200	10.00	9.89	2.31%	9.89	0.27%	0.741
DS6a	1e0a0c321c0c1c00	1806020006040600	7.43	7.35	2.31%	7.32	0.41%	0.550
DS6a	1e0a0c321c0c1c00	1806020006041600	4.88	4.83	2.31%	4.81	0.48%	0.362
DS6a	1e0a0c321c0c1c00	1806021006061e00	6.11	6.05	2.31%	6.04	0.89%	0.453
DS6a	1e120c3e1c0c1c00	18061216060c1e00	2.12	2.11	2.39%	2.09	1.13%	0.157
DS6a	1e1a0c321c0c1c00	1806020006060e00	5.56	5.51	2.49%	5.53	0.69%	0.414
DS6a	1e1a0c321c0c1c00	1806021006040e00	16.87	16.69	2.49%	16.64	0.69%	1.250
DS6a	1e1a0c321c0c1c00	1806021006041e00	11.93	11.81	2.49%	11.79	0.86%	0.885
DS6a	1e1a0c321c0c1c00	1806021006060e00	2.56	2.55	2.49%	2.55	0.73%	0.191
DS6a	1e1a0c3a1c0c1c00	1806020006040e00	8.66	8.59	2.60%	8.59	0.65%	0.644
DS6a	1e1a0c3a1c0c1c00	1806021006040e00	7.93	7.84	2.60%	7.83	0.69%	0.588
DS6a	1e1a0c3a1c0c1c00	1806021006041e00	1.24	1.23	2.60%	1.23	0.86%	0.092
DS6a	1e1a0c3e1c0c1c00	0000000000000000	0.06	0.05	2.69%	0.00	0.00%	0.002
DS6a	1e1a0c3e1c0c1c00	1806000006040e00	7.85	7.81	2.69%	7.54	0.61%	0.577
DS6a	1e1a0c3e1c0c1c00	1806020006041e00	5.96	5.88	2.65%	5.89	0.81%	0.441
DS6a	1e1a0c3e1c0c1c00	1806021006041e00	3.56	3.52	2.69%	3.52	0.86%	0.264
DS6a	1e1a0c3e1c0c1c00	18060210060c1e00	15.72	15.56	2.69%	15.51	0.92%	1.165
DS6a	1e1a0c3e1c0c1c00	1806021206041e00	10.09	9.95	2.69%	9.97	0.89%	0.747

Continued on the next page

Table A.2: List of subdatasets

DS	M1 Detector Mask	M2 Detector Mask	Run Time (days)	M1 L.T. (days)	M1 Eff.	M2 L.T. (days)	M2 Eff.	Exposure (kg·y)
DS6a	1e1a0c3e1c0c1c00	18060214060c0e00	5.65	5.60	2.69%	5.66	0.80%	0.422
DS6a	1e1a0c3e1c0c1c00	18060214060c1e00	7.83	7.76	2.69%	7.74	0.98%	0.581
DS6a	1e1a0c3e1c0c1c00	18060214060e1e00	58.28	57.56	2.67%	57.43	0.95%	4.311
DS6a	1e1a0c3e1c0c1c00	1806121206041e00	1.00	0.98	2.69%	1.00	1.01%	0.074
DS6a	1e1a0c3e1c0c1c00	18061212060c1e00	12.96	12.80	2.69%	12.80	1.07%	0.959
DS6a	1e1a0c3e1c0c1c00	18061212060c1e00	26.05	25.76	2.69%	25.72	1.13%	1.930
DSTotal	–	–	621.97	615.24	2.35%	487.97	1.00%	41.923

Table A.2: List of each subdataset with its livetime, detection efficiency measured for the $\beta\beta$ E.S.to 0_1^+ decay, and total isotopic exposure. Note the large variance in the detection efficiency.

A.2 $2\nu\beta\beta$ to 0_1^+

Note that both the 559 and 563 keV peaks will be shown together since they use the same sets of cuts.

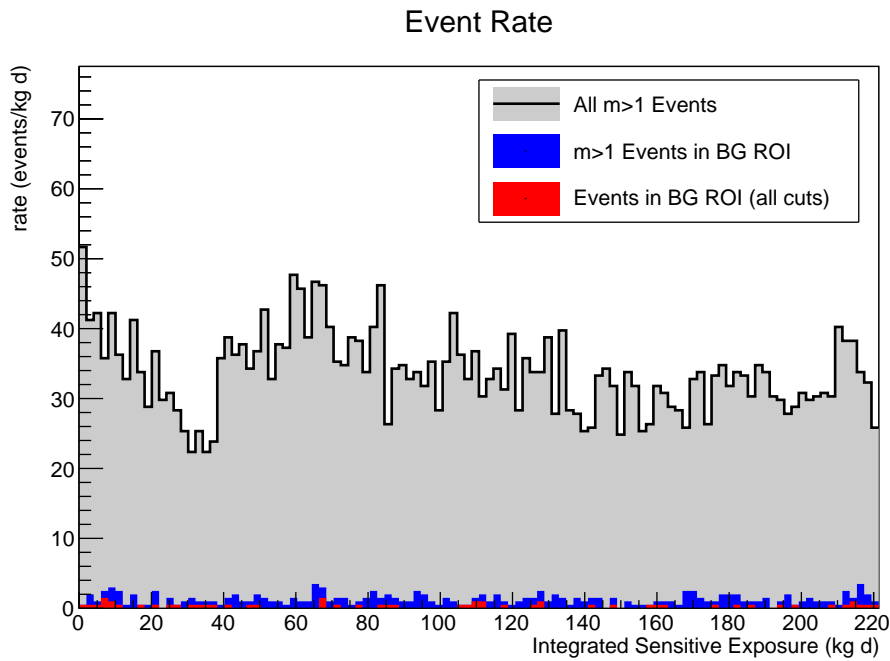


Figure A.3: Module 1 Background rate vs sensitive exposure, defined as the detection efficiency for the $\beta\beta$ E.S.to 0_1^+ decay multiplied by the integrated exposure over all ^{76}Ge in module 1.

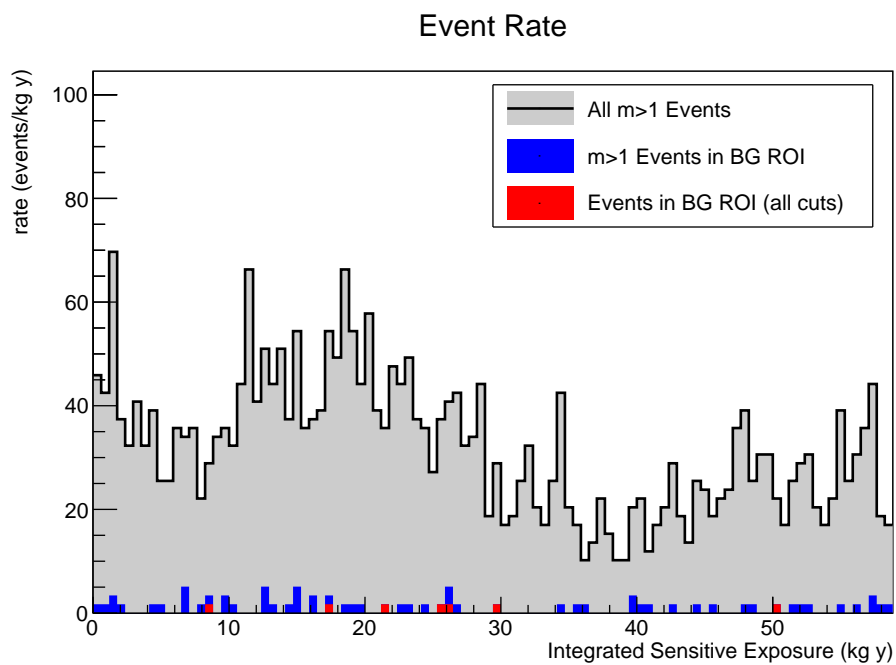


Figure A.4: Module 2 Background rate vs sensitive exposure.

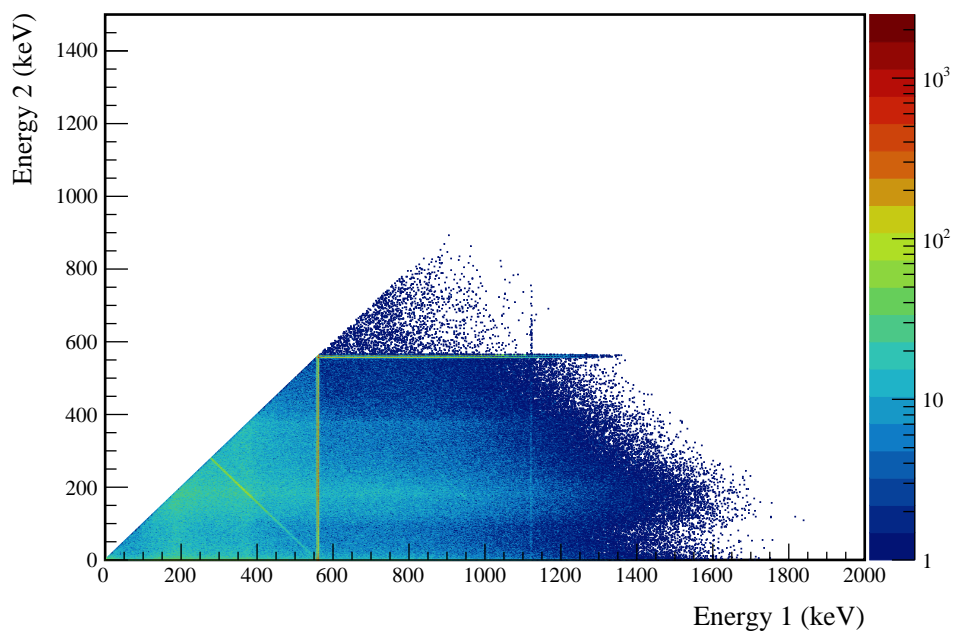


Figure A.5: Simulated multiplicity 2 energy spectrum of the $2\nu\beta\beta$ to 0_1^+ decay mode

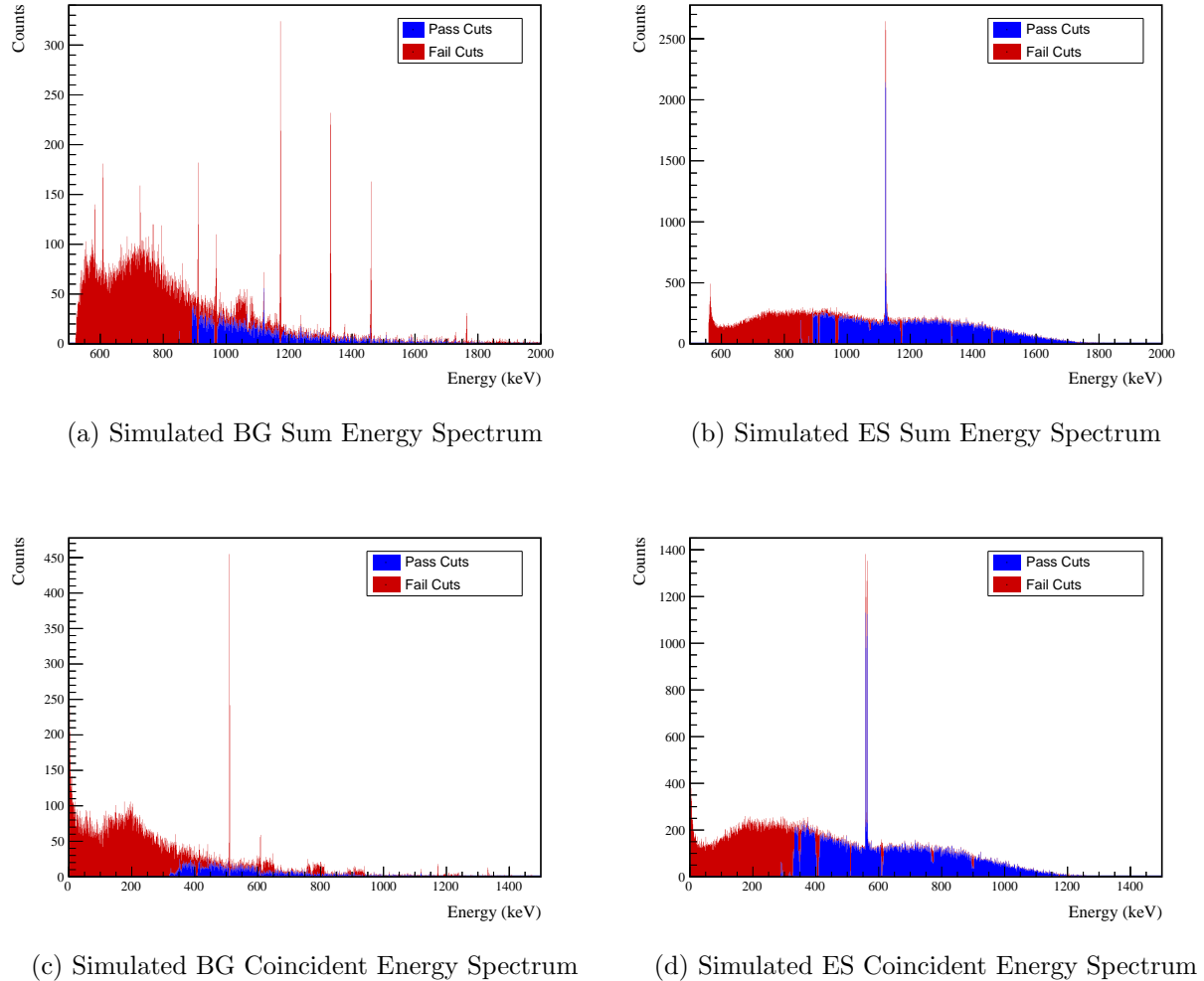
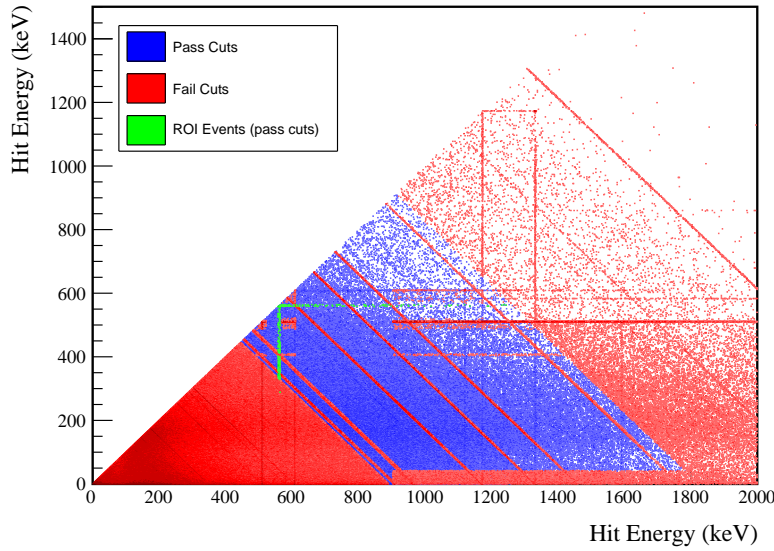


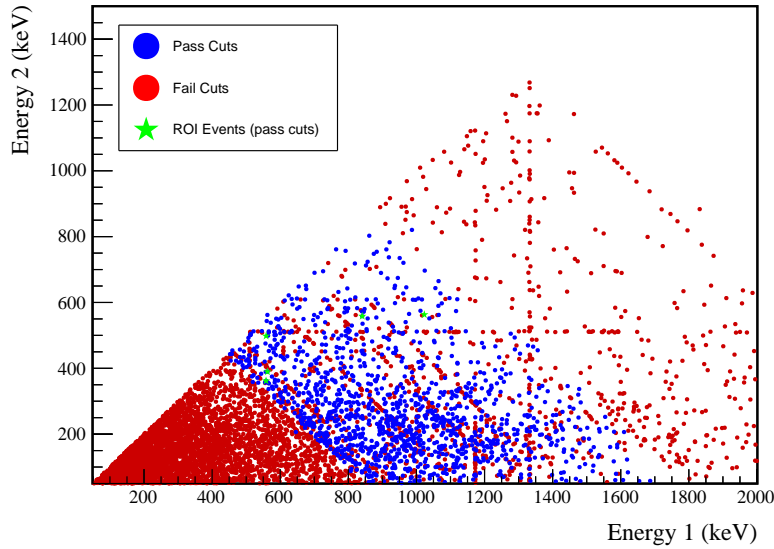
Figure A.6: Sum energy and coincident energy spectra for the 559 and 563 keV peaks.

Table A.3: Table of energy estimation uncertainties for the 559 and 563 keV peaks.

DS	E_{peak} (keV)	σ_{fit} (keV)	σ_{disfit} (keV)	σ (keV)	$f_{i,fit}$ (keV)	τ_{fit} (keV)	$\delta_{i,fit}$ (keV)	$\delta_{\mu,NL}$ (keV)	$\delta_{\mu,drift}$ (keV)	$\delta_{\mu,etalk}$ (keV)	$\delta_{\mu,peak}$ (keV)	δ_{μ} (keV)	FWHM (keV)	$\delta_{fwhm,fit}$ (keV)	$\delta_{fwhm,etalk}$ (keV)	$\delta_{fwhm,drift}$ (keV)	δ_{FWHM} (keV)	$\delta_{fwhm,ztak}$ (keV)	$\delta_{FWHM,ztak}$ (keV)	$E_{ROI,1}$ (keV)	$E_{ROI,2}$ (keV)	ϵ_{ROI}	$\sigma_{e,noi}$
DS1	559.101	0.460	0.063	0.464	0.230	0.515	0.001	0.104	0.002	0.012	0.005	0.105	1.152	0.001	0.039	0.011	0.040	0.035	558.230	559.823	0.859	0.016	
DS2	559.101	0.461	0.055	0.464	0.249	0.515	0.002	0.067	0.004	0.012	0.005	0.068	1.158	0.001	0.107	0.011	0.108	0.093	558.217	559.820	0.862	0.032	
DS3	559.101	0.470	0.066	0.474	0.224	0.505	0.001	0.026	0.024	0.012	0.005	0.038	1.174	0.001	0.073	0.011	0.074	0.063	558.218	559.838	0.868	0.022	
DS4	559.101	0.455	0.077	0.461	0.108	0.445	0.002	0.076	0.010	0.012	0.005	0.078	1.111	0.001	0.106	0.011	0.107	0.096	558.309	559.832	0.876	0.034	
DS5a	559.101	0.560	0.085	0.567	0.106	0.855	0.002	0.079	0.005	0.012	0.005	0.080	1.367	0.002	0.055	0.011	0.056	0.041	558.131	559.994	0.864	0.015	
DS5b	559.101	0.469	0.074	0.475	0.158	0.491	0.001	0.020	0.011	0.012	0.005	0.026	1.157	0.001	0.125	0.011	0.125	0.108	558.258	559.847	0.874	0.037	
DS5c	559.101	0.460	0.085	0.468	0.174	0.489	0.001	0.037	0.030	0.012	0.005	0.050	1.145	0.001	0.162	0.011	0.162	0.142	558.260	559.835	0.871	0.049	
DS6a	559.101	0.456	0.044	0.458	0.191	0.463	0.001	0.069	0.025	0.012	0.005	0.075	1.123	0.000	0.041	0.011	0.042	0.038	558.270	559.817	0.869	0.014	
DS1	563.178	0.461	0.064	0.466	0.230	0.518	0.001	0.104	0.002	0.012	0.005	0.105	1.156	0.001	0.039	0.011	0.040	0.035	562.303	563.902	0.859	0.016	
DS2	563.178	0.463	0.055	0.466	0.249	0.517	0.002	0.067	0.004	0.012	0.005	0.068	1.162	0.001	0.107	0.011	0.108	0.093	562.291	563.900	0.862	0.032	
DS3	563.178	0.471	0.066	0.476	0.224	0.508	0.001	0.026	0.024	0.012	0.005	0.038	1.179	0.001	0.073	0.011	0.074	0.063	562.291	563.918	0.867	0.022	
DS4	563.178	0.457	0.077	0.463	0.108	0.447	0.002	0.076	0.010	0.012	0.005	0.078	1.115	0.001	0.106	0.011	0.107	0.096	562.383	563.911	0.876	0.034	
DS5a	563.178	0.562	0.086	0.569	0.106	0.858	0.002	0.079	0.006	0.012	0.005	0.080	1.372	0.002	0.055	0.011	0.056	0.041	562.204	564.074	0.864	0.015	
DS5b	563.178	0.471	0.074	0.477	0.158	0.494	0.001	0.020	0.011	0.012	0.005	0.026	1.162	0.001	0.125	0.011	0.125	0.108	562.332	563.927	0.874	0.037	
DS5c	563.178	0.462	0.086	0.470	0.174	0.492	0.001	0.037	0.030	0.012	0.005	0.050	1.149	0.001	0.162	0.011	0.162	0.141	562.334	563.915	0.871	0.048	
DS6a	563.178	0.457	0.044	0.459	0.191	0.465	0.001	0.069	0.026	0.012	0.005	0.075	1.127	0.000	0.041	0.011	0.042	0.038	562.344	563.897	0.869	0.014	

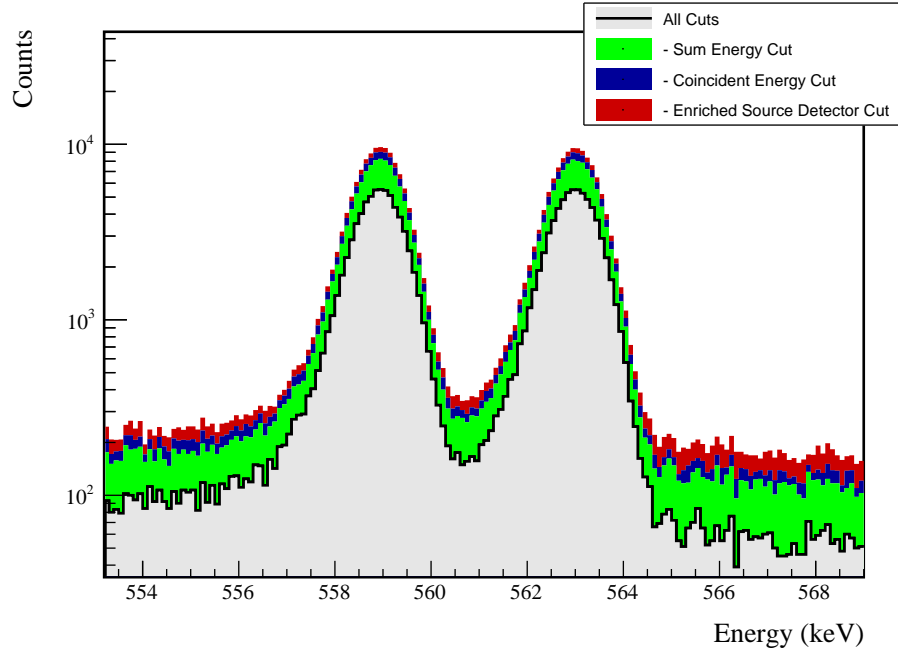


(a) Simulation



(b) Data

Figure A.7: Simulated and measured multiplicity 2 energy spectrum with sum and coincident energy cuts included for the 559 and 563 keV peaks.



(a) Effect of all cuts on ROI

Source	Module 1 efficiency	Module 2 efficiency
Multi-Detector with Full Energy γ	$5.7 \pm 0.2\%$	$3.1 \pm 0.5\%$
Region of Interest	$86.8 \pm 1.5\%$	$86.8 \pm 1.5\%$
Dead Layer	$74.8 \pm 4.3\%$	$63.5 \pm 6.4\%$
Detector Dead Times	$98.3 \pm 0.8\%$	$98.5 \pm 0.7\%$
Enriched Source Detector Cut	$96.9 \pm <0.1\%$	$90.5 \pm <0.1\%$
Coincident Energy Cut	$91.3 \pm 0.5\%$	$89.6 \pm 0.5\%$
Sum Energy Cut	$63.0 \pm 0.5\%$	$56.7 \pm 0.5\%$
Final Efficiency	$2.35 \pm 0.17\%$	$1.00 \pm 0.18\%$

(b) Table of efficiencies

Figure A.8: Plot showing effect of cuts applied sequentially on ROI peak and table of detection efficiencies for the 559 and 563 keV peaks.

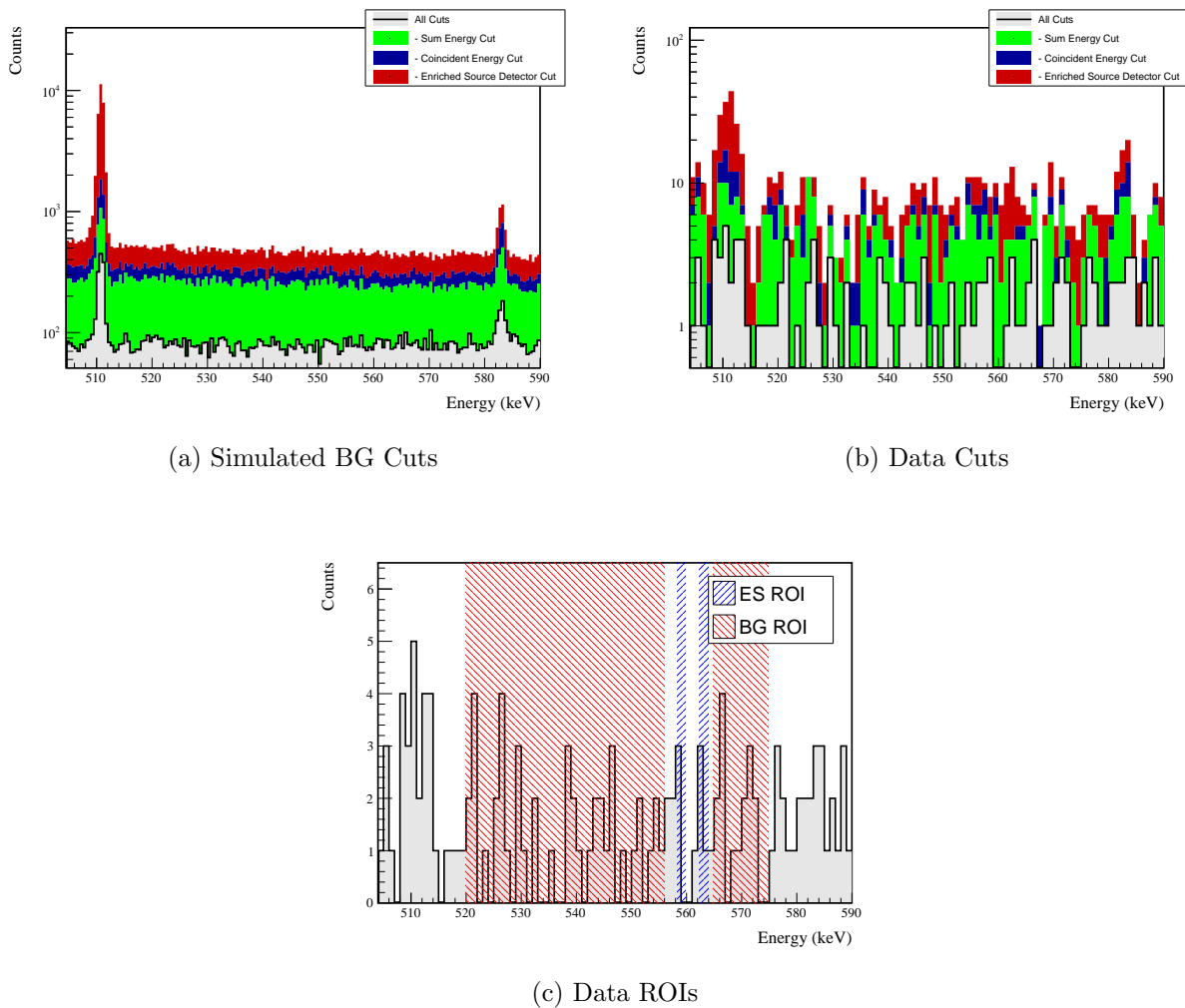


Figure A.9: Effect of all cuts applied to measured and simulated background data.

A.2. $2\nu\beta\beta$ TO 0_1^+

15

Cut Name	Cut Description	$\langle \epsilon_{total} \rangle$	$\hat{\epsilon}_{total}$	$\langle \epsilon_{unique} \rangle$	$\hat{\epsilon}_{unique}$	Sacrifice	ΔDP
Enriched Source		M1: 21.5 %	23.3 ^{+2.7} _{-2.5} %	3.2 %	2.3 ^{+1.1} _{-0.7} %	1.0 %	
Detector Cut	Any other detector: isEnr	M2: 40.5 %	63.8 ^{+6.0} _{-6.5} %	6.7 %	12.1 ^{+4.9} _{-3.6} %	2.9 %	9%
Coincident	No other detector: (((energy<40.8) (energy>403.4 && energy<409.2) (energy>509.2 && energy<512.2) (energy>608. && energy<611.4) (energy>1170.6 && energy<1175.6) (energy>1204.2 && energy<1208.2) (energy>1259.2) && isEnr) ((energy>42.2) (energy>487.6 && energy<522.) (energy>568.8 && energy<610.6) (energy>903.2) && !isEnr))	M1: 20.6 %	21.8 ^{+2.6} _{-2.4} %	3.5 %	1.9 ^{+1.0} _{-0.7} %	2.8 %	
Energy Cut		M2: 22.9 %	31.0 ^{+6.4} _{-5.7} %	3.2 %	1.7 ^{+2.7} _{-1.1} %	2.1 %	5%
Sum Energy Cut	Not: (sumE<852.2) (sumE>853. && sumE<855.4) (sumE>856.6 && sumE<877.8) (sumE>878. && sumE<891.) (sumE>906.8 && sumE<912.4) (sumE>911.8 && sumE<917.8) (sumE>1169.8 && sumE<1174.6) (sumE>1330. && sumE<1333.6) (sumE>1458. && sumE<1462.2) (sumE>1761.8 && sumE<1771.) (sumE>1824.6)	M1: 73.1 %	74.4 ^{+2.6} _{-2.8} %	44.8 %	44.4 \pm 3.0 %	29.8 %	19%
Combined Cuts		M1: 81.6 %	80.8 ^{+2.3} _{-2.5} %	—	—	41.0 %	29%
		M2: 86.9 %	89.7 ^{+3.3} _{-4.7} %	—	—	49.0 %	

Table A.4: Table of cut descriptions and efficiencies for simulated backgrounds and measured data for the 559 and 563 keV peaks.

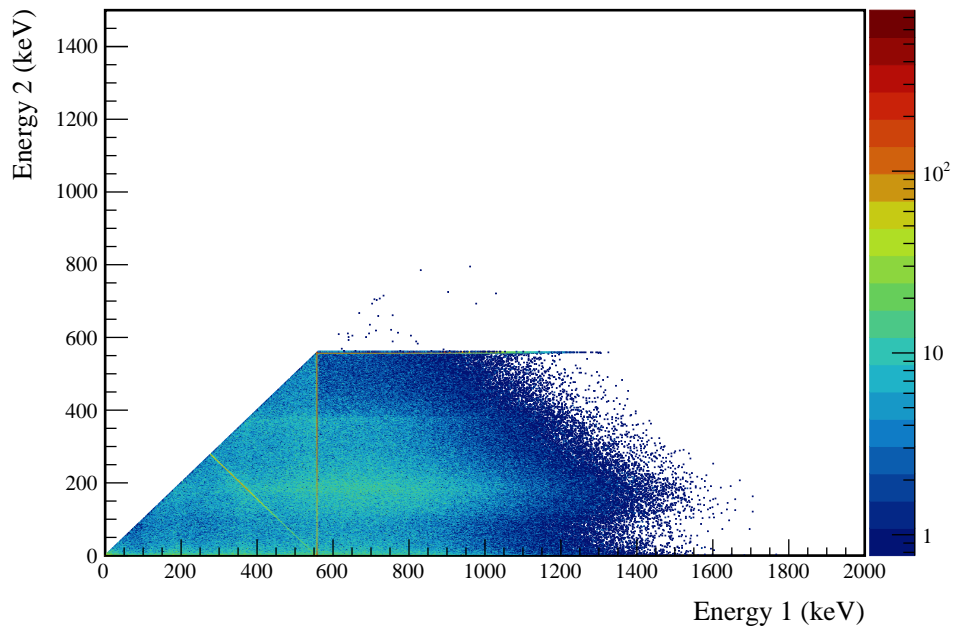
A.3 $2\nu\beta\beta$ to 2_1^+ 

Figure A.10: Simulated multiplicity 2 energy spectrum of the $2\nu\beta\beta$ to 2_1^+ decay mode

Table A.5: Table of energy estimation uncertainties for the 559 keV peak.

DS	E_{peak} (keV)	σ_{fit} (keV)	σ_{drift} (keV)	σ (keV)	$f_{i,fit}$	$f_{i,drift}$	τ_{fit} (keV)	τ_{drift} (keV)	$\delta_{\mu,NL}$ (keV)	$\delta_{\mu,fit}$ (keV)	$\delta_{\mu,drift}$ (keV)	δ_{peak} (keV)	δ_μ (keV)	FWHM	$\delta_{fwhm,fit}$ (keV)	$\delta_{fwhm,drift}$ (keV)	$\delta_{fwhm,peak}$ (keV)	δ_{FWHM} (keV)	δ_α	$E_{ROI,1}$ (keV)	$E_{ROI,2}$ (keV)	ϵ_{ROI}	$\sigma_{e_{ROI}}$
DS1	559.101	0.460	0.063	0.464	0.230	0.515	0.001	0.104	0.002	0.012	0.005	0.105	1.152	0.001	0.039	0.011	0.040	0.035	558.214	559.835	0.866	0.015	
DS2	559.101	0.461	0.055	0.464	0.249	0.515	0.002	0.067	0.004	0.012	0.005	0.068	1.158	0.001	0.107	0.011	0.108	0.093	558.201	559.833	0.868	0.031	
DS3	559.101	0.470	0.066	0.474	0.224	0.505	0.001	0.026	0.024	0.012	0.005	0.038	1.174	0.001	0.073	0.011	0.074	0.063	558.201	559.851	0.874	0.021	
DS4	559.101	0.455	0.077	0.461	0.108	0.445	0.002	0.076	0.010	0.012	0.005	0.078	1.111	0.001	0.106	0.011	0.107	0.096	558.295	559.844	0.882	0.033	
DS5a	559.101	0.560	0.085	0.567	0.106	0.855	0.002	0.079	0.005	0.012	0.005	0.080	1.367	0.002	0.055	0.011	0.056	0.041	558.114	560.009	0.870	0.015	
DS5b	559.101	0.469	0.074	0.475	0.158	0.491	0.001	0.020	0.011	0.012	0.005	0.026	1.157	0.001	0.125	0.011	0.125	0.108	558.243	559.860	0.880	0.036	
DS5c	559.101	0.460	0.085	0.468	0.174	0.489	0.001	0.037	0.030	0.012	0.005	0.050	1.145	0.001	0.162	0.011	0.162	0.142	558.245	559.848	0.877	0.047	
DS6a	559.101	0.456	0.044	0.458	0.191	0.463	0.001	0.069	0.025	0.012	0.005	0.075	1.123	0.000	0.041	0.011	0.042	0.038	558.255	559.830	0.875	0.014	

Cut Name	Cut Description	$\langle \epsilon_{total} \rangle$	$\hat{\epsilon}_{total}$	$\langle \epsilon_{unique} \rangle$	$\hat{\epsilon}_{unique}$	Sacrifice	ΔDP
Enriched Source		M1: 21.5 %	23.0 $^{+2.7}_{-2.5}$ %	4.0 %	3.0 $^{+1.2}_{-0.9}$ %	1.6 %	17%
Detector Cut	Any other detector: isEnr	M2: 40.6 %	63.8 $^{+6.0}_{-6.5}$ %	7.7 %	15.5 $^{+5.3}_{-4.2}$ %	3.5 %	
Multiplicity 2		M1: 15.0 %	16.6 $^{+2.4}_{-2.2}$ %	0.6 %	0.0 $^{+0.4}_{-0.0}$ %	0.0 %	
Cut	m==2	M2: 11.5 %	17.2 $^{+5.5}_{-4.4}$ %	0.7 %	1.7 $^{+2.7}_{-1.1}$ %	0.0 %	2%
	No other detector: ((energy<316.8) (energy>329.8 && energy>366.6) (energy>398.6 && energy<420.) (energy>509.6 && energy<512.2) (energy>606.6 && energy>615.6) (energy>1116.4 && energy<121.6) (energy>1144. && energy>1260.8) (energy>1265.2) && isEnr)	M1: 61.7 %	54.7 \pm 3.1 %	3.4 %	1.1 $^{+0.9}_{-0.5}$ %	0.6 %	11%
Coincident		M2: 47.3 %	27.6 $^{+6.2}_{-5.5}$ %	3.1 %	0.0 $^{+1.7}_{-0.0}$ %	0.6 %	
Energy Cut							
Sum Energy Cut	Not: (sumE<875.6) (sumE>886.4 && sumE<925.4) (sumE>957.4 && sumE<978.8) (sumE>1165.4 && sumE<1174.6) (sumE>1330. && sumE<1333.6) (sumE>1457. && sumE<1462.4) (sumE>1702. && sumE<1819.4) (sumE>1824.2)	M1: 76.1 %	78.1 $^{+2.4}_{-2.6}$ %	5.7 %	7.5 $^{+1.8}_{-1.5}$ %	0.8 %	17%
Combined Cuts		M2: 77.2 %	72.4 $^{+5.5}_{-6.2}$ %	4.0 %	1.7 $^{+2.7}_{-1.1}$ %	0.8 %	
	M1: 89.9 %	86.8 $^{+1.9}_{-2.2}$ %	—	—	31.0 %	35.1 %	84%
	M2: 92.9 %	96.6 $^{+1.7}_{-3.3}$ %	—	—	—	—	

Table A.6: Table of cut descriptions and efficiencies for simulated backgrounds and measured data for the 559 keV peak.

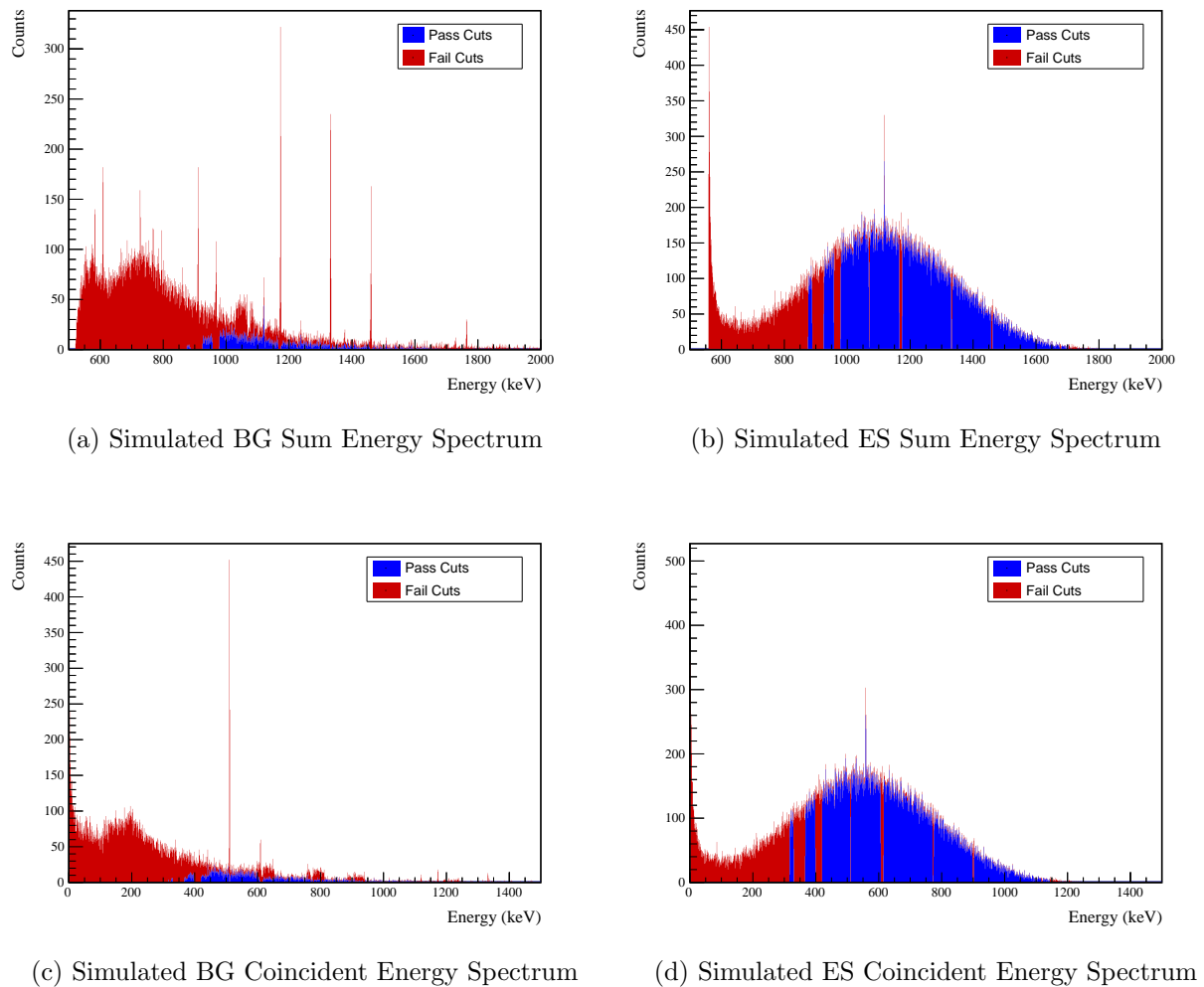


Figure A.11: Sum energy and coincident energy spectra for the 559 keV peak.

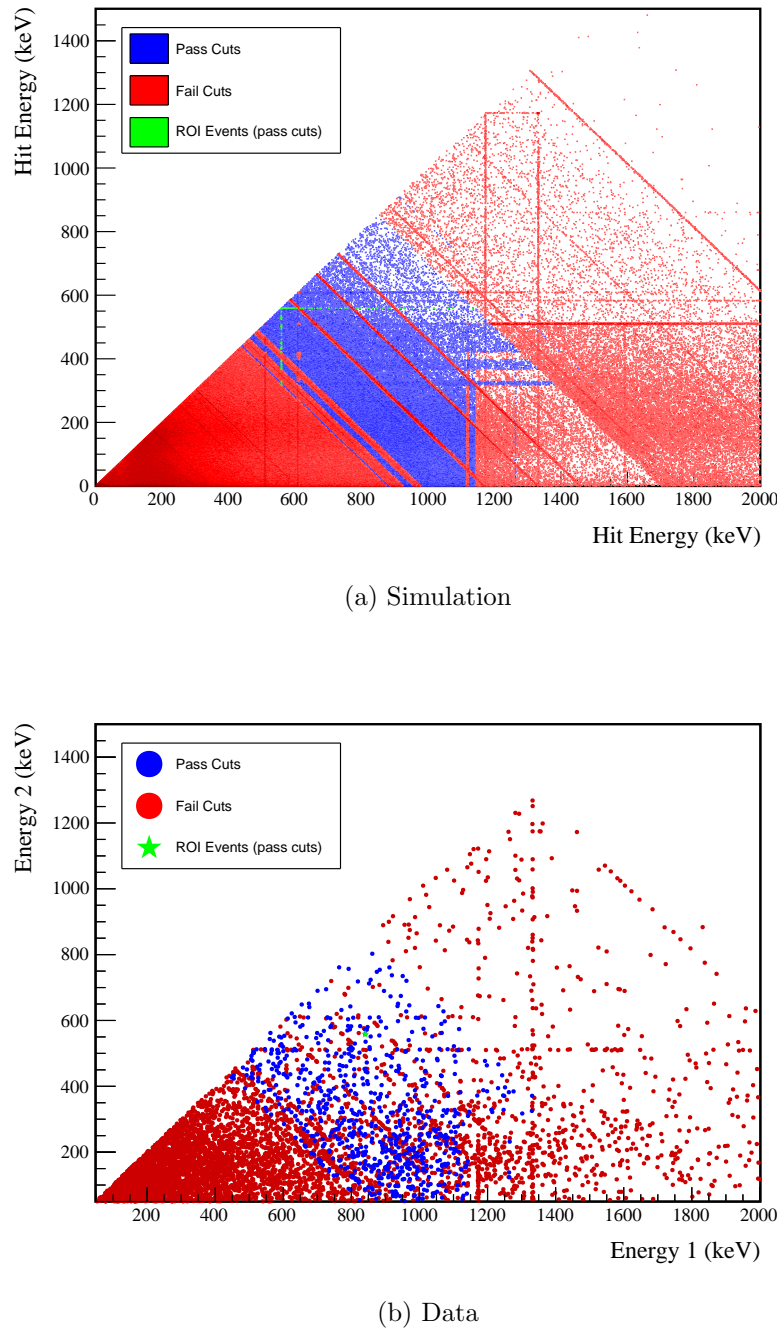
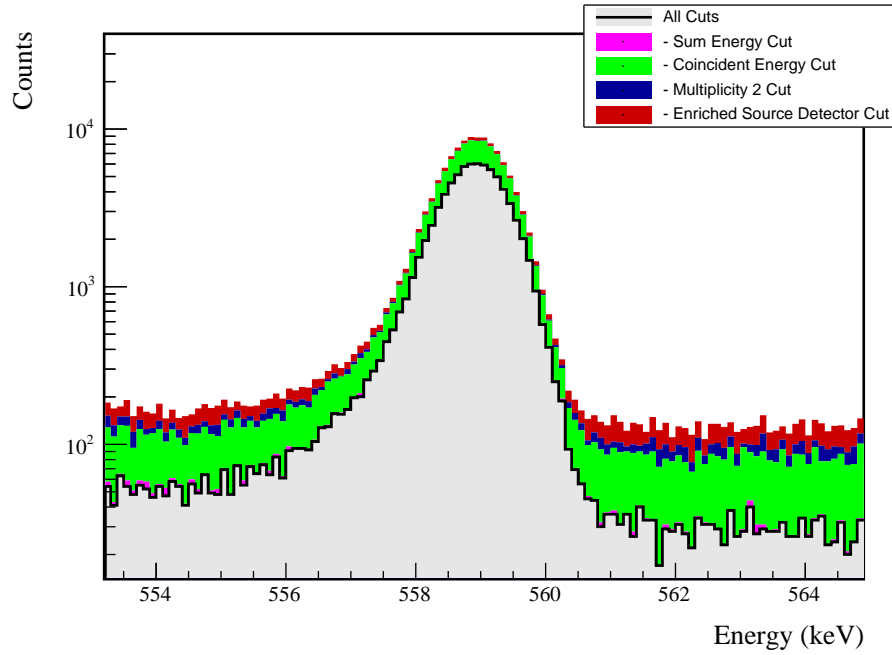


Figure A.12: Simulated and measured multiplicity 2 energy spectrum with sum and coincident energy cuts included for the 559 keV peak.



(a) Effect of all cuts on ROI

Source	Module 1 efficiency	Module 2 efficiency
Multi-Detector with Full Energy γ	$2.9 \pm 0.2\%$	$1.5 \pm 0.5\%$
Region of Interest	$87.4 \pm 2.0\%$	$87.4 \pm 2.0\%$
Dead Layer	$71.5 \pm 4.9\%$	$60.2 \pm 7.0\%$
Detector Dead Times	$98.3 \pm 0.8\%$	$98.6 \pm 0.7\%$
Enriched Source Detector Cut	$97.5 \pm <0.1\%$	$94.1 \pm <0.1\%$
Multiplicity 2 Cut	$99.5 \pm <0.1\%$	$99.7 \pm <0.1\%$
Coincident Energy Cut	$72.3 \pm 0.5\%$	$71.6 \pm 0.5\%$
Sum Energy Cut	$71.4 \pm 0.5\%$	$69.1 \pm 0.5\%$
Final Efficiency	$1.35 \pm 0.14\%$	$0.58 \pm 0.19\%$

(b) Table of efficiencies

Figure A.13: Plot showing effect of cuts applied sequentially on ROI peak and table of detection efficiencies for the 559 keV peak.

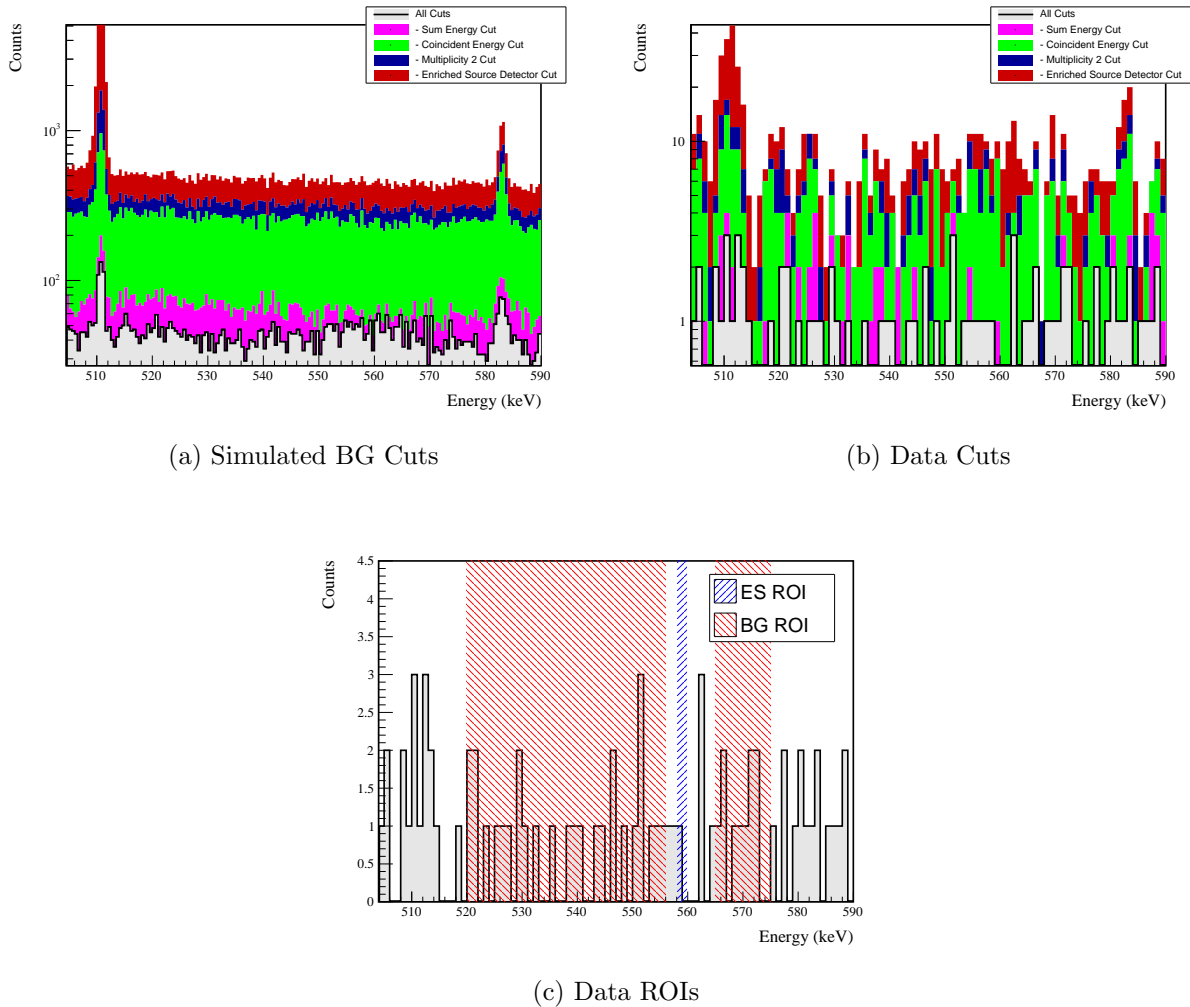


Figure A.14: Effect of all cuts applied to measured and simulated background data.

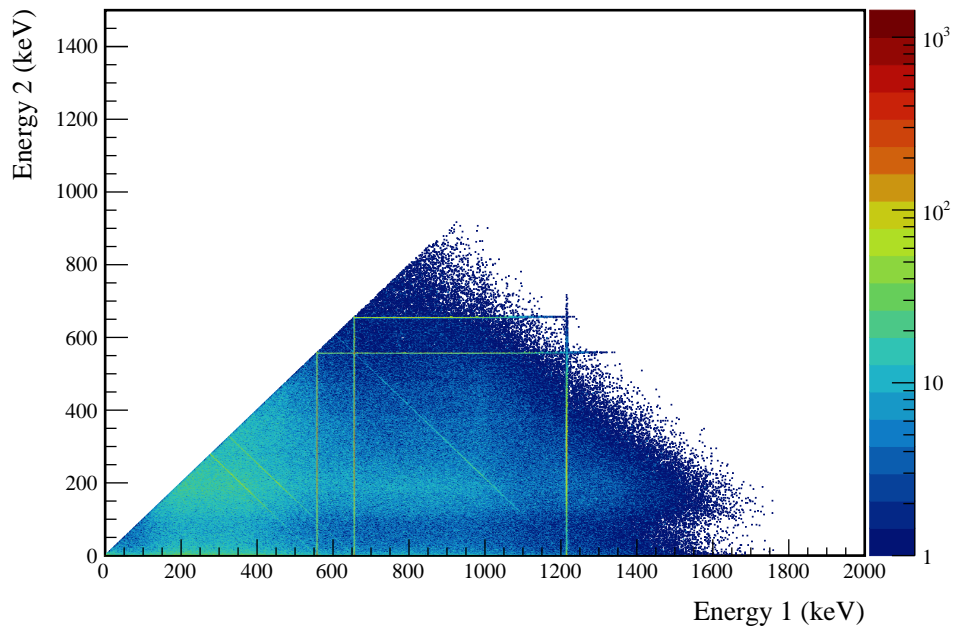
A.4 $2\nu\beta\beta$ to 2_2^+ 

Figure A.15: Simulated multiplicity 2 energy spectrum of the $2\nu\beta\beta$ to 2_2^+ decay mode

A.4.1 559 keV peak

Table A.7: Table of energy estimation uncertainties for the 559 keV peak.

DS	E_{peak} (keV)	σ_{fit} (keV)	σ_{drift} (keV)	σ (keV)	$f_{i,fit}$	$f_{i,drift}$	τ_{fit} (keV)	$\delta_{\mu,NL}$ (keV)	$\delta_{\mu,fit}$ (keV)	$\delta_{\mu,drift}$ (keV)	δ_{peak} (keV)	δ_μ (keV)	FWHM	$\delta_{fwhm,fit}$ (keV)	$\delta_{fwhm,drift}$ (keV)	$\delta_{fwhm,peak}$ (keV)	δ_{FWHM} (keV)	δ_α	$E_{ROI,1}$ (keV)	$E_{ROI,2}$ (keV)	ϵ_{ROI}	$\sigma_{e_{ROI}}$
DS1	559.101	0.460	0.063	0.464	0.230	0.515	0.001	0.104	0.002	0.012	0.005	0.105	1.152	0.001	0.039	0.011	0.040	0.035	558.243	559.812	0.854	0.016
DS2	559.101	0.461	0.055	0.464	0.249	0.515	0.002	0.067	0.004	0.012	0.005	0.068	1.158	0.001	0.107	0.011	0.108	0.093	558.231	559.810	0.857	0.033
DS3	559.101	0.470	0.066	0.474	0.224	0.505	0.001	0.026	0.024	0.012	0.005	0.038	1.174	0.001	0.073	0.011	0.074	0.063	558.231	559.827	0.862	0.022
DS4	559.101	0.455	0.077	0.461	0.108	0.445	0.002	0.076	0.010	0.012	0.005	0.078	1.111	0.001	0.106	0.011	0.107	0.096	558.321	559.821	0.871	0.035
DS5a	559.101	0.560	0.085	0.567	0.106	0.855	0.002	0.079	0.005	0.012	0.005	0.080	1.367	0.002	0.055	0.011	0.056	0.041	558.145	559.981	0.859	0.015
DS5b	559.101	0.469	0.074	0.475	0.158	0.491	0.001	0.020	0.011	0.012	0.005	0.026	1.157	0.001	0.125	0.011	0.125	0.108	558.270	559.836	0.869	0.038
DS5c	559.101	0.460	0.085	0.468	0.174	0.489	0.001	0.037	0.030	0.012	0.005	0.050	1.145	0.001	0.162	0.011	0.162	0.142	558.273	559.824	0.866	0.050
DS6a	559.101	0.456	0.044	0.458	0.191	0.463	0.001	0.069	0.025	0.012	0.005	0.075	1.123	0.000	0.041	0.011	0.042	0.038	558.282	559.806	0.864	0.015

A.4. $2\nu\beta\beta$ TO 2_2^+

25

Cut Name	Cut Description	$\langle \epsilon_{total} \rangle$	$\hat{\epsilon}_{total}$	$\langle \epsilon_{unique} \rangle$	$\hat{\epsilon}_{unique}$	Sacrifice	ΔDP
Enriched Source	Any other detector: isEnv	M1: 21.5 %	$23.0^{+2.7}_{-2.5}$ %	6.1 %	$6.0^{+1.6}_{-1.3}$ %	1.8 %	10%
Detector Cut	No other detector: (((energy<41.) (energy>509.8 && energy<512.2) (energy>608.2 && energy<612.6) (energy>1203. && energy<1208.4) (energy>1307.4) && isEnv) (((energy<40.4) (energy>509. && energy<513.2) (energy>604. && energy<610.) (energy>894.8)) && !isEnv)	M2: 40.6 %	$63.8^{+6.0}_{-6.5}$ %	11.9 %	$17.2^{+5.5}_{-4.4}$ %	5.0 %	
Coincident		M1: 19.2 %	$20.8^{+2.6}_{-2.4}$ %	3.5 %	$2.3^{+1.1}_{-0.8}$ %	2.9 %	
Energy Cut		M2: 21.2 %	$32.8^{+6.4}_{-5.8}$ %	3.2 %	$5.2^{+3.7}_{-2.2}$ %	2.3 %	2%
	Not: (sumE<810.) (sumE>908.2 && sumE<912.4) (sumE>967.6 && sumE<970.) (sumE>1168.8 && sumE<1174.6) (sumE>1330.4 && sumE<1333.6) (sumE>1459.4 && sumE<1461.8) (sumE>1761.8 && sumE<1767.2) (sumE>1906.)	M1: 61.2 %	61.5 ± 3.0 %	36.0 %	$35.5^{+3.0}_{-2.9}$ %	16.4 %	18%
Sum Energy Cut		M2: 62.3 %	$56.9^{+6.3}_{-6.6}$ %	27.0 %	$17.2^{+5.5}_{-4.4}$ %	17.2 %	
Combined Cuts		M1: 72.1 %	$71.3^{+2.7}_{-2.9}$ %	—	—	26.1 %	32%
		M2: 79.9 %	$86.2^{+3.9}_{-5.1}$ %	—	—	34.4 %	

Table A.8: Table of cut descriptions and efficiencies for simulated backgrounds and measured data for the 559 keV peak.

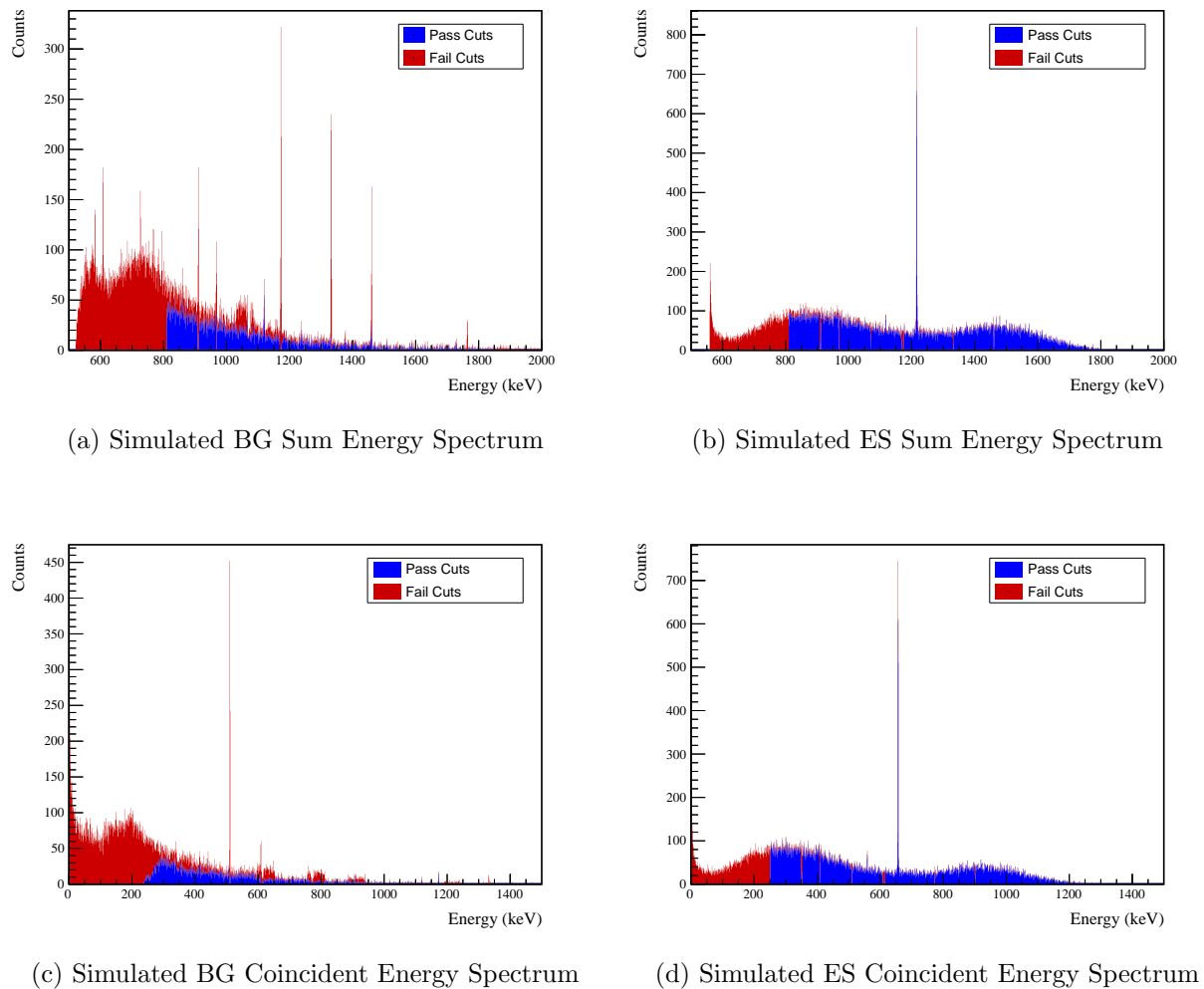
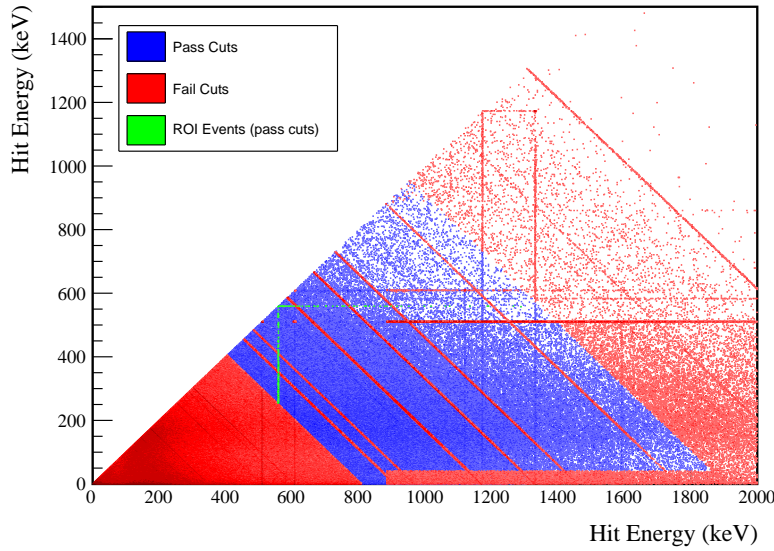
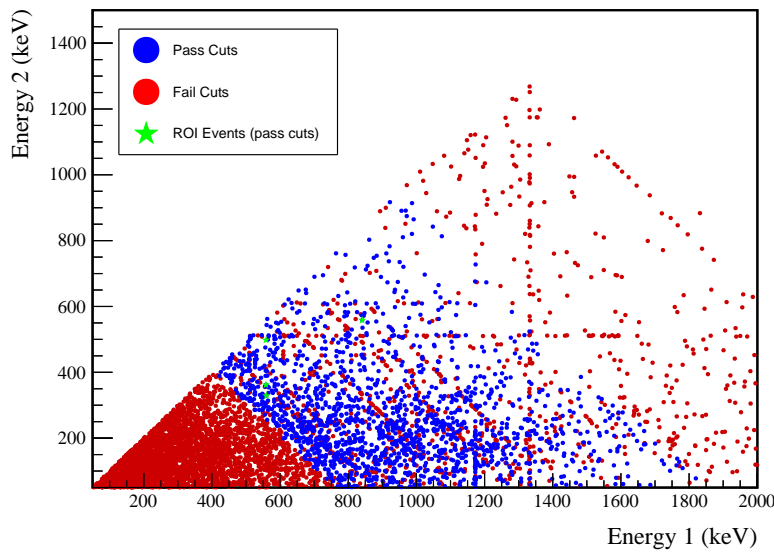


Figure A.16: Sum energy and coincident energy spectra for the 559 keV peak.

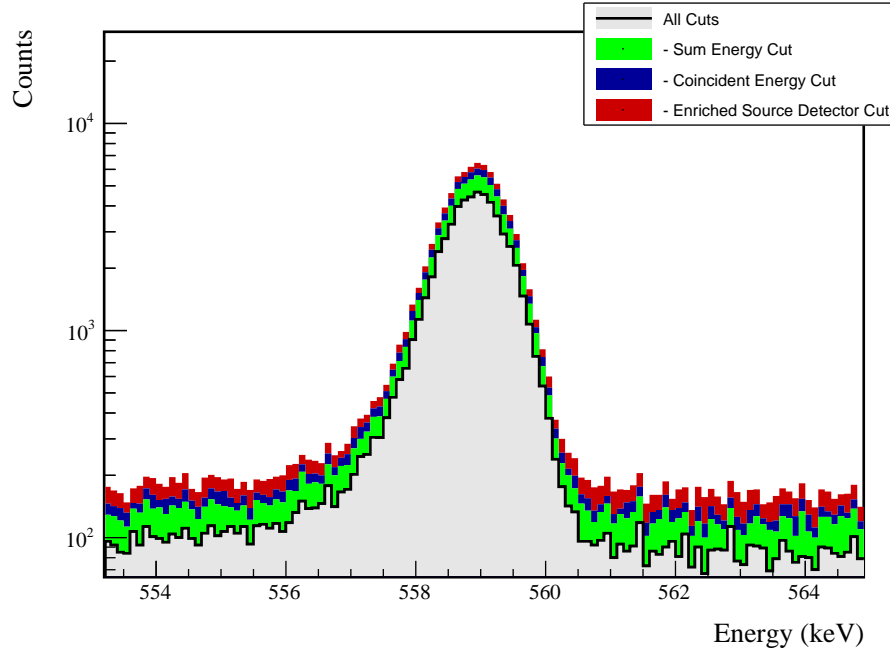


(a) Simulation



(b) Data

Figure A.17: Simulated and measured multiplicity 2 energy spectrum with sum and coincident energy cuts included for the 559 keV peak.



(a) Effect of all cuts on ROI

Source	Module 1 efficiency	Module 2 efficiency
Multi-Detector with Full Energy γ	$1.9 \pm 0.2\%$	$1.1 \pm 0.5\%$
Region of Interest	$86.2 \pm 2.1\%$	$86.2 \pm 2.1\%$
Dead Layer	$75.5 \pm 4.2\%$	$65.5 \pm 6.0\%$
Detector Dead Times	$98.4 \pm 0.8\%$	$98.6 \pm 0.7\%$
Enriched Source Detector Cut	$96.7 \pm <0.1\%$	$90.2 \pm <0.1\%$
Coincident Energy Cut	$93.0 \pm 0.5\%$	$91.2 \pm 0.5\%$
Sum Energy Cut	$78.9 \pm 0.5\%$	$73.4 \pm 0.5\%$
Final Efficiency	$0.98 \pm 0.12\%$	$0.44 \pm 0.20\%$

(b) Table of efficiencies

Figure A.18: Plot showing effect of cuts applied sequentially on ROI peak and table of detection efficiencies for the 559 keV peak.

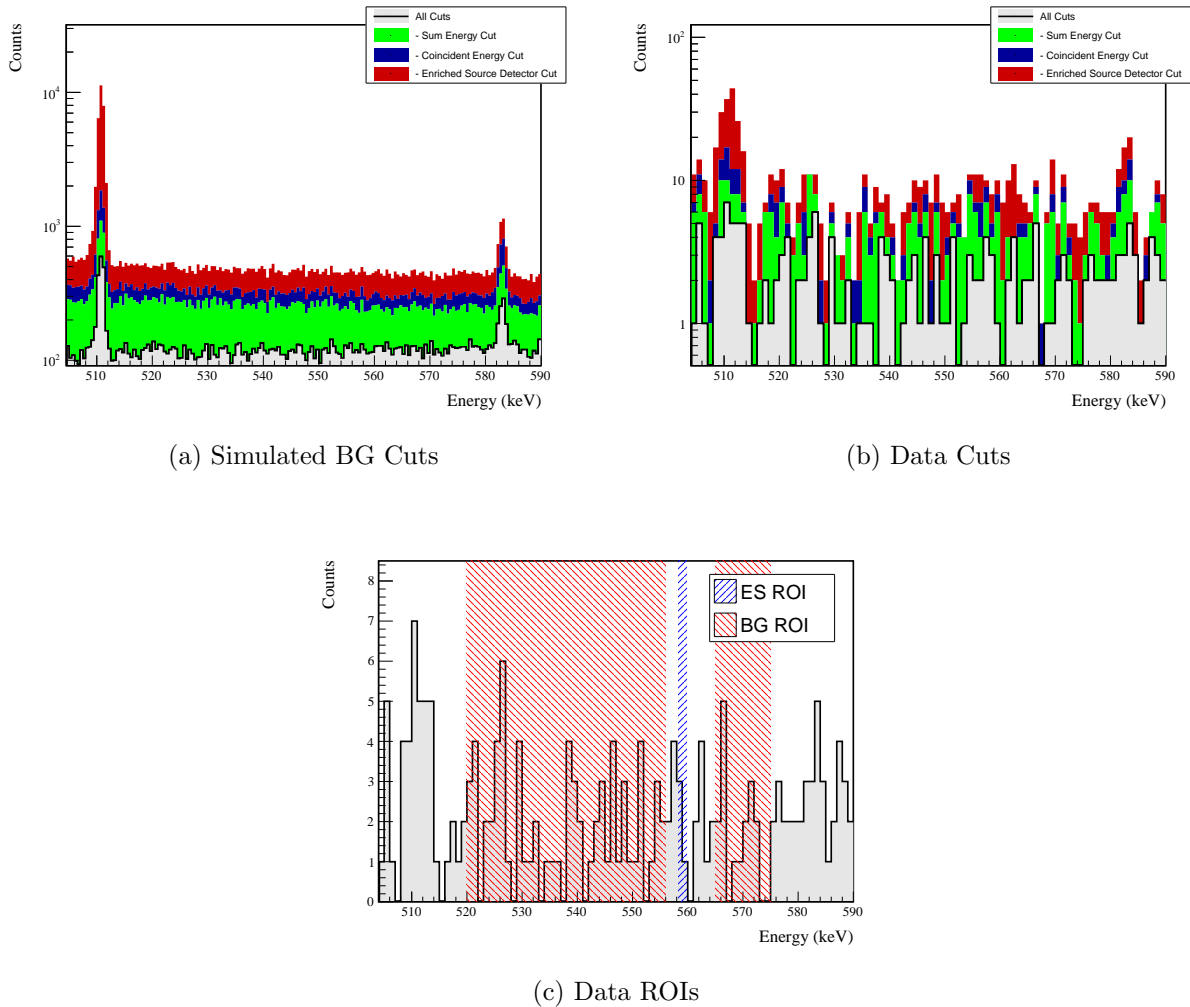
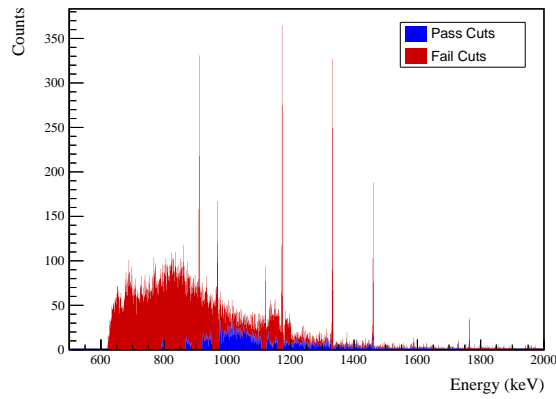
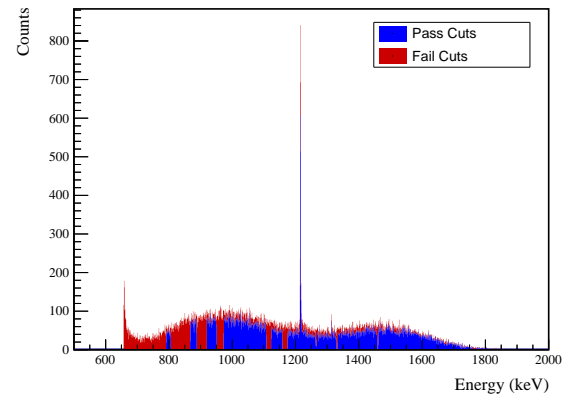


Figure A.19: Effect of all cuts applied to measured and simulated background data.

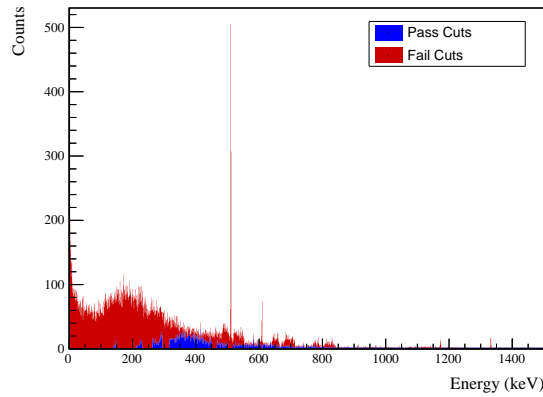
A.4.2 657 keV peak



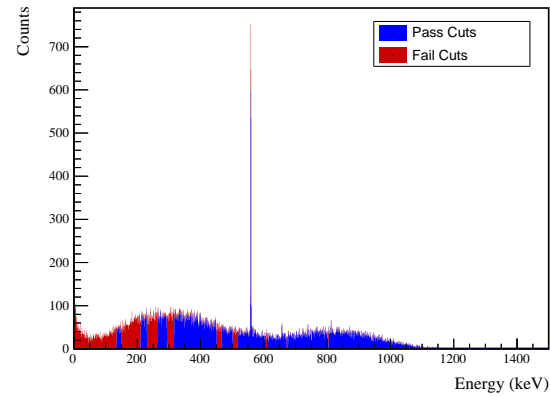
(a) Simulated BG Sum Energy Spectrum



(b) Simulated ES Sum Energy Spectrum



(c) Simulated BG Coincident Energy Spectrum

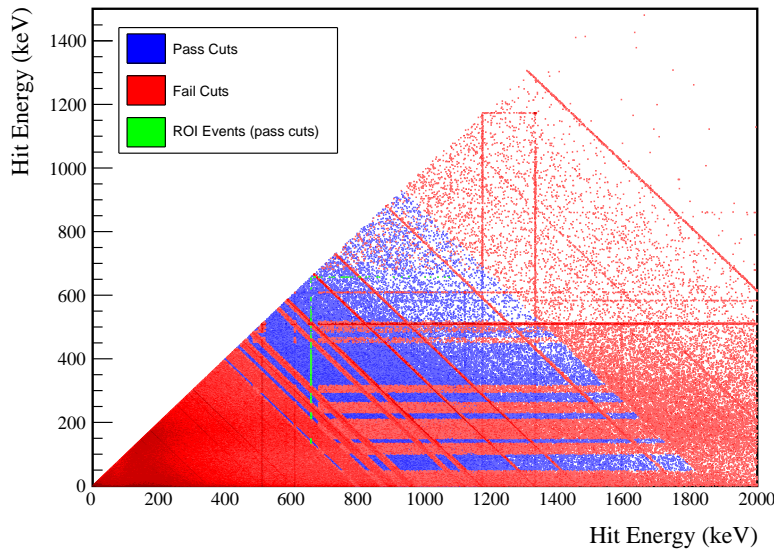


(d) Simulated ES Coincident Energy Spectrum

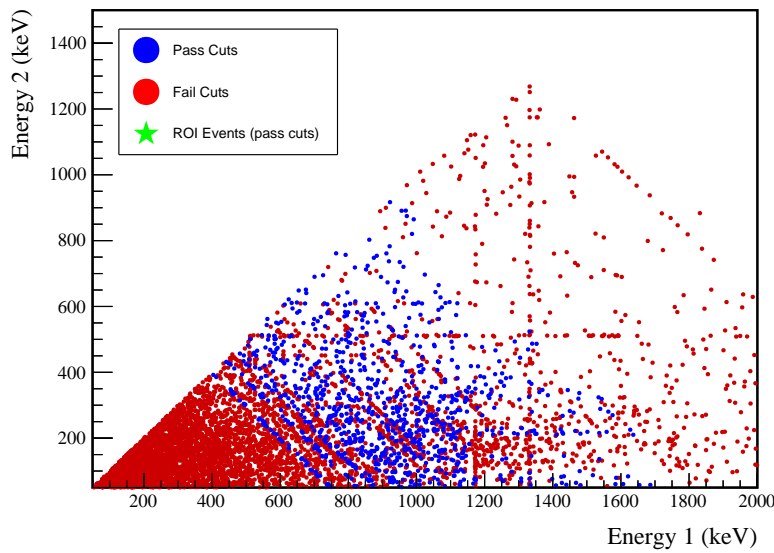
Figure A.20: Sum energy and coincident energy spectra for the 657 keV peak.

Table A.9: Table of energy estimation uncertainties for the 657 keV peak.

DS	E_{peak} (keV)	σ_{fit} (keV)	σ_{drift} (keV)	σ (keV)	$f_{i,fit}$	$f_{i,drift}$	τ_{fit} (keV)	$\delta_{\mu,NL}$ (keV)	$\delta_{\mu,drift}$ (keV)	$\delta_{\mu,peak}$ (keV)	δ_μ (keV)	FWHM	$\delta_{fwhm,fit}$ (keV)	$\delta_{fwhm,drift}$ (keV)	$\delta_{fwhm,peak}$ (keV)	$E_{ROI,1}$ (keV)	$E_{ROI,2}$ (keV)	ϵ_{ROI}	$\sigma_{e_{ROI}}$			
DS1	657.041	0.500	0.074	0.505	0.230	0.579	0.002	0.104	0.003	0.012	0.005	0.105	1.256	0.001	0.039	0.011	0.040	0.032	656.067	657.845	0.867	0.014
DS2	657.041	0.502	0.064	0.506	0.249	0.580	0.002	0.067	0.005	0.012	0.005	0.068	1.263	0.001	0.107	0.011	0.108	0.085	656.052	657.843	0.869	0.028
DS3	657.041	0.510	0.078	0.516	0.224	0.568	0.002	0.026	0.028	0.012	0.005	0.040	1.278	0.001	0.073	0.011	0.074	0.058	656.056	657.862	0.874	0.019
DS4	657.041	0.493	0.090	0.501	0.108	0.490	0.002	0.076	0.012	0.012	0.005	0.078	1.207	0.001	0.106	0.011	0.107	0.088	656.161	657.852	0.884	0.030
DS5a	657.041	0.606	0.100	0.614	0.106	0.924	0.002	0.079	0.006	0.012	0.005	0.080	1.481	0.002	0.055	0.011	0.056	0.038	655.966	658.029	0.872	0.013
DS5b	657.041	0.509	0.087	0.517	0.158	0.562	0.001	0.020	0.013	0.012	0.005	0.027	1.259	0.001	0.125	0.011	0.125	0.100	656.101	657.871	0.880	0.033
DS5c	657.041	0.500	0.100	0.510	0.174	0.555	0.002	0.037	0.035	0.012	0.005	0.053	1.247	0.001	0.162	0.011	0.162	0.130	656.102	657.859	0.878	0.043
DS6a	657.041	0.495	0.051	0.497	0.191	0.524	0.001	0.069	0.030	0.012	0.005	0.076	1.221	0.001	0.041	0.011	0.042	0.035	656.115	657.837	0.876	0.013

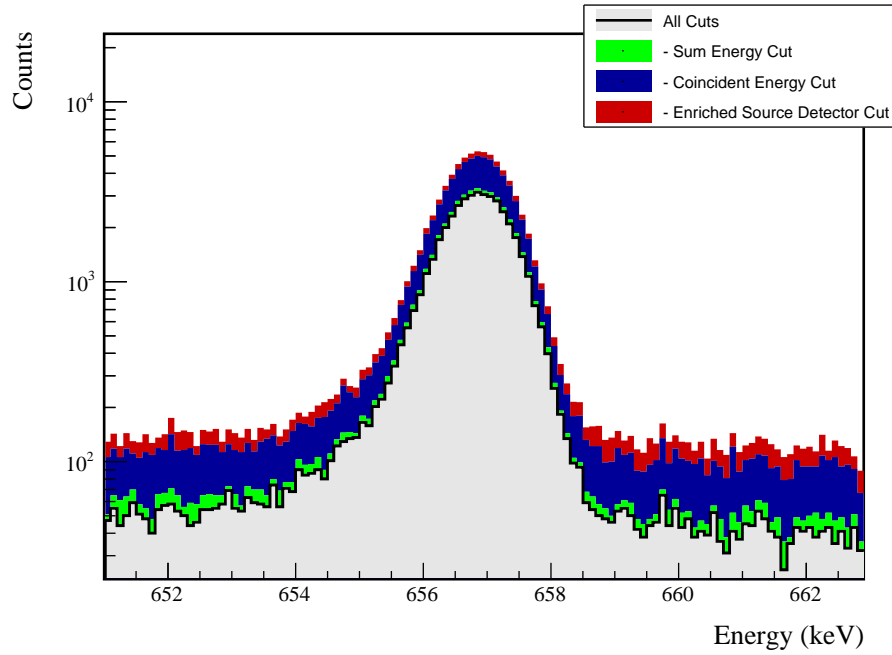


(a) Simulation



(b) Data

Figure A.21: Simulated and measured multiplicity 2 energy spectrum with sum and coincident energy cuts included for the 657 keV peak.



(a) Effect of all cuts on ROI

Source	Module 1 efficiency	Module 2 efficiency
Multi-Detector with Full Energy γ	$1.8 \pm 0.2\%$	$1.0 \pm 0.5\%$
Region of Interest	$87.5 \pm 1.8\%$	$87.5 \pm 1.8\%$
Dead Layer	$76.0 \pm 4.1\%$	$64.8 \pm 6.2\%$
Detector Dead Times	$98.5 \pm 0.7\%$	$98.7 \pm 0.6\%$
Enriched Source Detector Cut	$96.8 \pm <0.1\%$	$89.8 \pm <0.1\%$
Coincident Energy Cut	$66.2 \pm 0.5\%$	$68.6 \pm 0.5\%$
Sum Energy Cut	$74.6 \pm 0.5\%$	$69.4 \pm 0.5\%$
Final Efficiency	$0.75 \pm 0.10\%$	$0.34 \pm 0.17\%$

(b) Table of efficiencies

Figure A.22: Plot showing effect of cuts applied sequentially on ROI peak and table of detection efficiencies for the 657 keV peak.

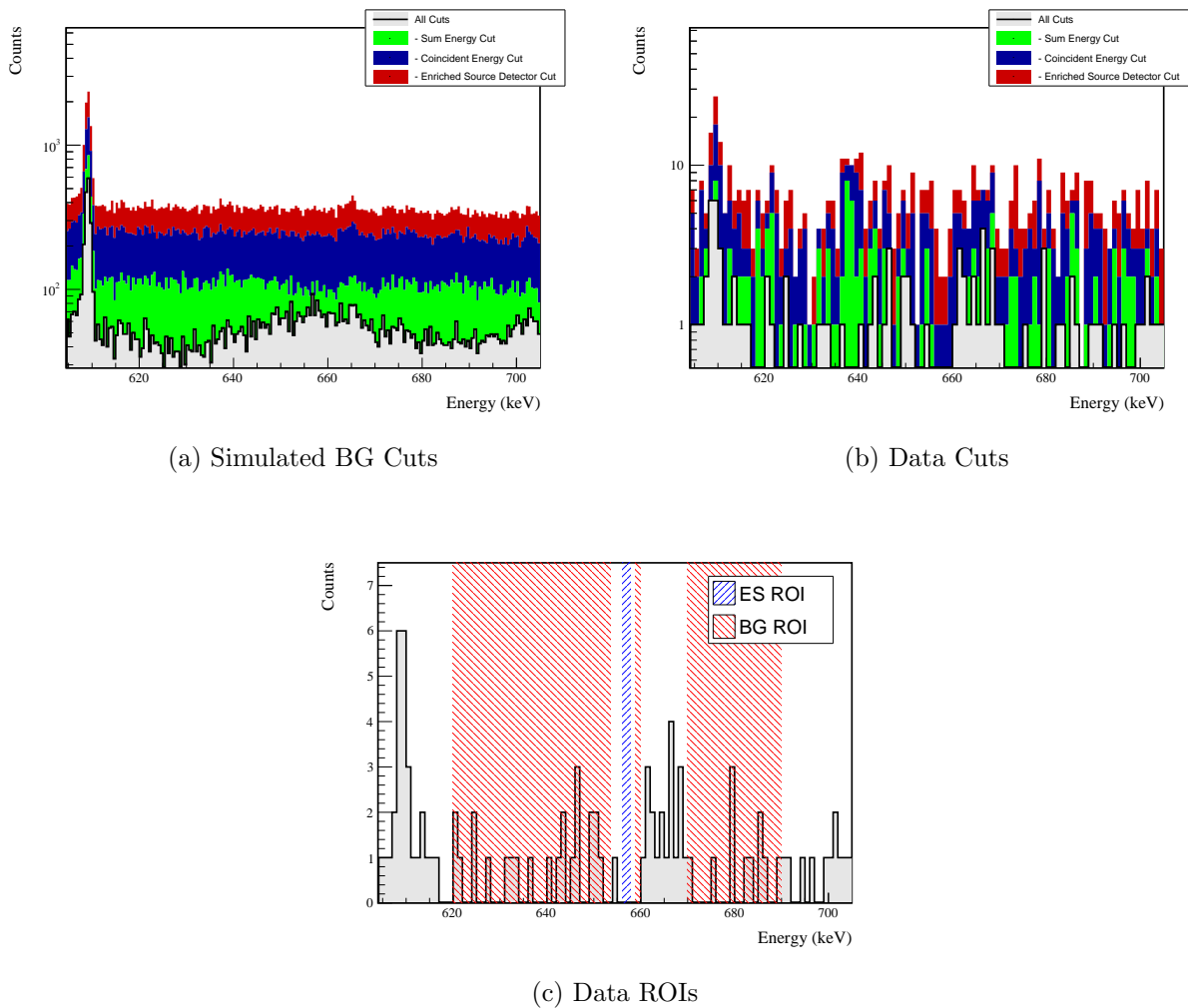


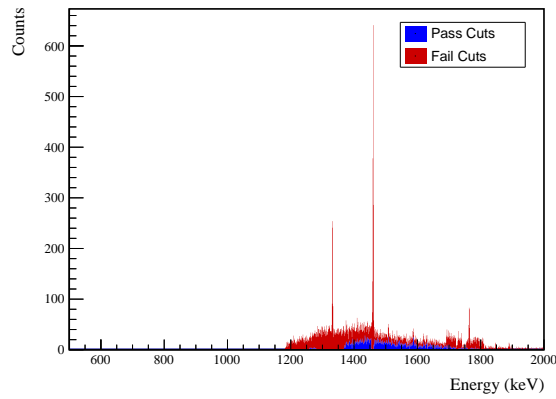
Figure A.23: Effect of all cuts applied to measured and simulated background data.

A.4. $2\nu\beta\beta$ TO 2_2^+

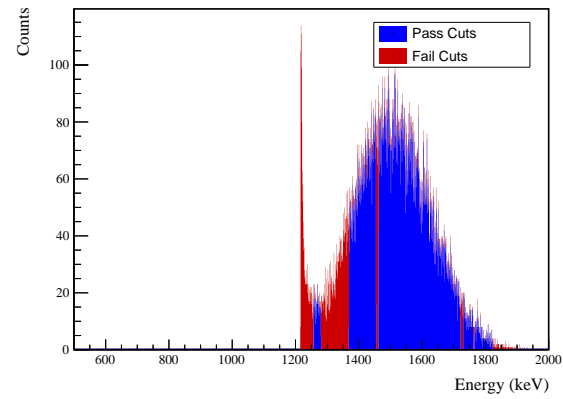
Cut Name	Cut Description	$\langle \epsilon_{total} \rangle$	$\hat{\epsilon}_{total}$	$\langle \epsilon_{unique} \rangle$	$\hat{\epsilon}_{unique}$	Sacrifice	ΔDP
Enriched Source		M1: 22.2 %	$23.4^{+2.9}_{-2.7}\%$	6.1 %	$5.2^{+1.7}_{-1.3}\%$	1.4 %	
Detector Cut	Any other detector: isEnr	M2: 41.6 %	$59.7^{+5.6}_{-5.9}\%$	11.8 %	$15.3^{+4.7}_{-3.8}\%$	4.5 %	17%
No other detector:	(((energy<48.) (energy>100.4 && energy<134.4) (energy>148.8 && energy>209.8) (energy>230.8 && energy<262.8) (energy>294.4 && energy<316.4) (energy>316.4 && energy<450.8 && energy<466.6) (energy>502.2 && energy<517.2) (energy>606.4 && energy<610.4) (energy>1156.8) && isEnr) (energy<41.6) (energy>483.2 && energy<520.2) (energy>679.8) && !isEnr)						
Coincident		M1: 48.2 %	$50.6 \pm 3.3\%$	14.7 %	$19.9^{+2.8}_{-2.5}\%$	12.3 %	
Energy Cut		M2: 43.9 %	$38.9^{+5.9}_{-5.6}\%$	11.7 %	$9.7^{+4.1}_{-3.0}\%$	7.2 %	15%
Sum Energy Cut	Not: (sumE<791.6) (sumE>806.2 && sumE<867.6) (sumE>887.6 && sumE<920.) (sumE>950.8 && sumE<973.4) (sumE>1108. && sumE<1123.2) (sumE>1158.6 && sumE<1174.8) (sumE>1328.8 && sumE<1333.6) (sumE>1458.6 && sumE<1461.8) (sumE>1760. && sumE<1771.8) (sumE>1863.6)	M1: 62.0 %	$60.2 \pm 3.3\%$	20.2 %	$20.8^{+2.8}_{-2.5}\%$	3.5 %	34%
Combined Cuts		M1: 84.8 %	$87.0^{+2.1}_{-2.4}\%$	—	—	39.7 %	36%
		M2: 88.7 %	$95.8^{+1.8}_{-3.0}\%$	—	—	43.3 %	

Table A.10: Table of cut descriptions and efficiencies for simulated backgrounds and measured data for the 657 keV peak.

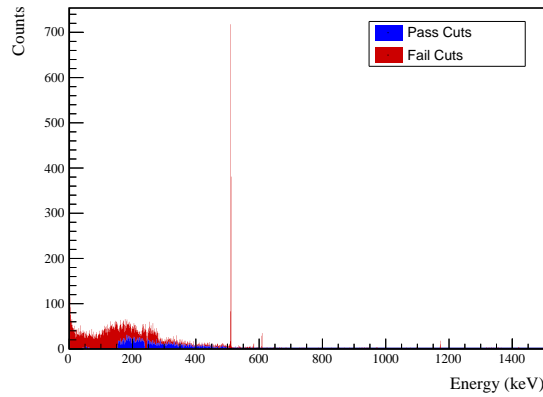
A.4.3 1216 keV peak



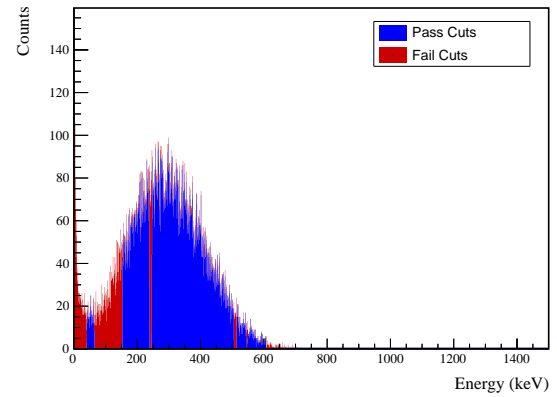
(a) Simulated BG Sum Energy Spectrum



(b) Simulated ES Sum Energy Spectrum



(c) Simulated BG Coincident Energy Spectrum



(d) Simulated ES Coincident Energy Spectrum

Figure A.24: Sum energy and coincident energy spectra for the 1216 keV peak.

Table A.11: Table of energy estimation uncertainties for the 1216 keV peak.

DS	E_{peak} (keV)	$\sigma_{t_{fit}}$ (keV)	$\sigma_{\mu, drift}$ (keV)	σ (keV)	$f_{t, fit}$ (keV)	τ_{fit} (keV)	$\delta_{t_{fit}}$ (keV)	$\delta_{\mu,NL}$ (keV)	$\delta_{\mu,drift}$ (keV)	$\delta_{t_{peak}}$ (keV)	$\delta_{\mu,peak}$ (keV)	δ_μ (keV)	FWHM (keV)	$\delta_{fwhm, fit}$ (keV)	$\delta_{fwhm,drift}$ (keV)	$\delta_{fwhm,x talk}$ (keV)	δ_{FWHM} (keV)	δ_α	$E_{ROI,1}$ (keV)	$E_{ROI,2}$ (keV)	ϵ_{ROI}	$\sigma_{\epsilon_{ROI}}$
DS1	1216.104	0.705	0.137	0.718	0.230	0.945	0.003	0.104	0.005	0.012	0.020	0.107	1.787	0.001	0.039	0.011	0.040	0.023	1214.713	1217.245	0.862	0.009
DS2	1216.104	0.710	0.119	0.720	0.249	0.951	0.003	0.067	0.008	0.012	0.020	0.072	1.803	0.001	0.107	0.011	0.108	0.060	1214.686	1217.245	0.862	0.020
DS3	1216.104	0.715	0.144	0.729	0.224	0.925	0.003	0.026	0.051	0.012	0.020	0.062	1.812	0.001	0.073	0.011	0.074	0.041	1214.702	1217.263	0.867	0.014
DS4	1216.104	0.697	0.167	0.717	0.108	0.746	0.003	0.076	0.022	0.012	0.020	0.083	1.726	0.001	0.106	0.011	0.107	0.062	1214.847	1217.261	0.884	0.021
DS5a	1216.104	0.838	0.185	0.859	0.106	1.316	0.004	0.079	0.012	0.012	0.020	0.083	2.070	0.002	0.055	0.011	0.056	0.027	1214.604	1217.483	0.872	0.009
DS5b	1216.104	0.716	0.161	0.734	0.158	0.963	0.002	0.020	0.024	0.012	0.020	0.039	1.791	0.001	0.125	0.011	0.125	0.070	1214.764	1217.282	0.873	0.023
DS5c	1216.104	0.703	0.185	0.727	0.174	0.932	0.003	0.037	0.066	0.012	0.020	0.079	1.783	0.001	0.162	0.011	0.162	0.091	1214.759	1217.269	0.871	0.030
DS6a	1216.104	0.693	0.095	0.700	0.191	0.873	0.002	0.069	0.055	0.012	0.020	0.092	1.723	0.001	0.041	0.011	0.042	0.025	1214.792	1217.224	0.870	0.009

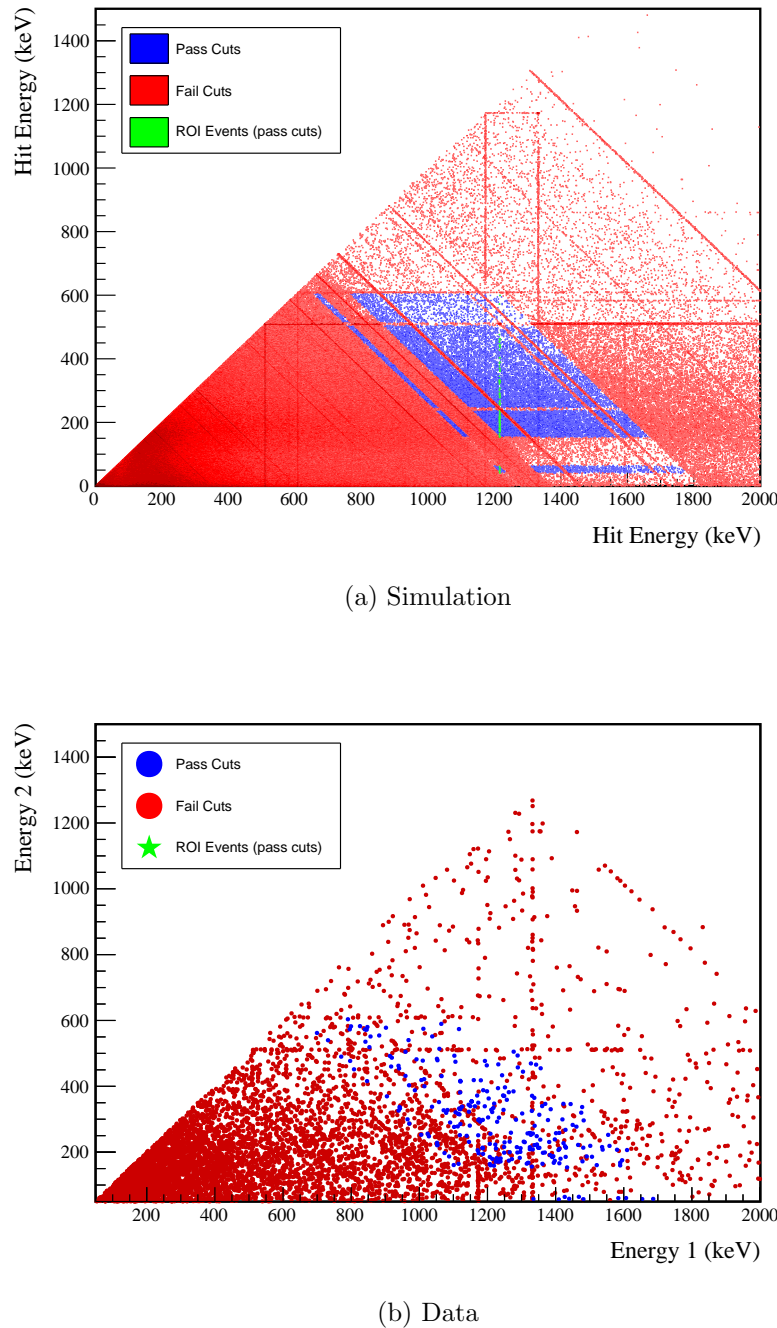
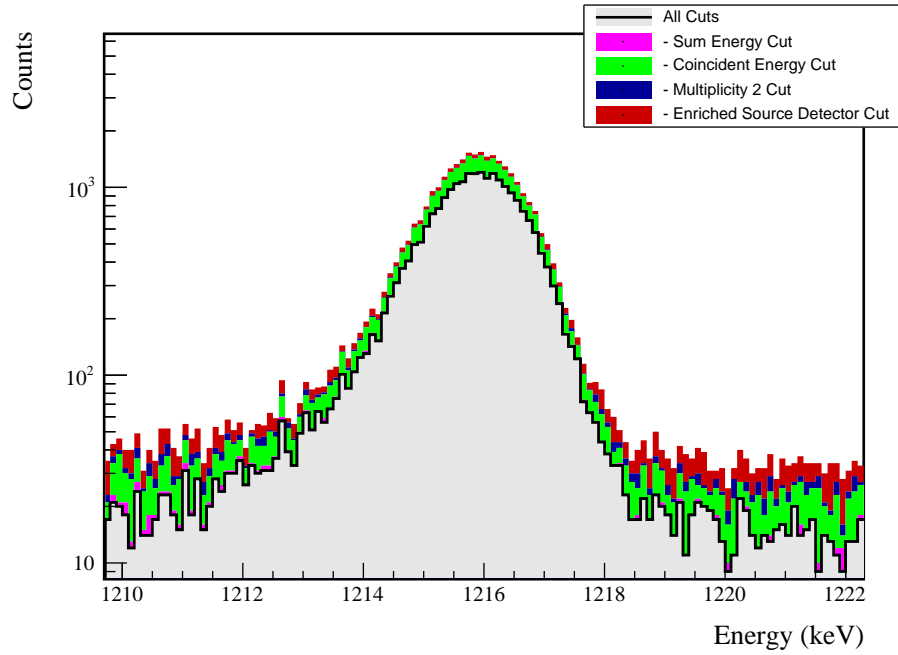


Figure A.25: Simulated and measured multiplicity 2 energy spectrum with sum and coincident energy cuts included for the 1216 keV peak.



(a) Effect of all cuts on ROI

Source	Module 1 efficiency	Module 2 efficiency
Multi-Detector with Full Energy γ	$0.8 \pm 0.2\%$	$0.4 \pm 0.5\%$
Region of Interest	$87.0 \pm 1.3\%$	$87.0 \pm 1.3\%$
Dead Layer	$73.7 \pm 4.5\%$	$61.8 \pm 6.7\%$
Detector Dead Times	$98.3 \pm 0.8\%$	$98.6 \pm 0.6\%$
Enriched Source Detector Cut	$97.3 \pm <0.1\%$	$93.3 \pm <0.1\%$
Multiplicity 2 Cut	$99.6 \pm <0.1\%$	$99.8 \pm <0.1\%$
Coincident Energy Cut	$82.7 \pm 0.5\%$	$82.5 \pm 0.5\%$
Sum Energy Cut	$82.0 \pm 0.5\%$	$80.5 \pm 0.5\%$
Final Efficiency	$0.41 \pm 0.11\%$	$0.17 \pm 0.21\%$

(b) Table of efficiencies

Figure A.26: Plot showing effect of cuts applied sequentially on ROI peak and table of detection efficiencies for the 1216 keV peak.

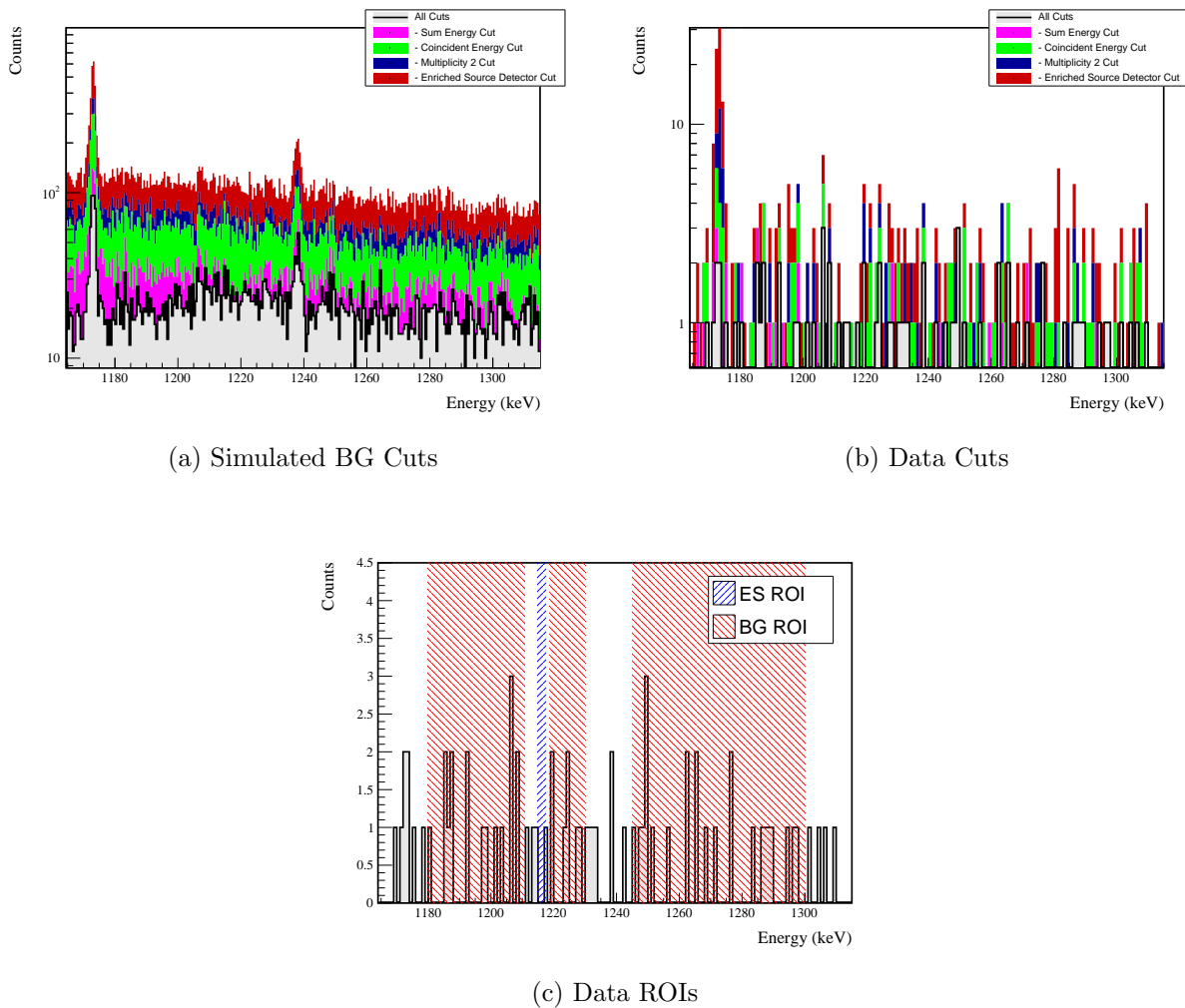


Figure A.27: Effect of all cuts applied to measured and simulated background data.

A.4. $2\nu\beta\beta$ TO 2_2^+

41

Cut Name	Cut Description	$\langle \epsilon_{total} \rangle$	$\hat{\epsilon}_{total}$	$\langle \epsilon_{unique} \rangle$	$\hat{\epsilon}_{unique}$	Sacrifice	ΔDP
Enriched Source	Any other detector: isEnr	M1: 25.2 %	24.7 $^{+3.5}_{-3.2}$ %	13.6 %	10.5 $^{+2.7}_{-2.2}$ %	2.1 %	23 %
Detector Cut		M2: 41.8 %	61.9 $^{+7.1}_{-7.7}$ %	23.7 %	33.3 $^{+7.6}_{-6.8}$ %	5.0 %	
Multiplicity 2		M1: 14.8 %	19.8 $^{+3.3}_{-2.9}$ %	3.5 %	2.5 $^{+1.5}_{-1.0}$ %	0.1 %	5 %
Cut	m==2	M2: 11.6 %	4.8 $^{+4.5}_{-2.4}$ %	3.0 %	0.0 $^{+2.3}_{-0.0}$ %	0.1 %	
Coincident	No other detector: ((energy<40.8) (energy>64.6 && energy<153.2) (energy>238.8 && energy<245.8) (energy>505.2 && energy<13.6) (energy>607.)) && isEnr)	M1: 36.0 %	39.5 $^{+3.9}_{-3.8}$ %	10.8 %	7.4 $^{+2.3}_{-1.8}$ %	0.2 %	16 %
Energy Cut		M2: 27.7 %	19.0 $^{+6.8}_{-5.3}$ %	9.4 %	7.1 $^{+5.0}_{-3.1}$ %	0.2 %	
Sum Energy Cut	Not: (sumE<1257.) (sumE>1281.8 && sumE<1368.4) (sumE>1454.2 && sumE<1462.6) (sumE>1721.6 && sumE<1730.2) (sumE>1761.8 && sumE<1766.) (sumE>1822.8)	M1: 44.2 %	47.5 \pm 3.9 %	11.4 %	7.4 $^{+2.3}_{-1.8}$ %	0.6 %	14 %
Combined Cuts		M2: 38.7 %	40.5 $^{+7.7}_{-7.3}$ %	6.7 %	0.0 $^{+2.3}_{-0.0}$ %	0.6 %	
		M1: 77.8 %	74.7 $^{+3.3}_{-3.6}$ %	—	—	20.7 %	48 %
		M2: 80.1 %	83.3 $^{+5.0}_{-6.5}$ %	—	—	24.9 %	

Table A.12: Table of cut descriptions and efficiencies for simulated backgrounds and measured data for the 1216 keV peak.

A.5 $0\nu\beta\beta$ **to** 0_1^+

Note that both the 559 and 563 keV peaks will be shown together since they use the same sets of cuts.

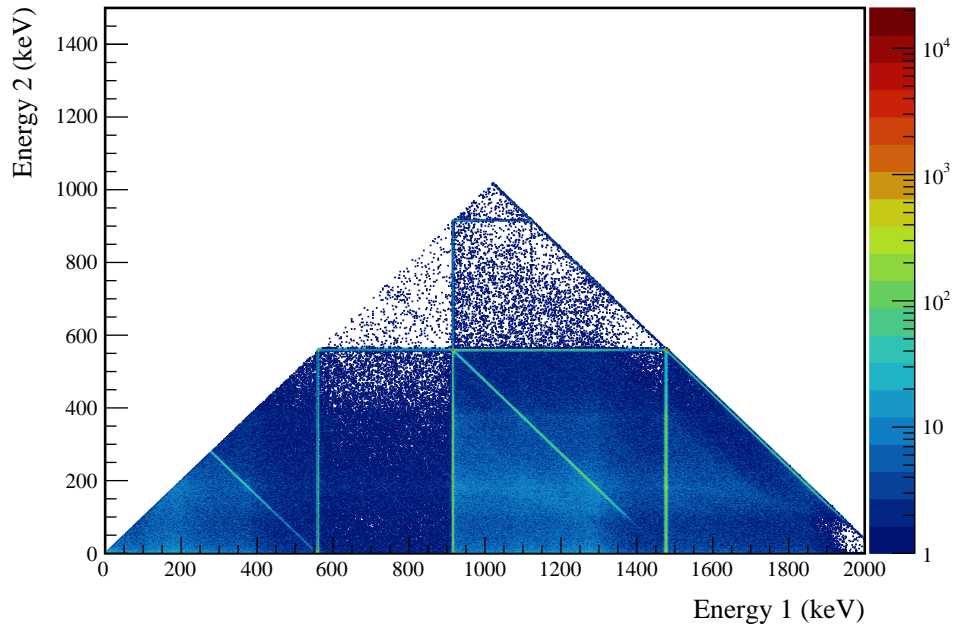


Figure A.28: Simulated multiplicity 2 energy spectrum of the $0\nu\beta\beta$ to 0_1^+ decay mode

Table A.13: Table of energy estimation uncertainties for the 559 and 563 keV peaks.

DS	E_{peak} (keV)	σ_{fit} (keV)	σ_{disfit} (keV)	σ (keV)	$f_{i,fit}$ (keV)	τ_{fit} (keV)	$\delta_{i,fit}$ (keV)	$\delta_{\mu,NL}$ (keV)	$\delta_{\mu,drift}$ (keV)	$\delta_{\mu,etalk}$ (keV)	$\delta_{\mu,peak}$ (keV)	δ_{μ} (keV)	FWHM (keV)	$\delta_{fwhm,fit}$ (keV)	$\delta_{fwhm,etalk}$ (keV)	$\delta_{fwhm,drift}$ (keV)	δ_{FWHM} (keV)	$\delta_{fwhm,ztalk}$ (keV)	$\delta_{FWHM,ztalk}$ (keV)	$E_{ROI,1}$ (keV)	$E_{ROI,2}$ (keV)	ϵ_{ROI}	$\sigma_{e,roi}$
DS1	559.101	0.460	0.063	0.464	0.230	0.515	0.001	0.104	0.002	0.012	0.005	0.105	1.152	0.001	0.039	0.011	0.040	0.035	558.141	559.892	0.891	0.014	
DS2	559.101	0.461	0.055	0.464	0.249	0.515	0.002	0.067	0.004	0.012	0.005	0.068	1.158	0.001	0.107	0.011	0.108	0.093	558.125	559.891	0.894	0.027	
DS3	559.101	0.470	0.066	0.474	0.224	0.505	0.001	0.026	0.024	0.012	0.005	0.038	1.174	0.001	0.073	0.011	0.074	0.063	558.128	559.909	0.898	0.019	
DS4	559.101	0.455	0.077	0.461	0.108	0.445	0.002	0.076	0.010	0.012	0.005	0.078	1.111	0.001	0.106	0.011	0.107	0.096	558.233	559.901	0.907	0.029	
DS5a	559.101	0.560	0.085	0.567	0.106	0.855	0.002	0.079	0.005	0.012	0.005	0.080	1.367	0.002	0.055	0.011	0.056	0.041	558.036	560.077	0.894	0.013	
DS5b	559.101	0.469	0.074	0.475	0.158	0.491	0.001	0.020	0.011	0.012	0.005	0.026	1.157	0.001	0.125	0.011	0.125	0.108	558.175	559.918	0.904	0.032	
DS5c	559.101	0.460	0.085	0.468	0.174	0.489	0.001	0.037	0.030	0.012	0.005	0.050	1.145	0.001	0.162	0.011	0.162	0.142	558.176	559.905	0.902	0.042	
DS6a	559.101	0.456	0.044	0.458	0.191	0.463	0.001	0.069	0.025	0.012	0.005	0.075	1.123	0.000	0.041	0.011	0.042	0.038	558.187	559.886	0.900	0.012	
DS1	563.178	0.461	0.064	0.466	0.230	0.518	0.001	0.104	0.002	0.012	0.005	0.105	1.156	0.001	0.039	0.011	0.040	0.035	562.214	563.972	0.891	0.013	
DS2	563.178	0.463	0.055	0.466	0.249	0.517	0.002	0.067	0.004	0.012	0.005	0.068	1.162	0.001	0.107	0.011	0.108	0.093	562.198	563.971	0.893	0.027	
DS3	563.178	0.471	0.066	0.476	0.224	0.508	0.001	0.026	0.024	0.012	0.005	0.038	1.179	0.001	0.073	0.011	0.074	0.063	562.202	563.989	0.898	0.019	
DS4	563.178	0.457	0.077	0.463	0.108	0.447	0.002	0.076	0.010	0.012	0.005	0.078	1.115	0.001	0.106	0.011	0.107	0.096	562.307	563.980	0.907	0.029	
DS5a	563.178	0.562	0.086	0.569	0.106	0.858	0.002	0.079	0.006	0.012	0.005	0.080	1.372	0.002	0.055	0.011	0.056	0.041	562.109	564.157	0.894	0.013	
DS5b	563.178	0.471	0.074	0.477	0.158	0.494	0.001	0.020	0.011	0.012	0.005	0.026	1.162	0.001	0.125	0.011	0.125	0.108	562.248	563.998	0.904	0.032	
DS5c	563.178	0.462	0.086	0.470	0.174	0.492	0.001	0.037	0.030	0.012	0.005	0.050	1.149	0.001	0.162	0.011	0.162	0.141	562.250	563.985	0.902	0.041	
DS6a	563.178	0.457	0.044	0.459	0.191	0.465	0.001	0.069	0.026	0.012	0.005	0.075	1.127	0.000	0.041	0.011	0.042	0.038	562.260	563.965	0.900	0.012	

Cut Name	Cut Description	$\langle \epsilon_{total} \rangle$	$\hat{\epsilon}_{total}$	$\langle \epsilon_{unique} \rangle$	$\hat{\epsilon}_{unique}$	Sacrifice	ΔDP
Enriched Source	Any other detector: !isEnr	M1: 21.5 %	23.3 ^{+2.7} _{-2.5} %	0.5 %	1.1 ^{+0.9} _{-0.5} %	1.2 %	12%
Detector Cut	No other detector: (((energy<51.) (energy>504.6 && energy<525.2) (energy>587.9 && energy<853.2) (energy>117.2 && energy<1121.8) (energy>1170.6 && energy<1175.6) (energy>1330.2 && energy<1337.) (energy>1483.,) && isEnr) ((energy<44.8) (energy>1385.6.) && !isEnr))	M2: 40.5 %	63.8 ^{+6.0} _{-6.5} %	0.9 %	6.9 ^{+4.1} _{-2.6} %	2.7 %	
Coincident		M1: 26.2 %	28.9 ^{+2.9} _{-2.7} %	0.7 %	1.5 ^{+0.9} _{-0.6} %	3.9 %	
Energy Cut		M2: 24.8 %	29.3 ^{+6.3} _{-5.6} %	0.5 %	6.9 ^{+4.1} _{-2.6} %	2.7 %	9%
Sum Energy Cut	Not: (sumE<1472.) (sumE>1760.4 && sumE<1765.8) (sumE>2042.8)	M1: 97.1 %	94.7 ^{+1.2} _{-1.5} %	54.1 %	51.5 ± 3.1 %	12.8 %	261%
Combined Cuts		M2: 97.6 %	84.5 ^{+4.2} _{-5.3} %	40.6 %	24.1 ^{+6.0} _{-5.2} %	16.4 %	
		M1: 98.3 %	97.7 ^{+0.7} _{-1.1} %	—	—	25.7 %	
		M2: 99.1 %	98.3 ^{+1.1} _{-2.7} %	—	—	35.8 %	317%

Table A.14: Table of cut descriptions and efficiencies for simulated backgrounds and measured data for the 559 and 563 keV peaks.

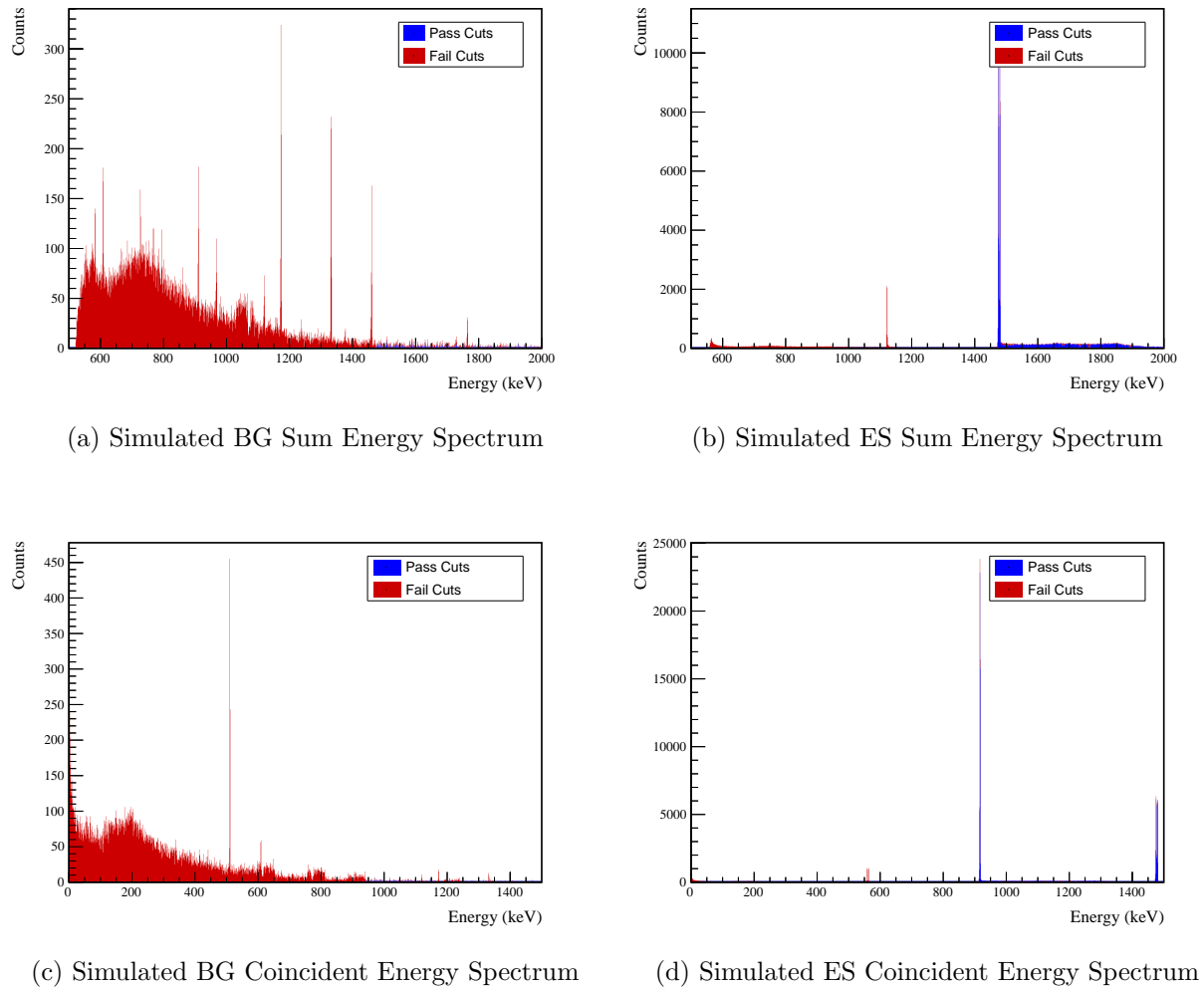
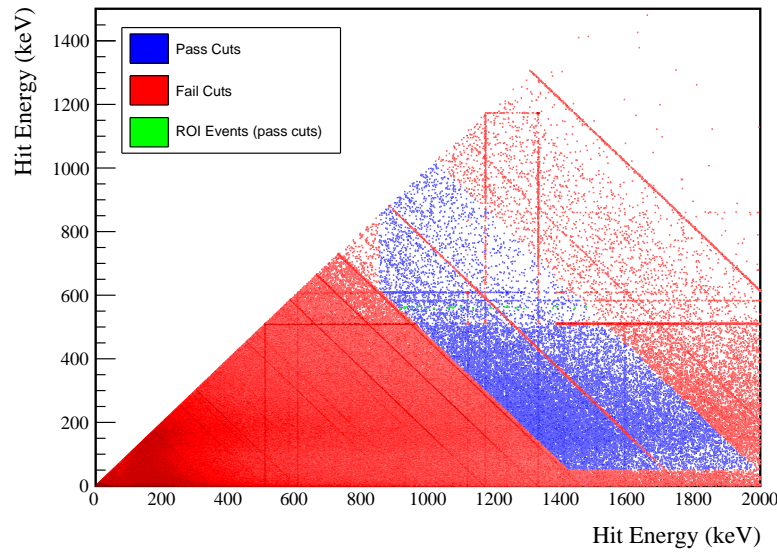
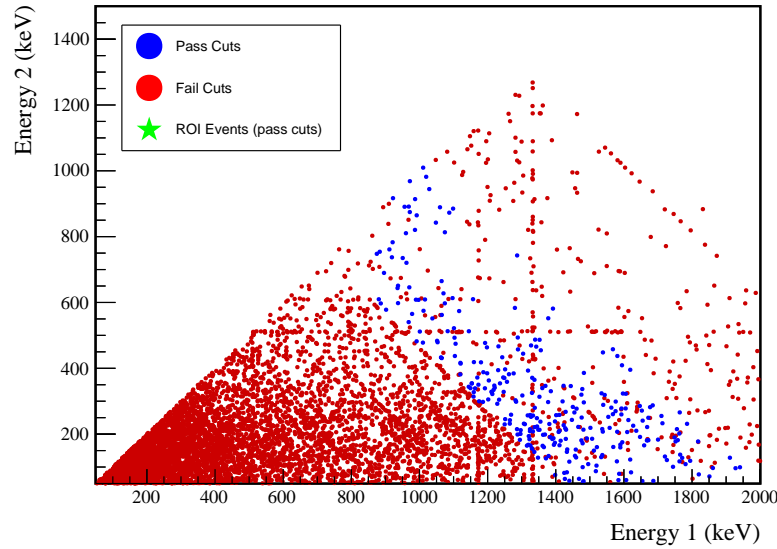


Figure A.29: Sum energy and coincident energy spectra for the 559 and 563 keV peaks.

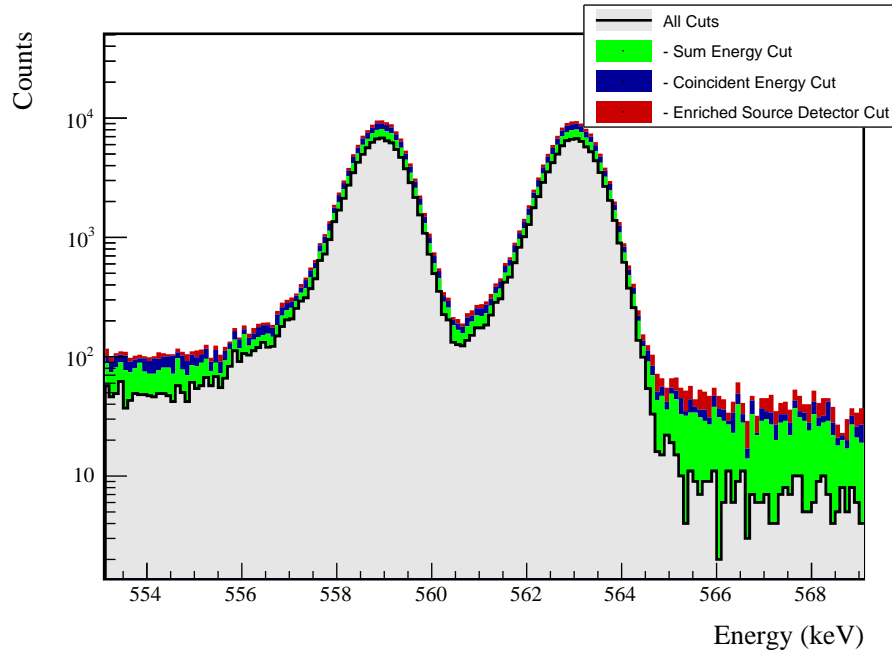


(a) Simulation



(b) Data

Figure A.30: Simulated and measured multiplicity 2 energy spectrum with sum and coincident energy cuts included for the 559 and 563 keV peaks.



(a) Effect of all cuts on ROI

Source	Module 1 efficiency	Module 2 efficiency
Multi-Detector with Full Energy γ	$5.6 \pm 0.2\%$	$3.0 \pm 0.5\%$
Region of Interest	$89.8 \pm 1.3\%$	$89.8 \pm 1.3\%$
Dead Layer	$69.7 \pm 5.2\%$	$58.2 \pm 7.3\%$
Detector Dead Times	$98.4 \pm 0.8\%$	$98.6 \pm 0.6\%$
Enriched Source Detector Cut	$97.1 \pm <0.1\%$	$91.2 \pm <0.1\%$
Coincident Energy Cut	$89.4 \pm 0.3\%$	$87.8 \pm 0.3\%$
Sum Energy Cut	$79.7 \pm 0.3\%$	$70.3 \pm 0.3\%$
Final Efficiency	$3.00 \pm 0.25\%$	$1.27 \pm 0.26\%$

(b) Table of efficiencies

Figure A.31: Plot showing effect of cuts applied sequentially on ROI peak and table of detection efficiencies for the 559 and 563 keV peaks.

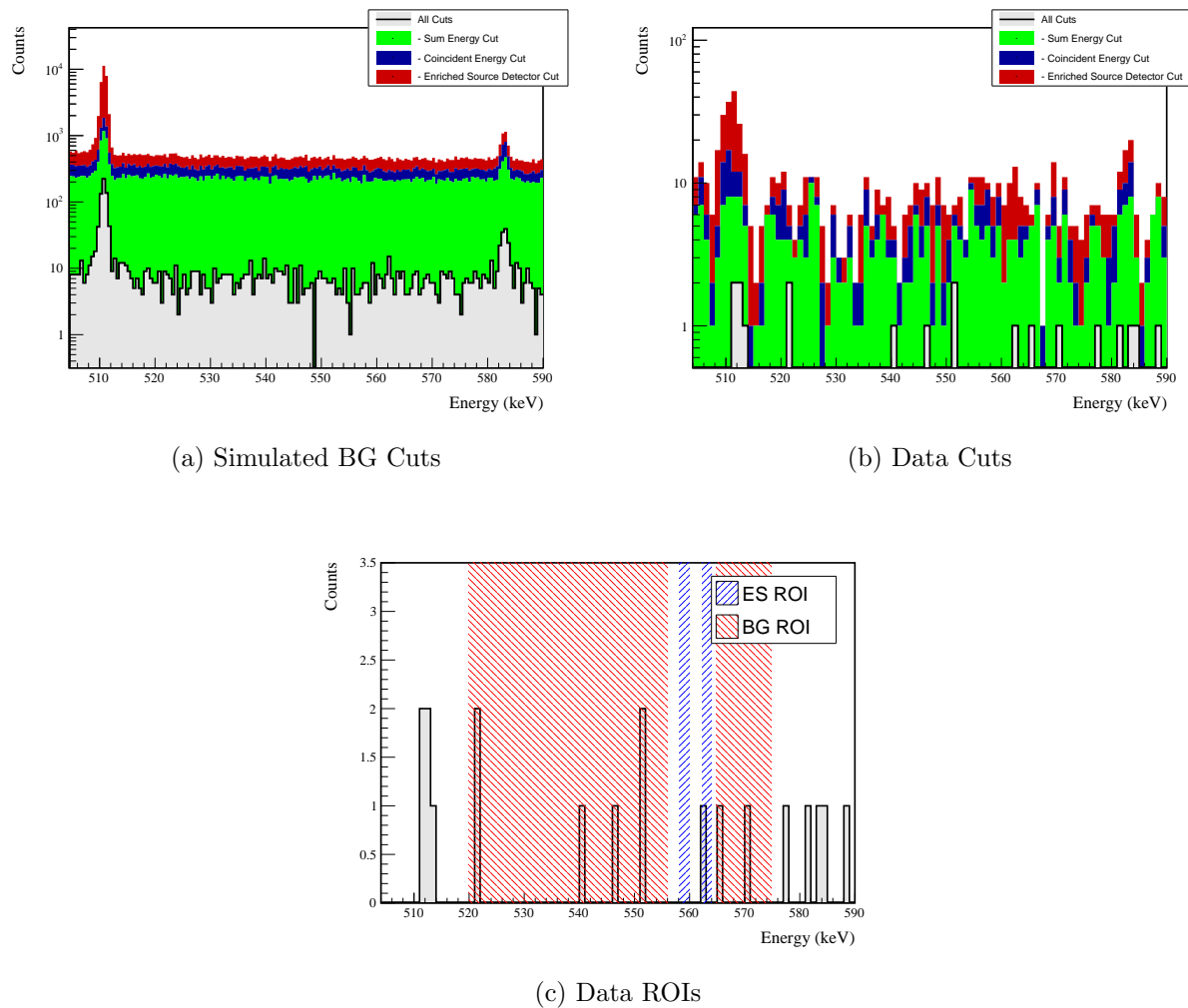


Figure A.32: Effect of all cuts applied to measured and simulated background data.

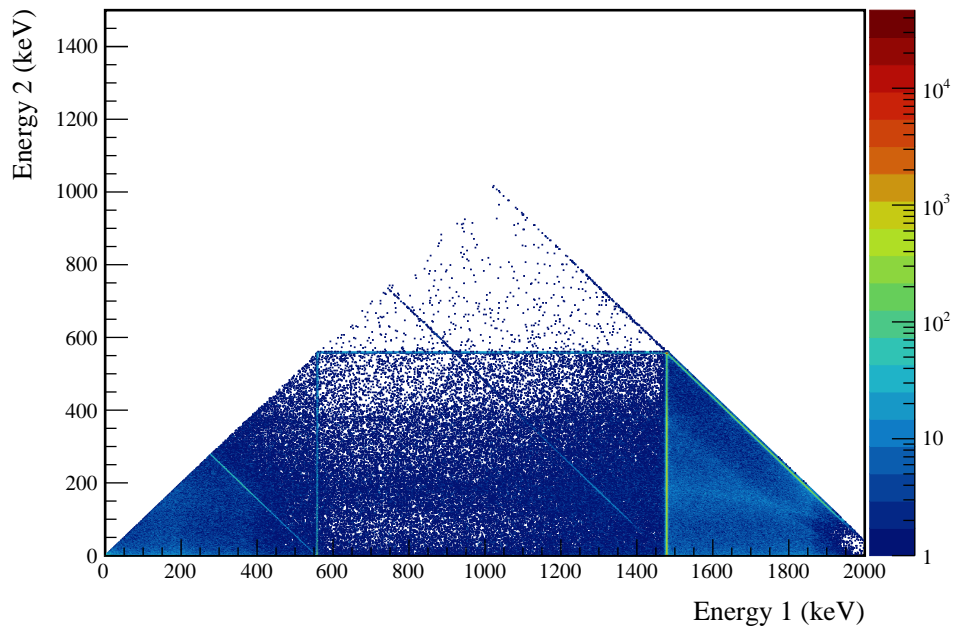
A.6 $0\nu\beta\beta$ to 2_1^+ 

Figure A.33: Simulated multiplicity 2 energy spectrum of the $0\nu\beta\beta$ to 2_1^+ decay mode

Table A.15: Table of energy estimation uncertainties for the 559 keV peak.

DS	E_{peak} (keV)	σ_{fit} (keV)	σ_{drift} (keV)	σ (keV)	$f_{i,fit}$	$f_{i,drift}$	τ_{fit} (keV)	$\delta_{\mu,NL}$ (keV)	$\delta_{\mu,drift}$ (keV)	$\delta_{\mu,peak}$ (keV)	δ_μ (keV)	FWHM (keV)	$\delta_{fwhm,fit}$ (keV)	$\delta_{fwhm,drift}$ (keV)	$\delta_{fwhm,peak}$ (keV)	δ_{FWHM} (keV)	δ_α	$E_{ROI,1}$ (keV)	$E_{ROI,2}$ (keV)	ϵ_{ROI}	$\sigma_{e_{ROI}}$	
DS1	559.101	0.460	0.063	0.464	0.230	0.515	0.001	0.104	0.002	0.012	0.005	0.105	1.152	0.001	0.039	0.011	0.040	0.035	558.032	559.959	0.915	0.011
DS2	559.101	0.461	0.055	0.464	0.249	0.515	0.002	0.067	0.004	0.012	0.005	0.068	1.158	0.001	0.107	0.011	0.108	0.093	558.035	559.957	0.917	0.023
DS3	559.101	0.470	0.066	0.474	0.224	0.505	0.001	0.026	0.024	0.012	0.005	0.038	1.174	0.001	0.073	0.011	0.074	0.063	558.039	559.977	0.921	0.016
DS4	559.101	0.455	0.077	0.461	0.108	0.445	0.002	0.076	0.010	0.012	0.005	0.078	1.111	0.001	0.106	0.011	0.107	0.096	558.161	559.966	0.929	0.024
DS5a	559.101	0.560	0.085	0.567	0.106	0.855	0.002	0.079	0.005	0.012	0.005	0.080	1.367	0.002	0.055	0.011	0.056	0.041	557.942	560.158	0.918	0.011
DS5b	559.101	0.469	0.074	0.475	0.158	0.491	0.001	0.020	0.011	0.012	0.005	0.026	1.157	0.001	0.125	0.011	0.125	0.108	558.094	559.986	0.927	0.027
DS5c	559.101	0.460	0.085	0.468	0.174	0.489	0.001	0.037	0.030	0.012	0.005	0.050	1.145	0.001	0.162	0.011	0.162	0.142	558.095	559.972	0.924	0.035
DS6a	559.101	0.456	0.044	0.458	0.191	0.463	0.001	0.069	0.025	0.012	0.005	0.075	1.123	0.000	0.041	0.011	0.042	0.038	558.106	559.951	0.923	0.010

A.6. $0\nu\beta\beta$ TO 2_1^+

51

Cut Name	Cut Description	$\langle \epsilon_{total} \rangle$	$\hat{\epsilon}_{total}$	$\langle \epsilon_{unique} \rangle$	$\hat{\epsilon}_{unique}$	Sacrifice	ΔDP
Enriched Source		M1: 21.5 %	$23.0^{+2.7}_{-2.5}\%$	0.0 %	$0.0^{+0.4}_{-0.0}\%$	1.9 %	-1%
Detector Cut	Any other detector: isEur	M2: 40.6 %	$63.8^{+6.0}_{-6.5}\%$	0.0 %	$0.0^{+1.7}_{-0.0}\%$	4.0 %	
Multiplicity 2		M1: 15.0 %	$16.6^{+2.4}_{-2.2}\%$	0.0 %	$0.0^{+0.4}_{-0.0}\%$	0.0 %	
Cut	m==2	M2: 11.5 %	$17.2^{+5.5}_{-4.4}\%$	0.0 %	$0.0^{+1.7}_{-0.0}\%$	0.0 %	0%
Coincident		M1: 100.0 %	$100.0^{+0.0}_{-0.4}\%$	64.6 %	$62.3 \pm 3.0\%$	18.3 %	
Energy Cut	Any other detector: energy>1472.4 && energy<1483.3	M2: 100.0 %	$100.0^{+0.0}_{-1.7}\%$	49.9 %	$25.9^{+6.1}_{-5.3}\%$	22.0 %	1046%
Combined Cuts		M1: 100.0 %	$100.0^{+0.0}_{-0.4}\%$	—	—	22.1 %	
		M2: 100.0 %	$100.0^{+0.0}_{-1.7}\%$	—	—	28.5 %	1273%

Table A.16: Table of cut descriptions and efficiencies for simulated backgrounds and measured data for the 559 keV peak.

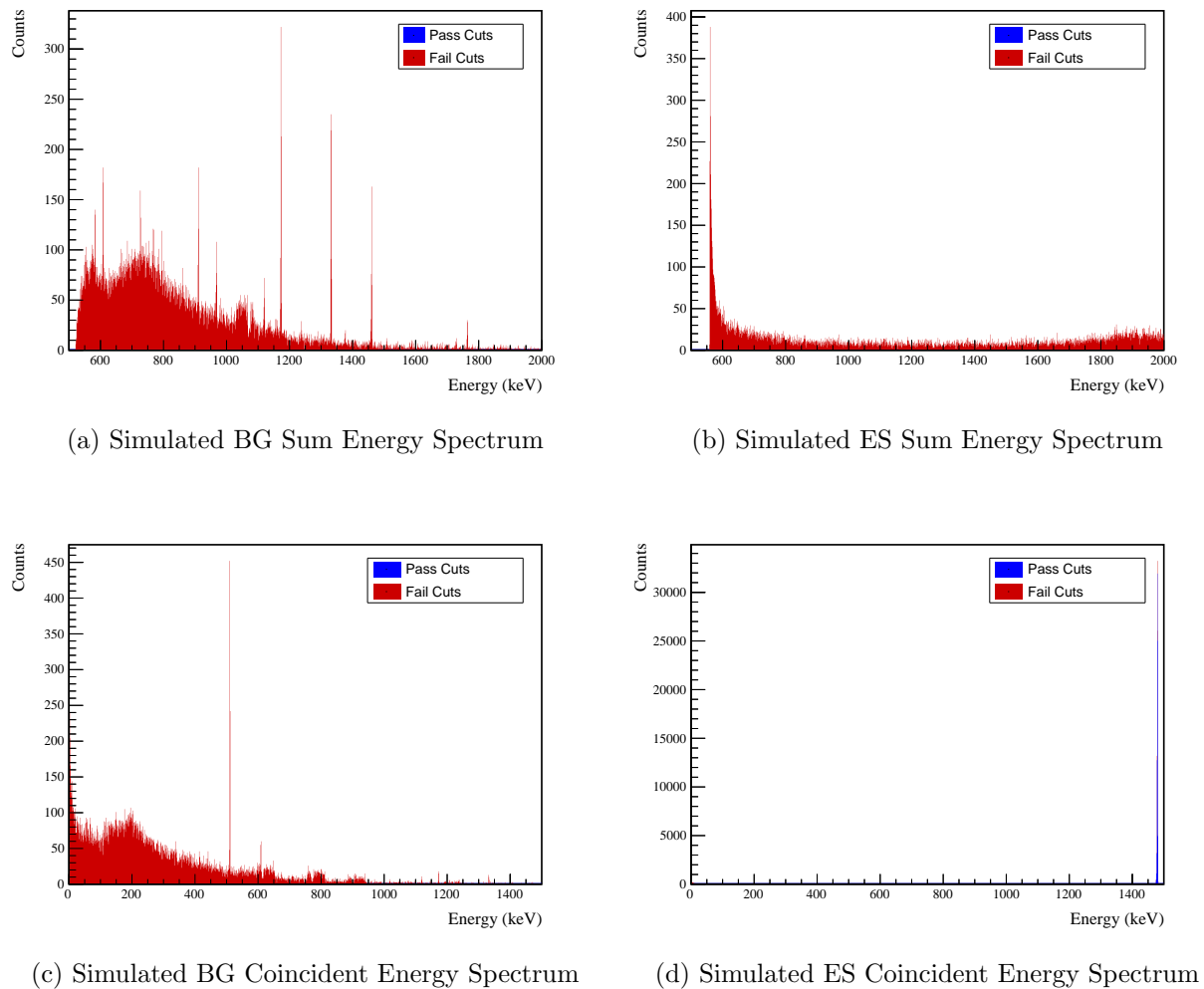


Figure A.34: Sum energy and coincident energy spectra for the 559 keV peak.

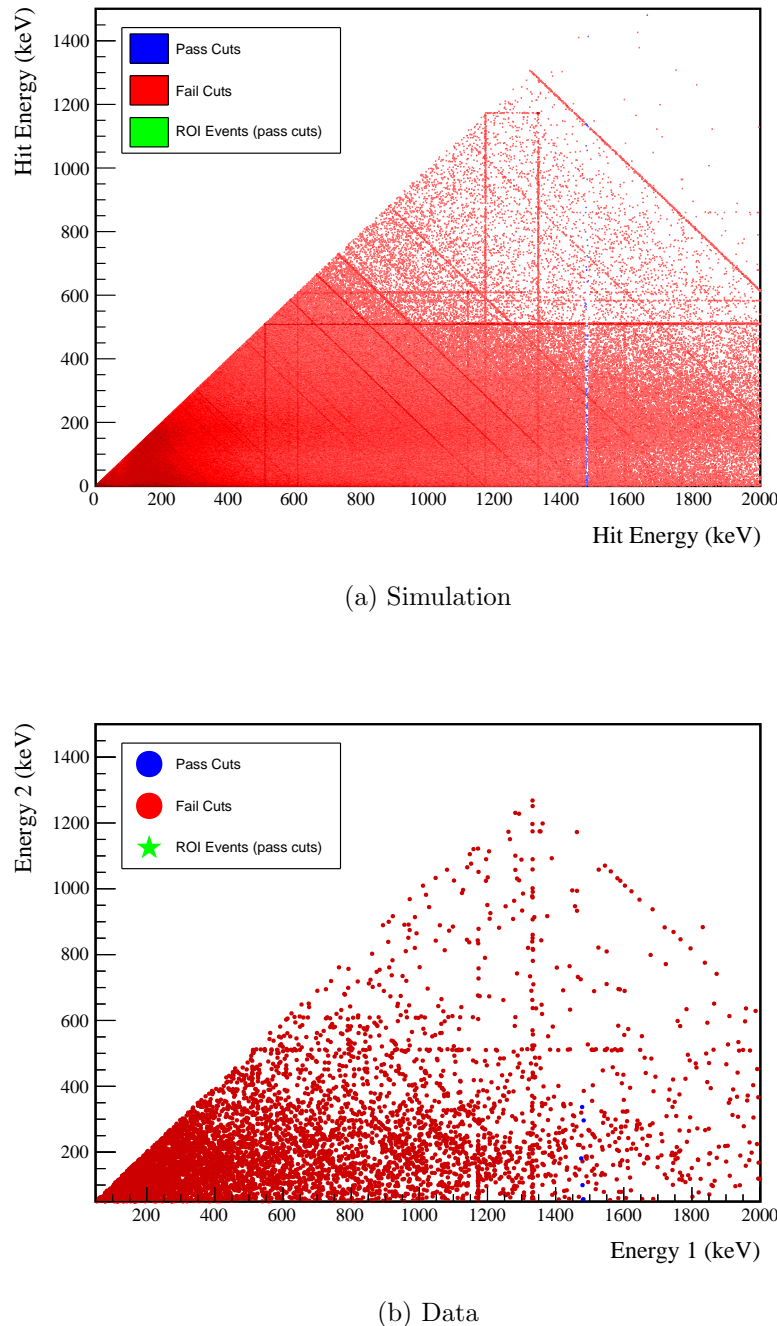
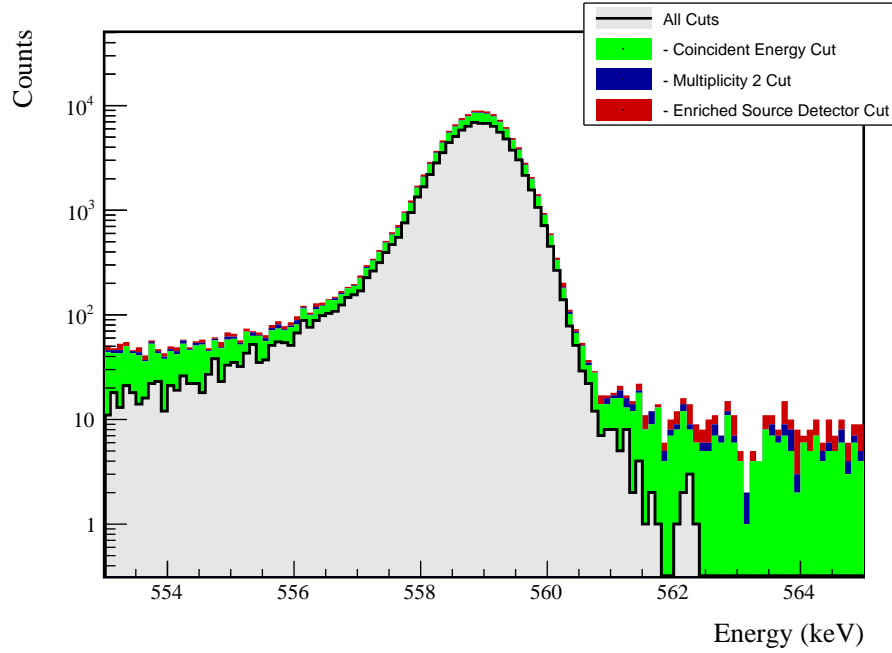


Figure A.35: Simulated and measured multiplicity 2 energy spectrum with sum and coincident energy cuts included for the 559 keV peak.



(a) Effect of all cuts on ROI

Source	Module 1 efficiency	Module 2 efficiency
Multi-Detector with Full Energy γ	$2.9 \pm 0.2\%$	$1.5 \pm 0.5\%$
Region of Interest	$92.2 \pm 1.5\%$	$92.2 \pm 1.5\%$
Dead Layer	$68.3 \pm 5.4\%$	$56.6 \pm 7.6\%$
Detector Dead Times	$98.4 \pm 0.8\%$	$98.6 \pm 0.7\%$
Enriched Source Detector Cut	$97.6 \pm <0.1\%$	$94.2 \pm <0.1\%$
Multiplicity 2 Cut	$98.7 \pm <0.1\%$	$99.2 \pm <0.1\%$
Coincident Energy Cut	$79.8 \pm 0.3\%$	$75.4 \pm 0.3\%$
Final Efficiency	$1.61 \pm 0.17\%$	$0.68 \pm 0.23\%$

(b) Table of efficiencies

Figure A.36: Plot showing effect of cuts applied sequentially on ROI peak and table of detection efficiencies for the 559 keV peak.

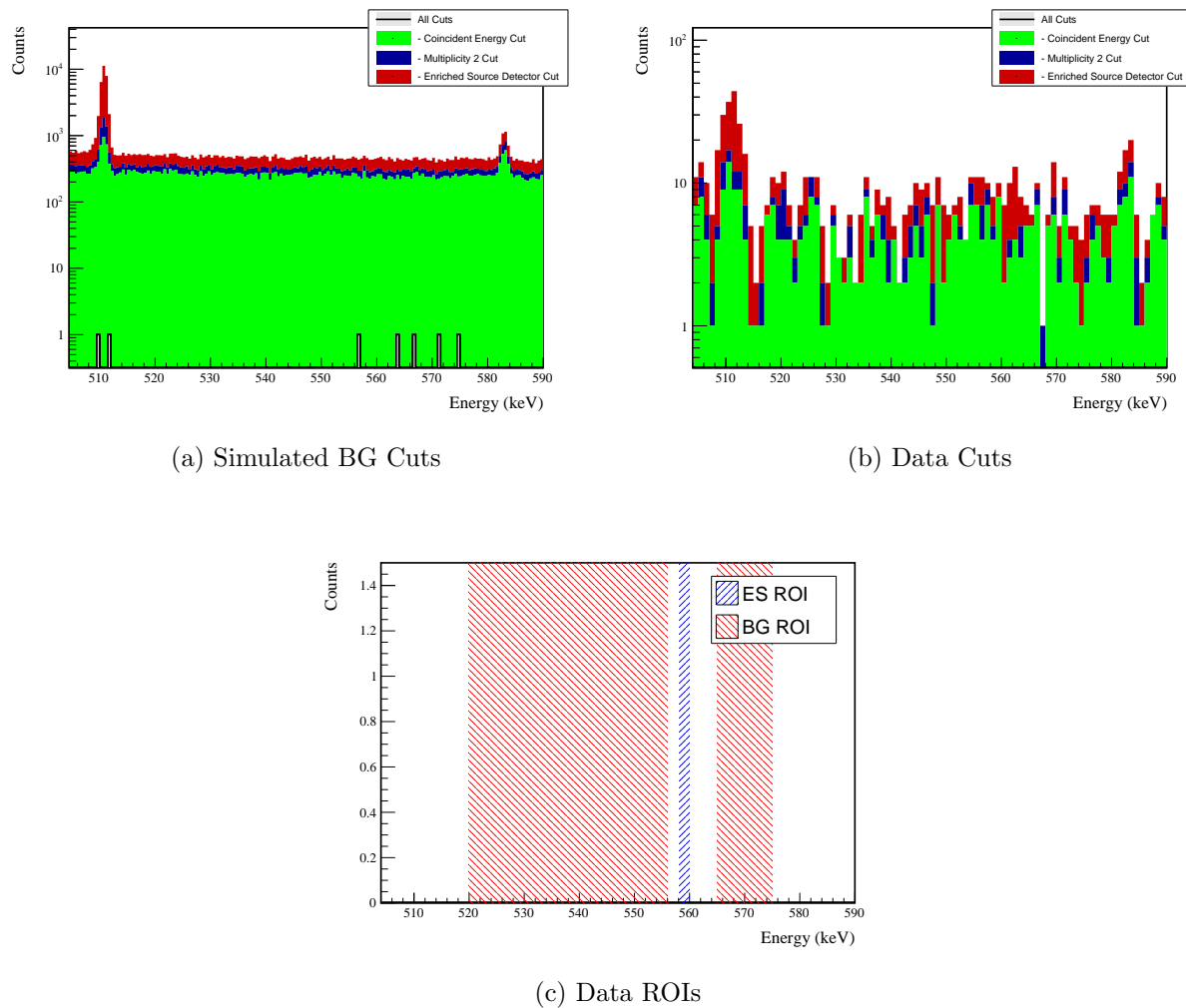


Figure A.37: Effect of all cuts applied to measured and simulated background data.

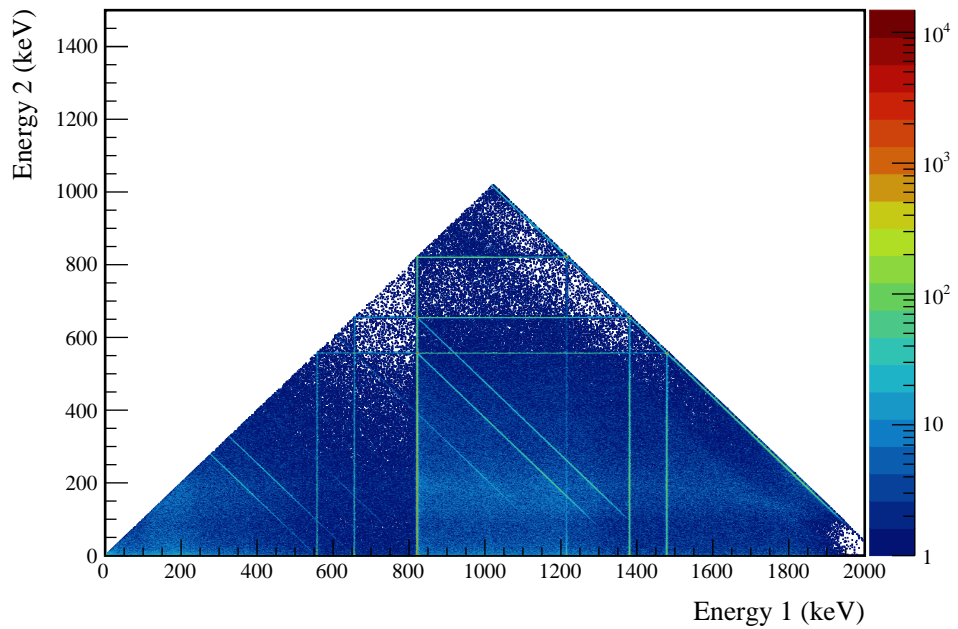
A.7 $0\nu\beta\beta$ **to** 2_2^+ 

Figure A.38: Simulated multiplicity 2 energy spectrum of the $0\nu\beta\beta$ to 2_2^+ decay mode

A.7.1 559 keV peak

Table A.17: Table of energy estimation uncertainties for the 559 keV peak.

DS	E_{peak} (keV)	σ_{fit} (keV)	σ_{drift} (keV)	σ (keV)	$f_{i,fit}$	$f_{i,drift}$	τ_{fit} (keV)	$\delta_{\mu,NL}$ (keV)	$\delta_{\mu,drift}$ (keV)	$\delta_{\mu,peak}$ (keV)	δ_μ (keV)	FWHM	$\delta_{fwhm,fit}$ (keV)	$\delta_{fwhm,drift}$ (keV)	$\delta_{fwhm,peak}$ (keV)	δ_{FWHM} (keV)	δ_α	$E_{ROI,1}$ (keV)	$E_{ROI,2}$ (keV)	ϵ_{ROI}	$\sigma_{e_{ROI}}$	
DS1	559.101	0.460	0.063	0.464	0.230	0.515	0.001	0.104	0.002	0.012	0.005	0.105	1.152	0.001	0.039	0.011	0.040	0.035	558.152	559.883	0.887	0.014
DS2	559.101	0.461	0.055	0.464	0.249	0.515	0.002	0.067	0.004	0.012	0.005	0.068	1.158	0.001	0.107	0.011	0.108	0.093	558.137	559.882	0.890	0.028
DS3	559.101	0.470	0.066	0.474	0.224	0.505	0.001	0.026	0.024	0.012	0.005	0.038	1.174	0.001	0.073	0.011	0.074	0.063	558.140	559.900	0.894	0.019
DS4	559.101	0.455	0.077	0.461	0.108	0.445	0.002	0.076	0.010	0.012	0.005	0.078	1.111	0.001	0.106	0.011	0.107	0.096	558.243	559.892	0.903	0.030
DS5a	559.101	0.560	0.085	0.567	0.106	0.855	0.002	0.079	0.005	0.012	0.005	0.080	1.367	0.002	0.055	0.011	0.056	0.041	558.049	560.067	0.891	0.013
DS5b	559.101	0.469	0.074	0.475	0.158	0.491	0.001	0.020	0.011	0.012	0.005	0.026	1.157	0.001	0.125	0.011	0.125	0.108	558.185	559.909	0.901	0.033
DS5c	559.101	0.460	0.085	0.468	0.174	0.489	0.001	0.037	0.030	0.012	0.005	0.050	1.145	0.001	0.162	0.011	0.162	0.142	558.187	559.896	0.898	0.042
DS6a	559.101	0.456	0.044	0.458	0.191	0.463	0.001	0.069	0.025	0.012	0.005	0.075	1.123	0.000	0.041	0.011	0.042	0.038	558.198	559.877	0.896	0.012

A.7. $0\nu\beta\beta$ TO 2_2^+

Cut Name	Cut Description	$\langle \epsilon_{total} \rangle$	$\hat{\epsilon}_{total}$	$\langle \epsilon_{unique} \rangle$	$\hat{\epsilon}_{unique}$	Sacrifice	ΔDP
Enriched Source	Any other detector: !isErr	M1: 21.5 % M2: 40.6 %	23.0 ^{+2.7} _{-2.5} % 63.8 ^{+6.0} _{-6.5} %	0.5 % 0.9 %	0.8 ^{+0.7} _{-0.4} % 6.9 ^{+4.1} _{-2.6} %	1.3 % 3.0 %	9%
Detector Cut	No other detector: (((energy<53.) (energy>591.4 && energy<631.6) (energy>1170.6 && energy<1175.6) (energy>1205. && energy<1208.) (energy>1337.) && energy<1331. (energy>492.6) && isErr) (energy<44.8) (energy>502.2 && energy<518.2) (energy>1375.4) && !isErr)	M1: 20.6 % M2: 21.3 %	21.9 ^{+2.6} _{-2.4} % 25.9 ^{+6.1} _{-5.3} %	0.4 % 0.3 %	1.1 ^{+0.9} _{-0.5} % 5.2 ^{+3.7} _{-2.2} %	2.3 % 1.4 %	5%
Coincident	Not: (sumE<1214.) (sumE>1216.2 && sumE<1378.) (sumE>383.6 && sumE<496.6) (sumE>1760.4 && sumE<1765.8) (sumE>2041.6)	M1: 97.2 % M2: 97.7 %	94.7 ^{+1.2} _{-1.5} % 86.2 ^{+3.9} _{-5.1} %	60.3 % 45.3 %	58.9 ± 3.1 % 27.6 ^{+6.2} _{-5.5} %	20.2 % 22.8 %	208%
Energy Cut		M1: 98.1 % M2: 99.0 %	97.0 ^{+0.9} _{-1.2} % 98.3 ^{+1.1} _{-2.7} %	— —	— —	30.5 % 39.9 %	244%
Sum Energy Cut							
Combined Cuts							

Table A.18: Table of cut descriptions and efficiencies for simulated backgrounds and measured data for the 559 keV peak.

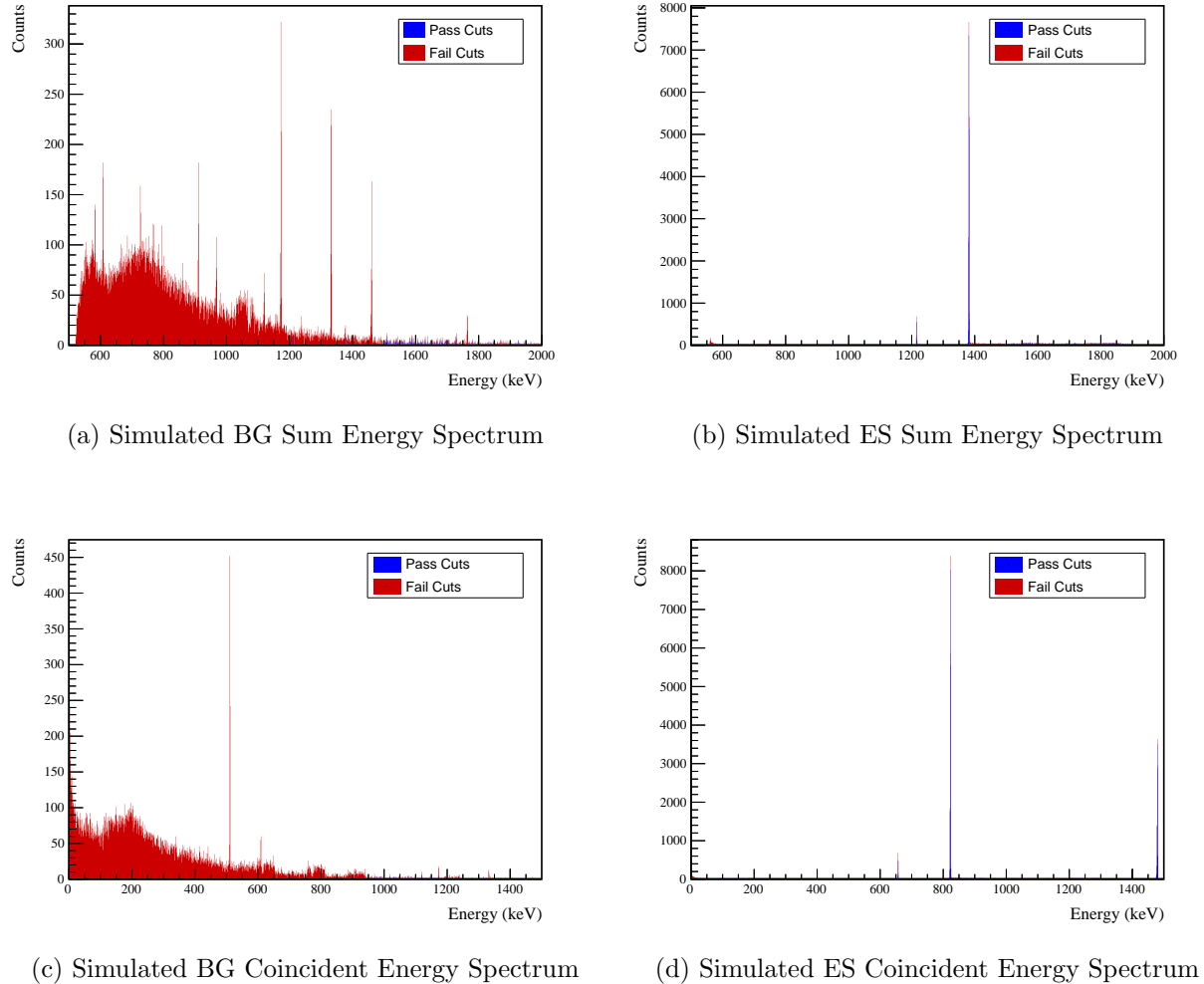
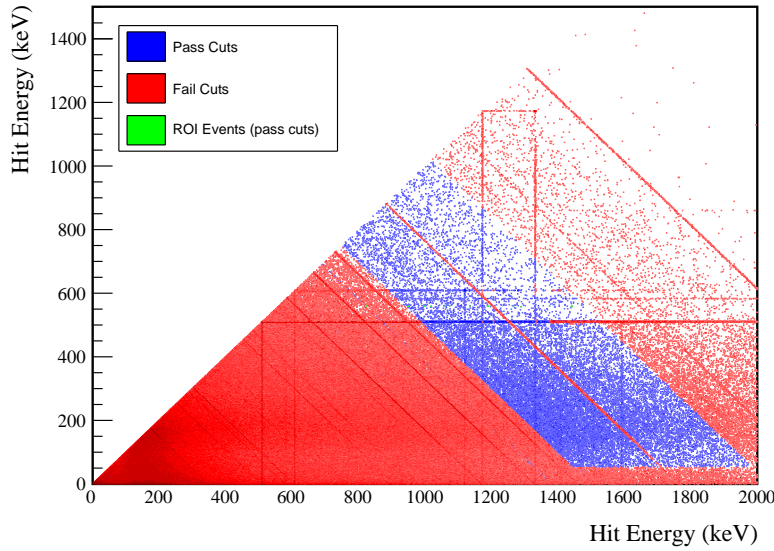
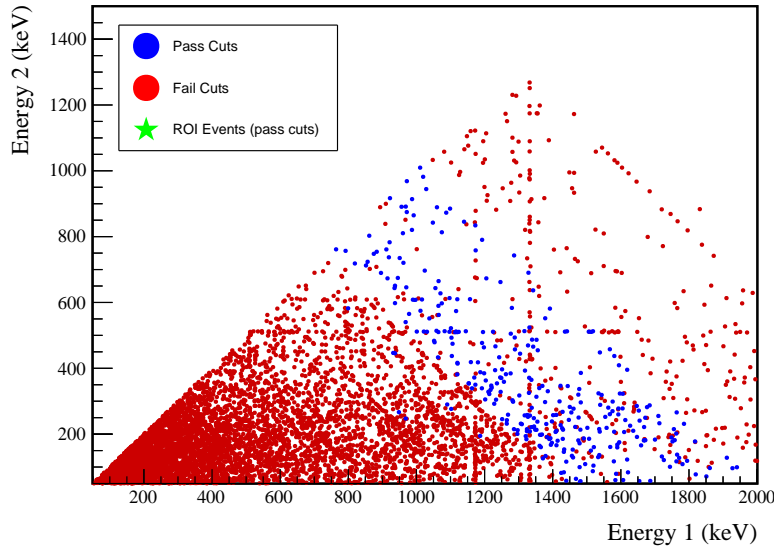


Figure A.39: Sum energy and coincident energy spectra for the 559 keV peak.

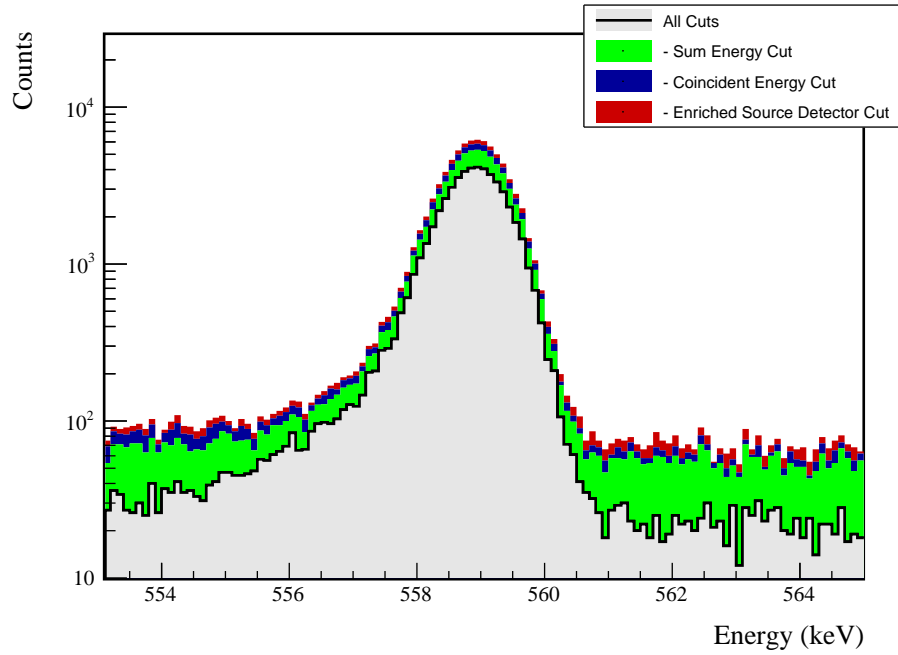


(a) Simulation



(b) Data

Figure A.40: Simulated and measured multiplicity 2 energy spectrum with sum and coincident energy cuts included for the 559 keV peak.



(a) Effect of all cuts on ROI

Source	Module 1 efficiency	Module 2 efficiency
Multi-Detector with Full Energy γ	$1.9 \pm 0.2\%$	$1.0 \pm 0.5\%$
Region of Interest	$89.5 \pm 1.8\%$	$89.5 \pm 1.8\%$
Dead Layer	$69.1 \pm 5.3\%$	$57.9 \pm 7.4\%$
Detector Dead Times	$98.4 \pm 0.8\%$	$98.6 \pm 0.7\%$
Enriched Source Detector Cut	$97.0 \pm <0.1\%$	$90.7 \pm <0.1\%$
Coincident Energy Cut	$92.3 \pm 0.3\%$	$90.6 \pm 0.3\%$
Sum Energy Cut	$73.4 \pm 0.3\%$	$65.1 \pm 0.3\%$
Final Efficiency	$0.94 \pm 0.13\%$	$0.40 \pm 0.19\%$

(b) Table of efficiencies

Figure A.41: Plot showing effect of cuts applied sequentially on ROI peak and table of detection efficiencies for the 559 keV peak.

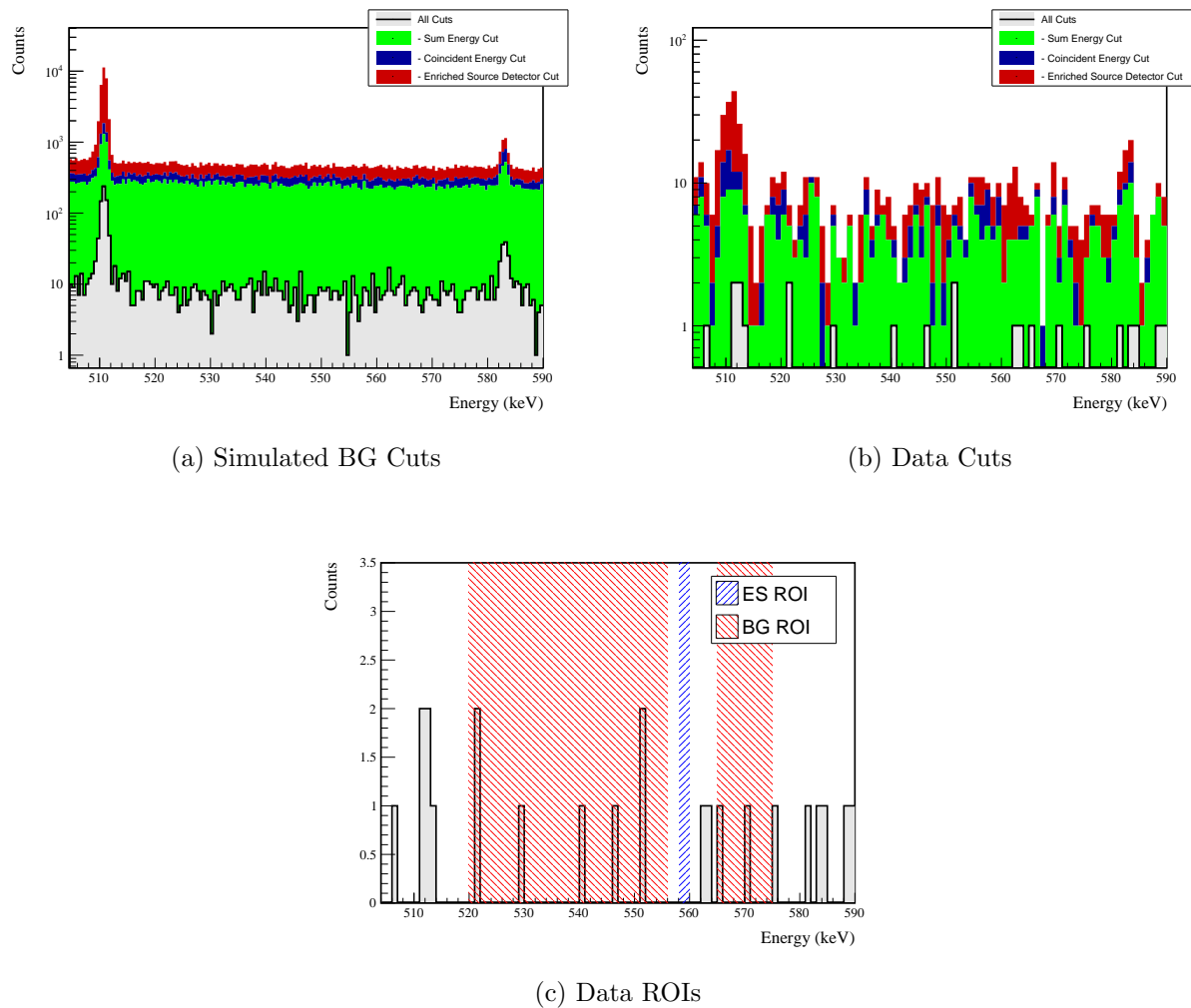
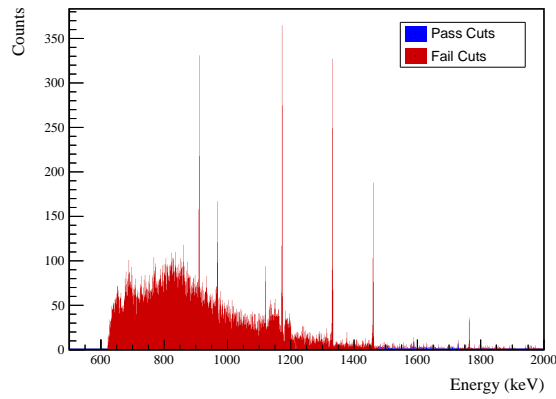
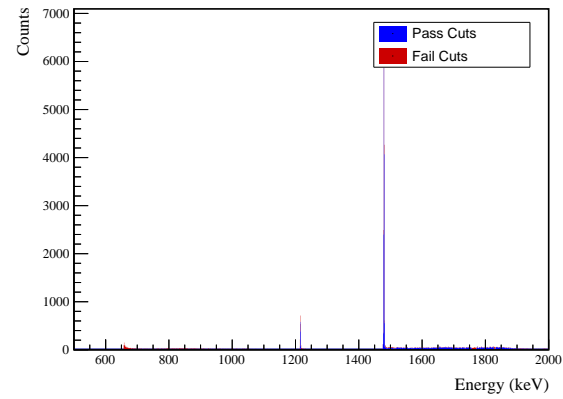


Figure A.42: Effect of all cuts applied to measured and simulated background data.

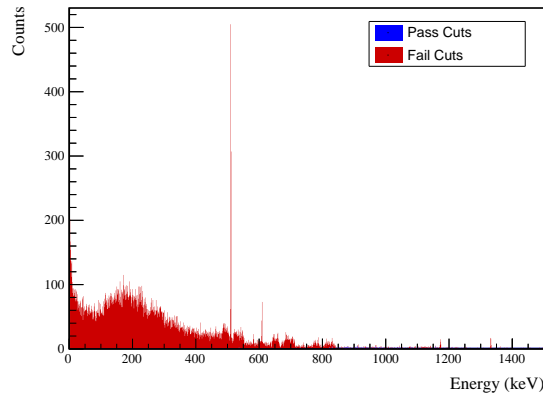
A.7.2 657 keV peak



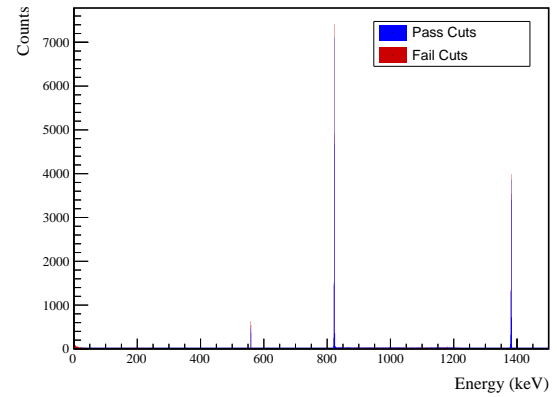
(a) Simulated BG Sum Energy Spectrum



(b) Simulated ES Sum Energy Spectrum



(c) Simulated BG Coincident Energy Spectrum



(d) Simulated ES Coincident Energy Spectrum

Figure A.43: Sum energy and coincident energy spectra for the 657 keV peak.

Table A.19: Table of energy estimation uncertainties for the 657 keV peak.

DS	E_{peak} (keV)	σ_{fit} (keV)	σ_{drift} (keV)	σ (keV)	$f_{i,fit}$	$f_{i,drift}$	τ_{fit} (keV)	$\delta_{\mu,NL}$ (keV)	$\delta_{\mu,drift}$ (keV)	$\delta_{\mu,peak}$ (keV)	δ_μ (keV)	FWHM	$\delta_{fwhm,fit}$ (keV)	$\delta_{fwhm,drift}$ (keV)	$\delta_{fwhm,peak}$ (keV)	$E_{ROI,1}$ (keV)	$E_{ROI,2}$ (keV)	ϵ_{ROI}	$\sigma_{e_{ROI}}$			
DS1	657.041	0.500	0.074	0.505	0.230	0.579	0.002	0.104	0.003	0.012	0.005	0.105	1.256	0.001	0.039	0.011	0.040	0.032	656.029	657.875	0.880	0.013
DS2	657.041	0.502	0.064	0.506	0.249	0.580	0.002	0.067	0.005	0.012	0.005	0.068	1.263	0.001	0.107	0.011	0.108	0.085	656.013	657.873	0.881	0.027
DS3	657.041	0.510	0.078	0.516	0.224	0.568	0.002	0.026	0.028	0.012	0.005	0.040	1.278	0.001	0.073	0.011	0.074	0.058	656.017	657.892	0.886	0.018
DS4	657.041	0.493	0.090	0.501	0.108	0.490	0.002	0.076	0.012	0.012	0.005	0.078	1.207	0.001	0.106	0.011	0.107	0.088	656.128	657.882	0.897	0.028
DS5a	657.041	0.606	0.100	0.614	0.106	0.924	0.002	0.079	0.006	0.012	0.005	0.080	1.481	0.002	0.055	0.011	0.056	0.038	655.925	658.065	0.885	0.013
DS5b	657.041	0.509	0.087	0.517	0.158	0.562	0.001	0.020	0.013	0.012	0.005	0.027	1.259	0.001	0.125	0.011	0.125	0.100	656.066	657.902	0.892	0.031
DS5c	657.041	0.500	0.100	0.510	0.174	0.555	0.002	0.037	0.035	0.012	0.005	0.053	1.247	0.001	0.162	0.011	0.162	0.130	656.066	657.888	0.890	0.041
DS6a	657.041	0.495	0.051	0.497	0.191	0.524	0.001	0.069	0.030	0.012	0.005	0.076	1.221	0.001	0.041	0.011	0.042	0.035	656.079	657.866	0.888	0.012

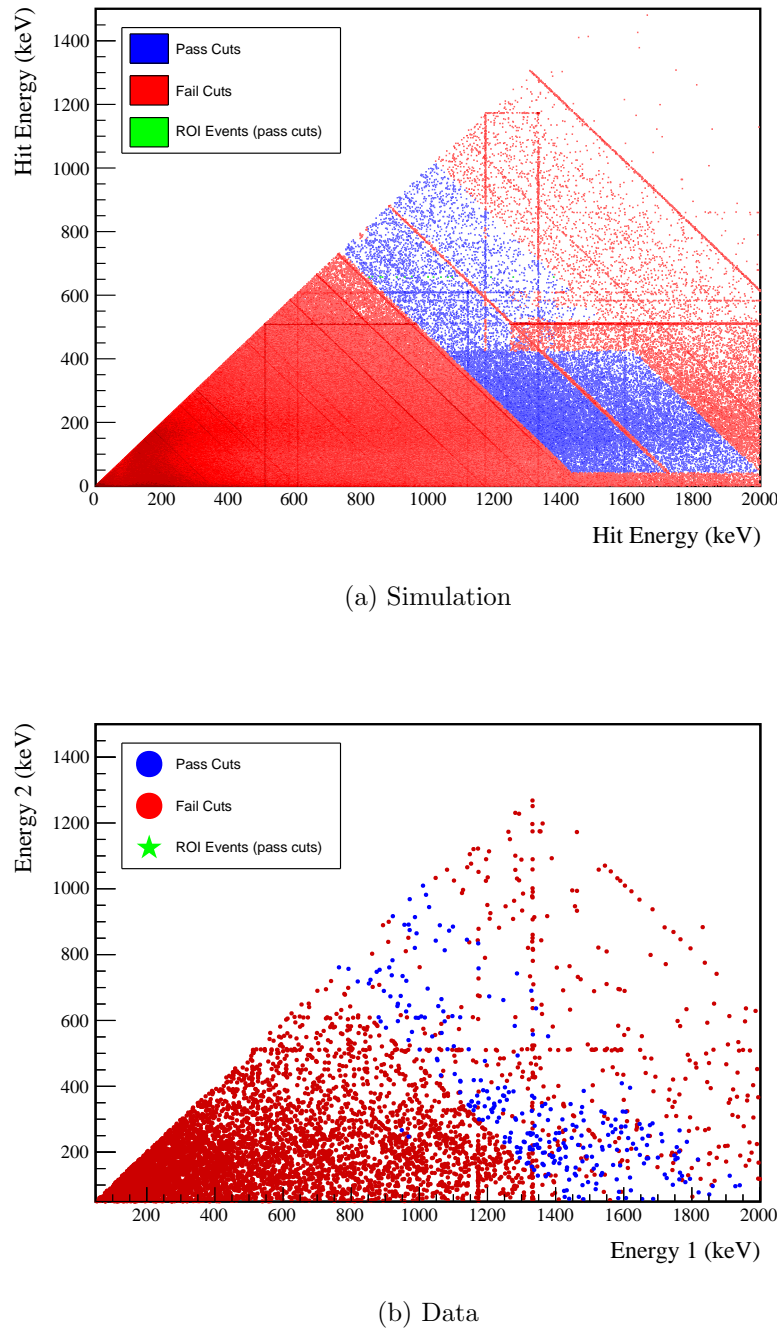
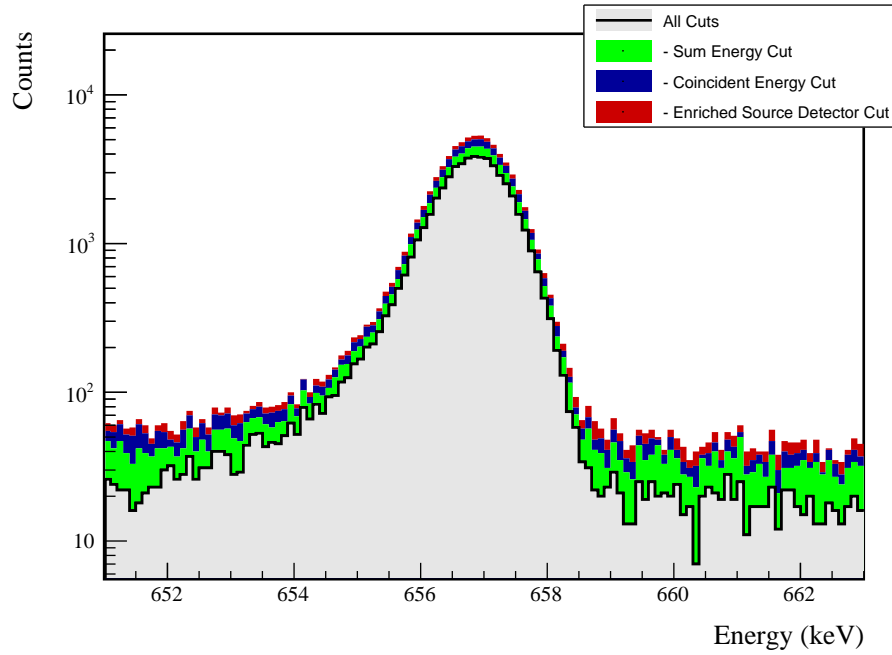


Figure A.44: Simulated and measured multiplicity 2 energy spectrum with sum and coincident energy cuts included for the 657 keV peak.



(a) Effect of all cuts on ROI

Source	Module 1 efficiency	Module 2 efficiency
Multi-Detector with Full Energy γ	$1.7 \pm 0.2\%$	$0.9 \pm 0.5\%$
Region of Interest	$88.7 \pm 1.7\%$	$88.7 \pm 1.7\%$
Dead Layer	$70.0 \pm 5.1\%$	$58.9 \pm 7.2\%$
Detector Dead Times	$98.4 \pm 0.8\%$	$98.6 \pm 0.6\%$
Enriched Source Detector Cut	$97.0 \pm <0.1\%$	$90.5 \pm <0.1\%$
Coincident Energy Cut	$89.9 \pm 0.3\%$	$88.1 \pm 0.3\%$
Sum Energy Cut	$80.9 \pm 0.3\%$	$71.9 \pm 0.3\%$
Final Efficiency	$0.93 \pm 0.13\%$	$0.39 \pm 0.21\%$

(b) Table of efficiencies

Figure A.45: Plot showing effect of cuts applied sequentially on ROI peak and table of detection efficiencies for the 657 keV peak.

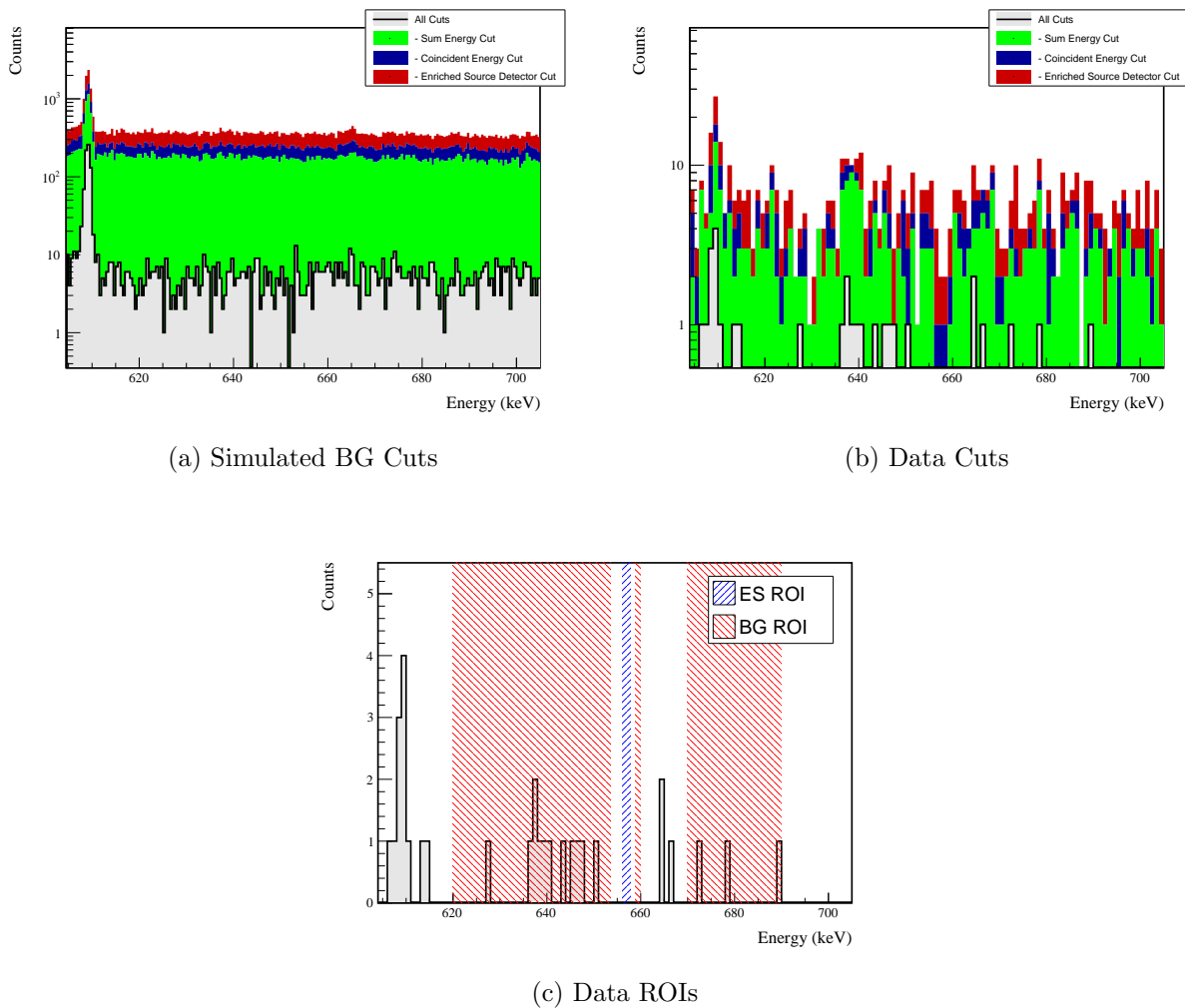
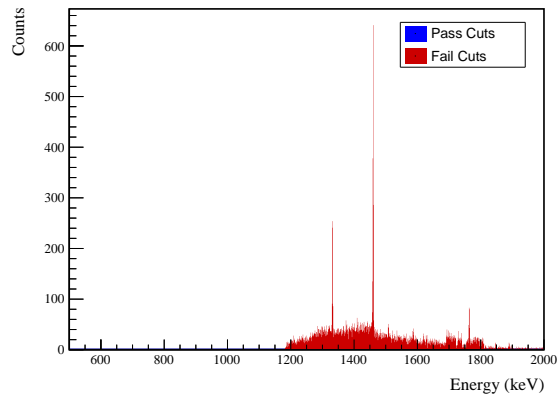


Figure A.46: Effect of all cuts applied to measured and simulated background data.

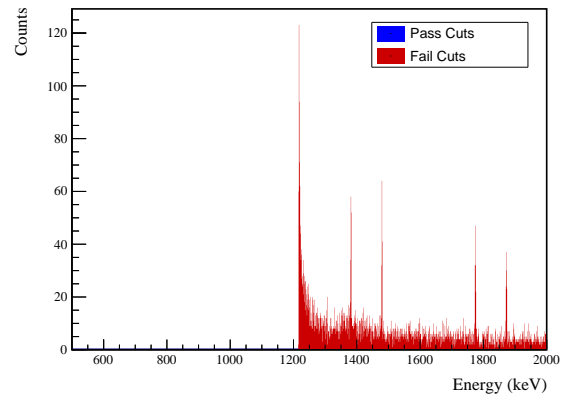
Cut Name	Cut Description	$\langle \epsilon_{total} \rangle$	$\hat{\epsilon}_{total}$	$\langle \epsilon_{unique} \rangle$	$\hat{\epsilon}_{unique}$	Sacrifice	ΔDP
Enriched Source	Any other detector: isEnv	M1: 22.2 % M2: 41.6 %	23.4 _{-2.7} ^{+2.9} % 59.7 _{-5.9} ^{+5.6} %	0.5 % 1.1 %	2.2 _{-0.8} ^{+1.2} % 2.8 _{-1.4} ^{+2.7} %	1.3 % 3.3 %	12%
Detector Cut	No other detector: ((energy<41.2) (energy>425.2 && energy<529.4) (energy>562.4 && energy<611.4) (energy>775.6 && energy<817.8) (energy>1169.6 && energy<1175.) (energy>1308. && energy<1333.2) (energy>1384.8) && isEnv) ((energy<40.6) (energy>489.6 && energy<521.) (energy>1248.)) && isEnv)	M1: 26.2 % M2: 25.5 %	25.1 _{-2.7} ^{+3.0} % 22.2 _{-4.5} ^{+5.3} %	0.7 % 0.6 %	2.6 _{-0.9} ^{+1.3} % 1.4 _{-0.9} ^{+2.2} %	4.0 % 2.8 %	8%
Coincident	Not: (sumE<1214.8) (sumE>1216.8 && sumE<1474.4) (sumE>1757.6 && sumE<1771.6) (sumE>2042.6)	M1: 97.0 % M2: 97.1 %	90.5 _{-2.1} ^{+1.8} % 93.1 _{-3.6} ^{+2.4} %	54.4 % 40.5 %	51.9 \pm 3.3 % 27.8 _{-4.9} ^{+5.6} %	12.3 % 15.3 %	232%
Energy Cut	M1: 98.4 % M2: 99.0 %	95.7 _{-1.5} ^{+1.2} % 98.6 _{-2.2} ^{+0.9} %	— —	— —	— —	24.8 % 35.0 %	281%
Sum Energy Cut							
Combined Cuts							

Table A.20: Table of cut descriptions and efficiencies for simulated backgrounds and measured data for the 657 keV peak.

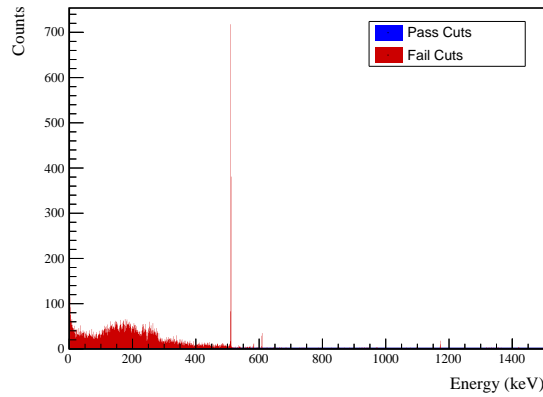
A.7.3 1216 keV peak



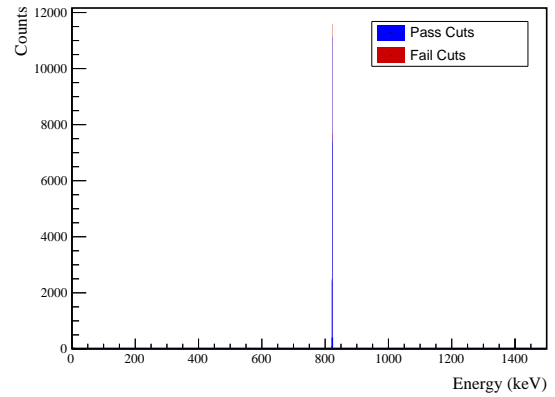
(a) Simulated BG Sum Energy Spectrum



(b) Simulated ES Sum Energy Spectrum



(c) Simulated BG Coincident Energy Spectrum

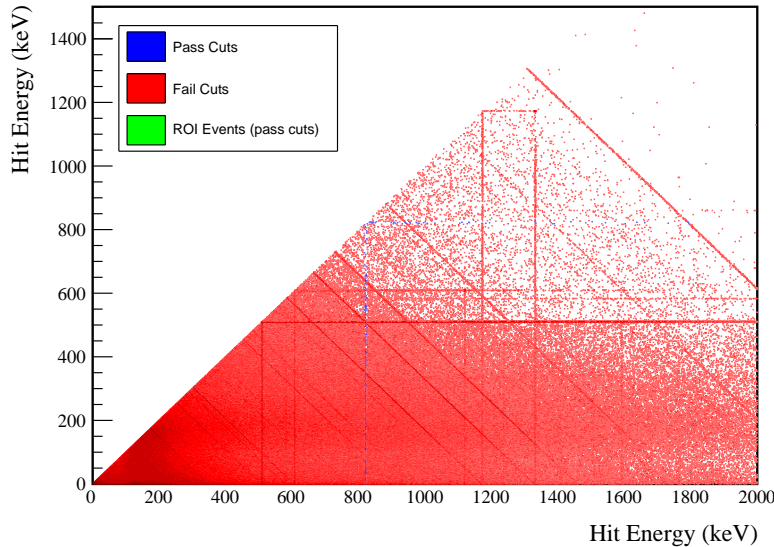


(d) Simulated ES Coincident Energy Spectrum

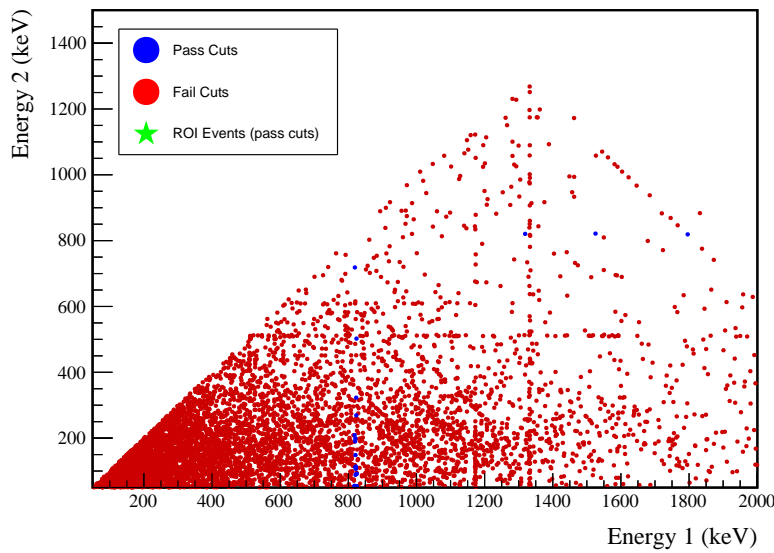
Figure A.47: Sum energy and coincident energy spectra for the 1216 keV peak.

Table A.21: Table of energy estimation uncertainties for the 1216 keV peak.

DS	E_{peak} (keV)	$\sigma_{T_{fit}}$ (keV)	$\sigma_{\mu,drift}$ (keV)	σ (keV)	$f_{t,fit}$ (keV)	T_{fit} (keV)	$\delta_{t,fit}$ (keV)	$\delta_{\mu,NL}$ (keV)	$\delta_{\mu,drift}$ (keV)	$\delta_{t,peak}$ (keV)	δ_μ (keV)	FWHM (keV)	$\delta_{f_{whm,drift}}$ (keV)	$\delta_{f_{whm,peak}}$ (keV)	$\delta_{f_{whm,drift}}$ (keV)	$\delta_{f_{whm,peak}}$ (keV)	δ_{FWHM} (keV)	δ_α	$E_{ROI,1}$ (keV)	$E_{ROI,2}$ (keV)	ϵ_{ROI}	$\sigma_{\epsilon_{ROI}}$
DS1	1216.104	0.705	0.137	0.718	0.230	0.945	0.003	0.104	0.005	0.012	0.020	0.107	1.787	0.001	0.039	0.011	0.040	0.023	1214.426	1217.449	0.914	0.006
DS2	1216.104	0.710	0.119	0.720	0.249	0.951	0.003	0.067	0.008	0.012	0.020	0.072	1.803	0.001	0.107	0.011	0.108	0.060	1214.387	1217.449	0.914	0.014
DS3	1216.104	0.715	0.144	0.729	0.224	0.925	0.003	0.026	0.051	0.012	0.020	0.062	1.812	0.001	0.073	0.011	0.074	0.041	1214.416	1217.470	0.917	0.010
DS4	1216.104	0.697	0.167	0.717	0.108	0.746	0.003	0.076	0.022	0.012	0.020	0.083	1.726	0.001	0.106	0.011	0.107	0.062	1214.621	1217.461	0.932	0.015
DS5a	1216.104	0.838	0.185	0.859	0.106	1.316	0.004	0.079	0.012	0.012	0.020	0.083	2.070	0.002	0.055	0.011	0.056	0.027	1214.323	1217.722	0.921	0.007
DS5b	1216.104	0.716	0.161	0.734	0.158	0.963	0.002	0.020	0.024	0.012	0.020	0.039	1.791	0.001	0.125	0.011	0.125	0.070	1214.506	1217.487	0.922	0.017
DS5c	1216.104	0.703	0.185	0.727	0.174	0.932	0.003	0.037	0.066	0.012	0.020	0.079	1.783	0.001	0.162	0.011	0.162	0.091	1214.497	1217.474	0.921	0.022
DS6a	1216.104	0.693	0.095	0.700	0.191	0.873	0.002	0.069	0.055	0.012	0.020	0.092	1.723	0.001	0.041	0.011	0.042	0.025	1214.535	1217.422	0.920	0.006

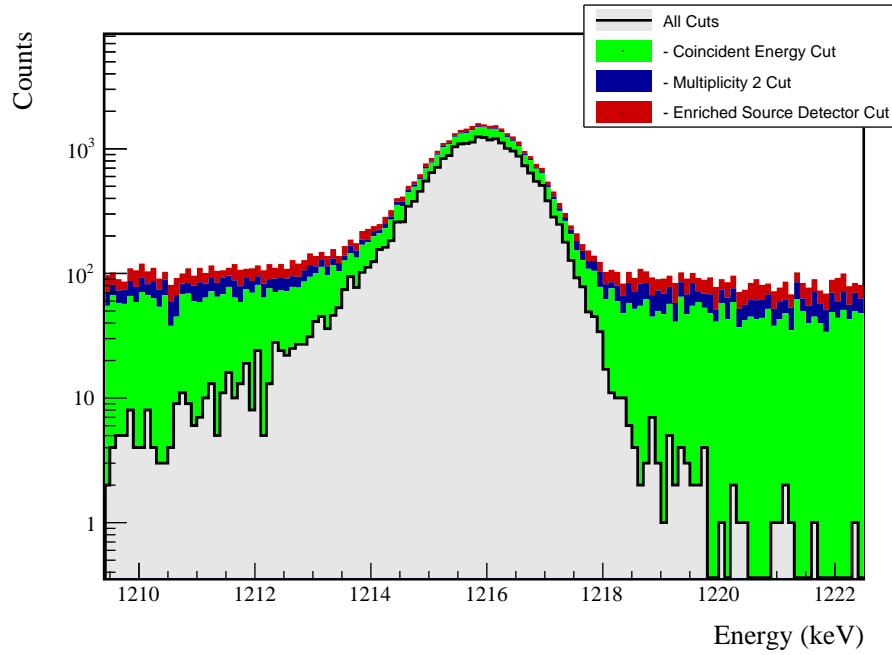


(a) Simulation



(b) Data

Figure A.48: Simulated and measured multiplicity 2 energy spectrum with sum and coincident energy cuts included for the 1216 keV peak.



(a) Effect of all cuts on ROI

Source	Module 1 efficiency	Module 2 efficiency
Multi-Detector with Full Energy γ	$0.8 \pm 0.2\%$	$0.4 \pm 0.5\%$
Region of Interest	$92.0 \pm 0.9\%$	$92.0 \pm 0.9\%$
Dead Layer	$69.2 \pm 5.2\%$	$58.6 \pm 7.2\%$
Detector Dead Times	$98.3 \pm 0.8\%$	$98.6 \pm 0.7\%$
Enriched Source Detector Cut	$96.4 \pm <0.1\%$	$91.7 \pm <0.1\%$
Multiplicity 2 Cut	$97.4 \pm <0.1\%$	$98.2 \pm <0.1\%$
Coincident Energy Cut	$77.7 \pm 0.3\%$	$74.4 \pm 0.3\%$
Final Efficiency	$0.43 \pm 0.12\%$	$0.18 \pm 0.21\%$

(b) Table of efficiencies

Figure A.49: Plot showing effect of cuts applied sequentially on ROI peak and table of detection efficiencies for the 1216 keV peak.

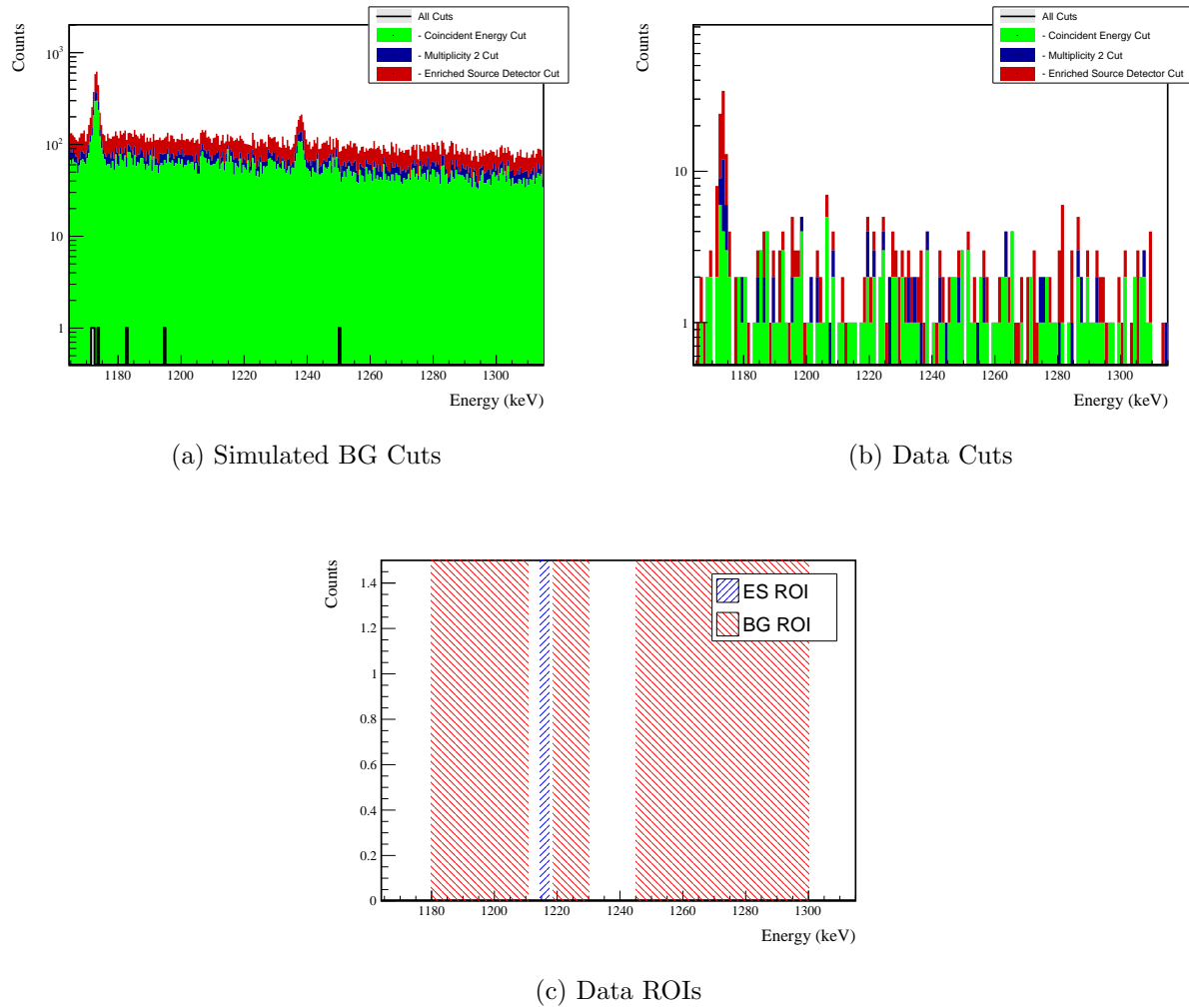


Figure A.50: Effect of all cuts applied to measured and simulated background data.

Cut Name	Cut Description	$\langle \epsilon_{total} \rangle$	$\hat{\epsilon}_{total}$	$\langle \epsilon_{unique} \rangle$	$\hat{\epsilon}_{unique}$	Sacrifice	ΔDP
Enriched Source		M1: 25.2 %	$24.7^{+3.5}_{-3.2}\%$	0.0 %	$0.0^{+0.6}_{-0.0}\%$	1.9 %	0%
Detector Cut	Any other detector: isEnv	M2: 41.8 %	$61.9^{+7.1}_{-7.7}\%$	0.0 %	$0.0^{+2.3}_{-0.0}\%$	3.8 %	
Multiplicity 2		M1: 14.8 %	$19.8^{+3.3}_{-2.9}\%$	0.0 %	$0.0^{+0.6}_{-0.0}\%$	0.0 %	1%
Cut	m==2	M2: 11.6 %	$4.8^{+4.5}_{-2.4}\%$	0.0 %	$0.0^{+2.3}_{-0.0}\%$	0.0 %	
Coincident		M1: 100.0 %	$100.0^{+0.0}_{-0.6}\%$	61.6 %	$59.3^{+3.8}_{-3.9}\%$	18.1 %	
Energy Cut	Any other detector: energy>817.7 && energy<825.4	M2: 100.0 %	$100.0^{+0.0}_{-2.3}\%$	48.9 %	$35.7^{+7.6}_{-7.0}\%$	19.6 %	781%
Combined Cuts		M1: 100.0 %	$100.0^{+0.0}_{-0.6}\%$	—	—	24.2 %	936%
		M2: 100.0 %	$100.0^{+0.0}_{-2.3}\%$	—	—	29.4 %	

Table A.22: Table of cut descriptions and efficiencies for simulated backgrounds and measured data for the 1216 keV peak.